Allgemeine Relativitätstheorie mit dem Computer

ZOOM ONLINE MEETING
JOHANN WOLFGANG GOETHE UNIVERSITÄT
18. JUNI, 2021

Aufgrund der Corona Krise findet die Vorlesung und die Übungstermine auch in diesem Semester nur Online statt.

MATTHIAS HANAUSKE

FRANKFURT INSTITUTE FOR ADVANCED STUDIES
JOHANN WOLFGANG GOETHE UNIVERSITÄT
INSTITUT FÜR THEORETISCHE PHYSIK
ARBEITSGRUPPE RELATIVISTISCHE ASTROPHYSIK
D-60438 FRANKFURT AM MAIN
GERMANY

10. Vorlesung

Teil III

Computersimulationen mit dem Einstein-Toolkit

In diesem Teil wird ein Einblick in die allgemein-relativistische Simulation auf Supercomputern gegeben. Unter Zuhilfenahme des Einstein-Toolkits werden unterschiedliche, realistische Systeme betrachtet (z.B. Neutronenstern-Kollisionen mit Aussendung von Gravitationswellen)

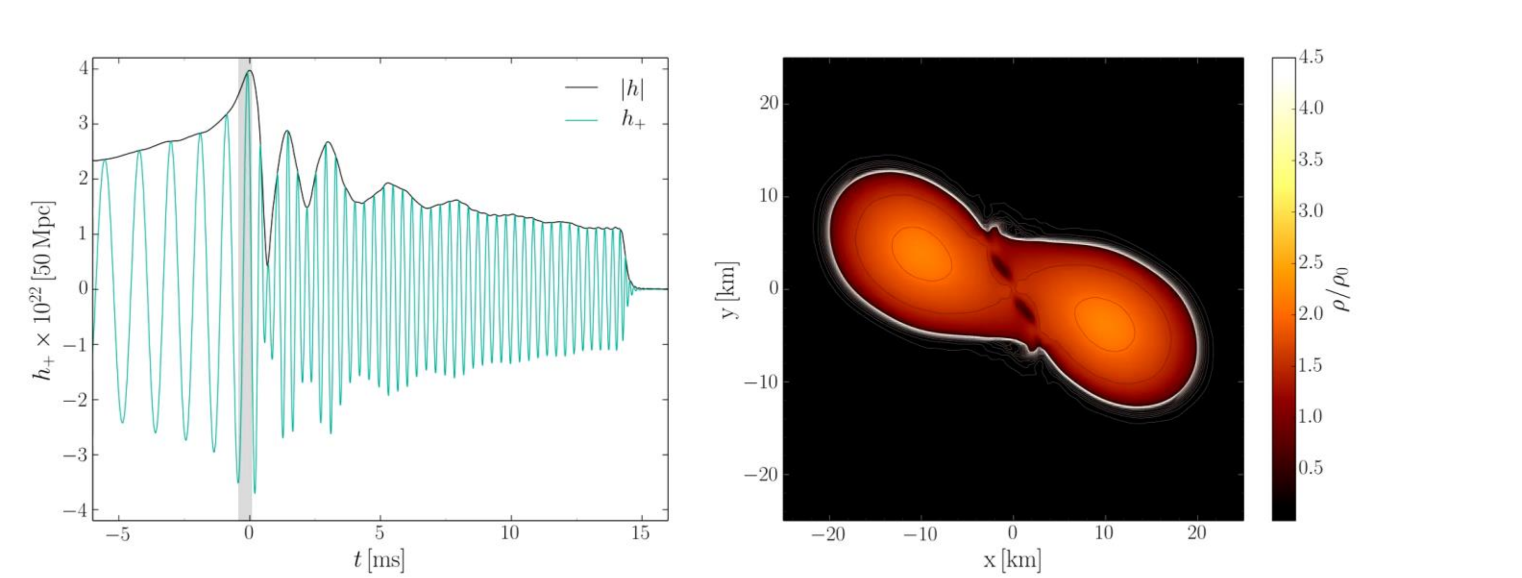

Das Einstein Toolkit: Weitere Informationen

einstein toolkit

- Welcome
- About the Toolkit
  - Members
  - Maintainers
  - Governance
  - Capabilities
  - Gallery
  - Releases
  - Tools
- Download
- Community Services
  - Wiki
  - Blog
  - Support
  - Seminars
  - Issue Tracker
- Documentation
  - Tutorial for New Users
  - Citing

Welcome

The Einstein Toolkit Consortium is developing and supporting open software for relativistic astrophysics. Our aim is to provide the core computational tools that can enable new science, broaden our community, facilitate interdisciplinary research and take advantage of emerging petascale computers and advanced cyberinfrastructure.

Please read our pages about the Einstein Toolkit, its governance, and how to get started with the toolkit for more information.

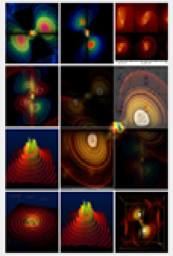

EinsteinToolkit@Flickr

Download

November 2014: We are pleased to announce the tenth release (code name "Herschel") of the Einstein Toolkit, an open, community developed software infrastructure for relativistic astrophysics.

https://www.youtube.com/watch?v=EO4d32ch6OI
https://www.youtube.com/watch?v=p5bq2iUO3DE
https://www.youtube.com/watch?v=MNpyd_o0MT4
https://www.youtube.com/watch?v=Qg6PwRI2uS8
https://www.youtube.com/watch?v=ZW3aV7U-aik

David Radice - Homepage

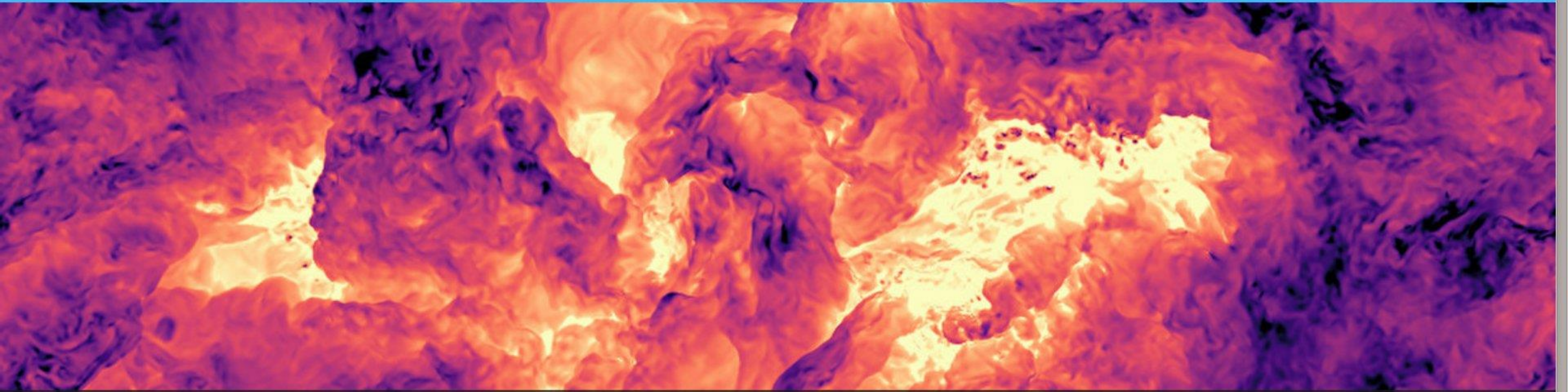

WhiskyTHC: the General-Relativistic Templated Hydrodynamics Code

Download

Gravitationswellen gefunden: LIGO!!!

<u>Kollision zweier Schwarzer Löcher GW150914</u>

Massen: 36 & 29 Sonnenmassen

Abstand zur Erde 410 Mpc (1.34 Milliarden Lichtjahre)

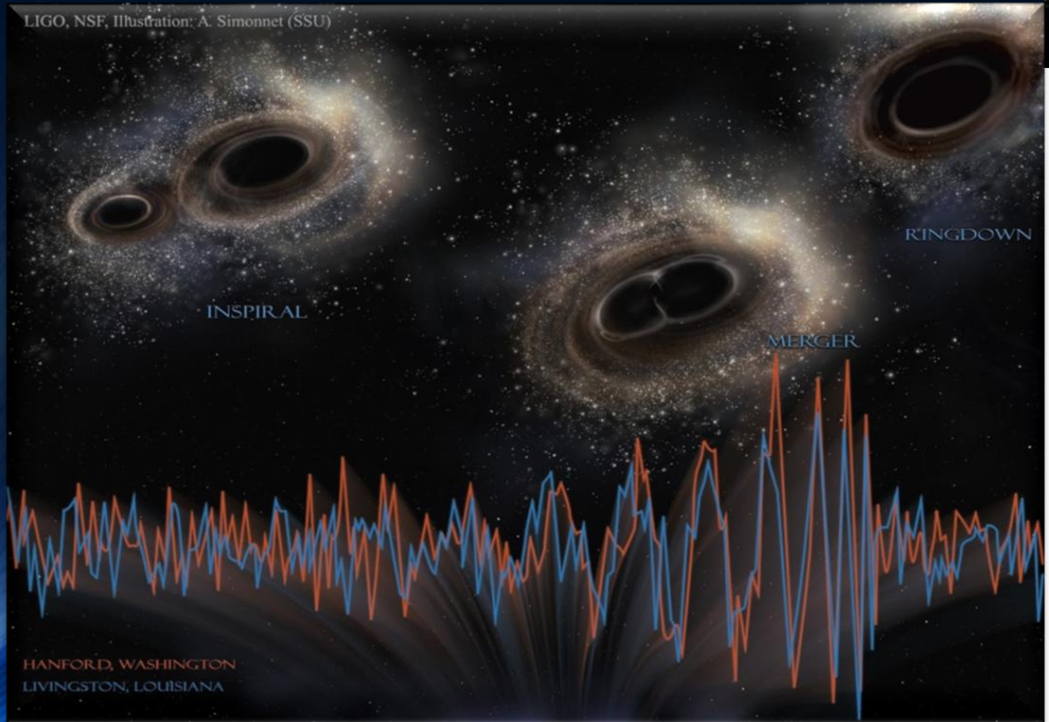

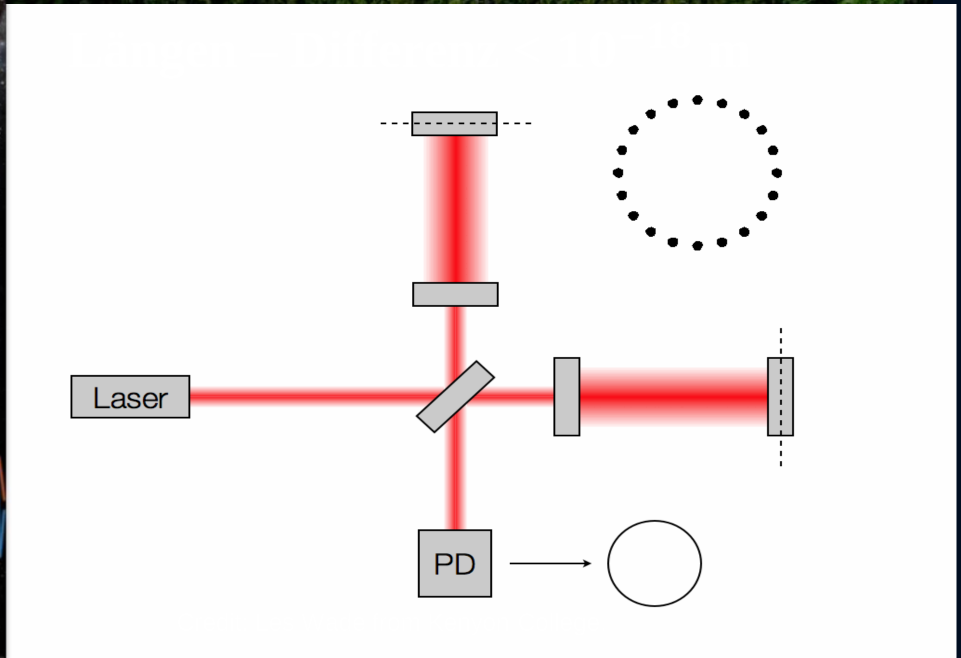

Die neue Art unser Universum zu betrachten

Lange Zeit über war das Studium von astrophysikalischen Vorgängen auf den mit den Augen sichtbaren Bereich limitiert und optische Teleskope entwickelten sich erst ab dem 16. Jahrhundert. Die Wahrnehmung des Universums in den anderen Frequenzbereichen der elektromagnetischen Strahlung wurde durch die Radio-, Infrarot- und Röntgen-Teleskope möglich und entwickelte sich erst im 20. Jahrhundert.

GSFC/NASA

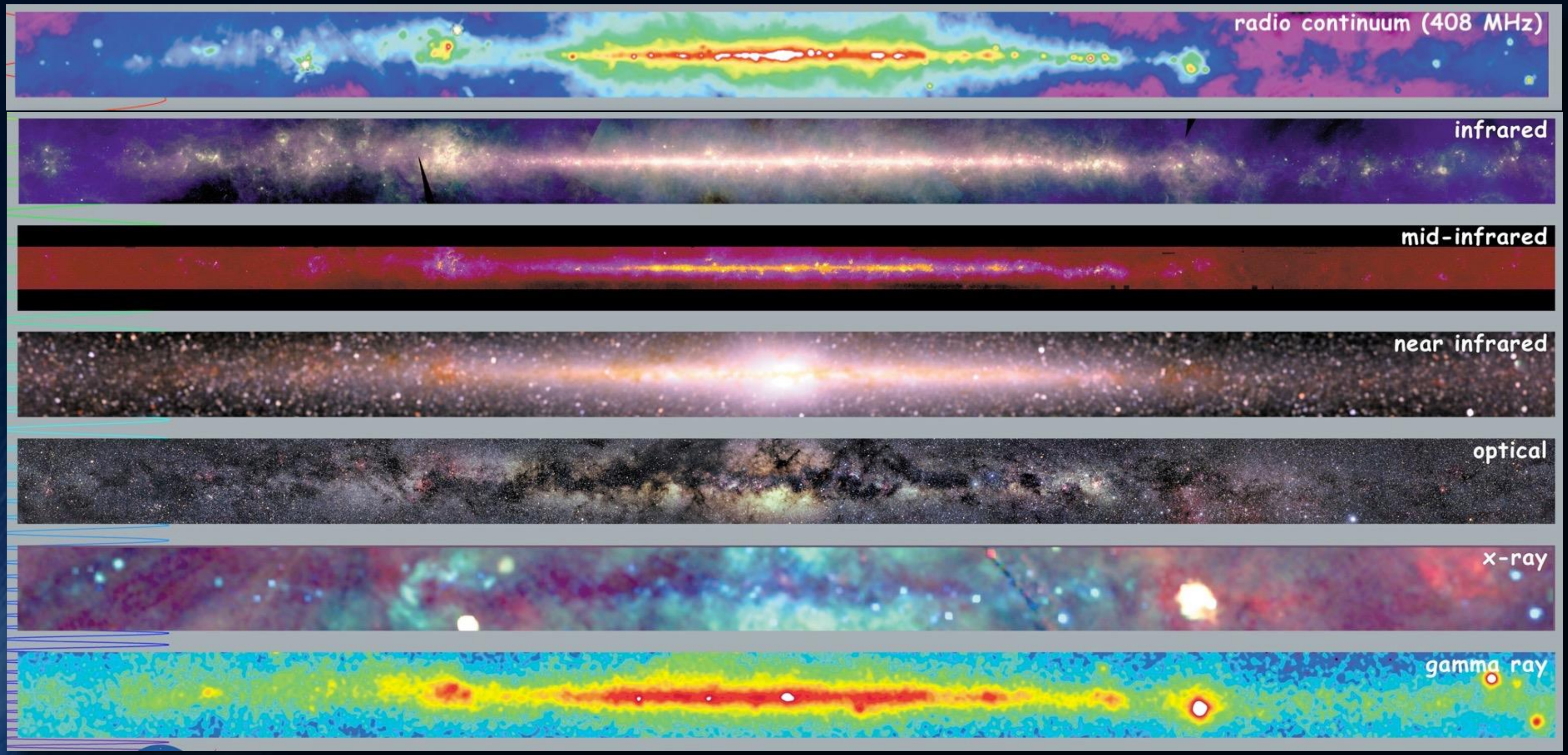

Radio

w-IR

m-IR

n-IR

Optisch

Röntgen

Gamma

Gravitations-
wellen

Erkenntnisse mittels elektromagnetische Strahlung

Es ist so als ob die Menschheit eine neue wundersame Brille hat, ein neues Sinnesorgan, mit welchem sie nun, zuvor unbeobachtbare Ereignisse in unserem Universum, wahrnehmen kann.

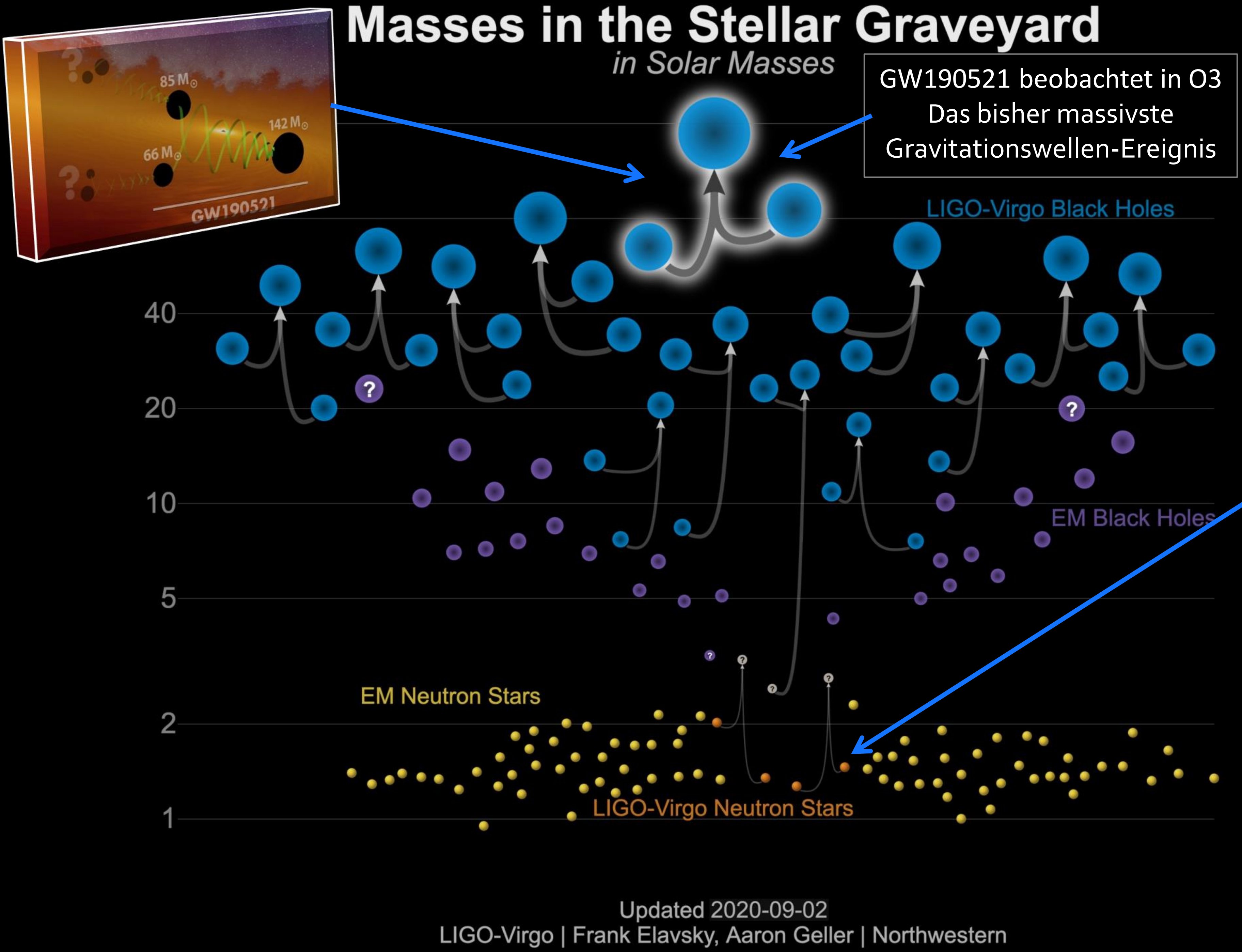

GW190521 beobachtet in O3
Das bisher massivste
Gravitationswellen-Ereignis

Detektierte Gravitationswellen

In den ersten beiden Beobachtungsläufen (O1+O2) konnten 11 Gravitationswellen detektiert werden, wobei einer dieser Gravitationswellen (GW170817) durch die Kollision zweier Neutronensterne verursacht wurde welche sich vor ungefähr 130 Millionen Jahren ereignete.

The long-awaited event GW170817

	Low-spin priors ($|\chi| \leq 0.05$)	High-spin priors ($|\chi| \leq 0.89$)
Primary mass m_1	$1.36–1.60\ M_\odot$	$1.36–2.26\ M_\odot$
Secondary mass m_2	$1.17–1.36\ M_\odot$	$0.86–1.36\ M_\odot$
Chirp mass $\mathcal{M}$	$1.188^{+0.004}_{-0.002} M_\odot$	$1.188^{+0.004}_{-0.002} M_\odot$
Mass ratio m_2/m_1	0.7–1.0	0.4–1.0
Total mass m_{tot}	$2.74^{+0.04}_{-0.01} M_\odot$	$2.82^{+0.47}_{-0.09} M_\odot$
Radiated energy E_{rad}	$> 0.025 M_\odot c^2$	$> 0.025 M_\odot c^2$
Luminosity distance D_{L}	40^{+8}_{-14} Mpc	40^{+8}_{-14} Mpc
Viewing angle Θ	$\leq 55°$	$\leq 56°$
Using NGC 4993 location	$\leq 28°$	$\leq 28°$
Combined dimensionless tidal deformability $\tilde{\Lambda}$	≤ 800	≤ 700
Dimensionless tidal deformability $\Lambda(1.4 M_\odot)$	≤ 800	≤ 1400

The second event: GW190425

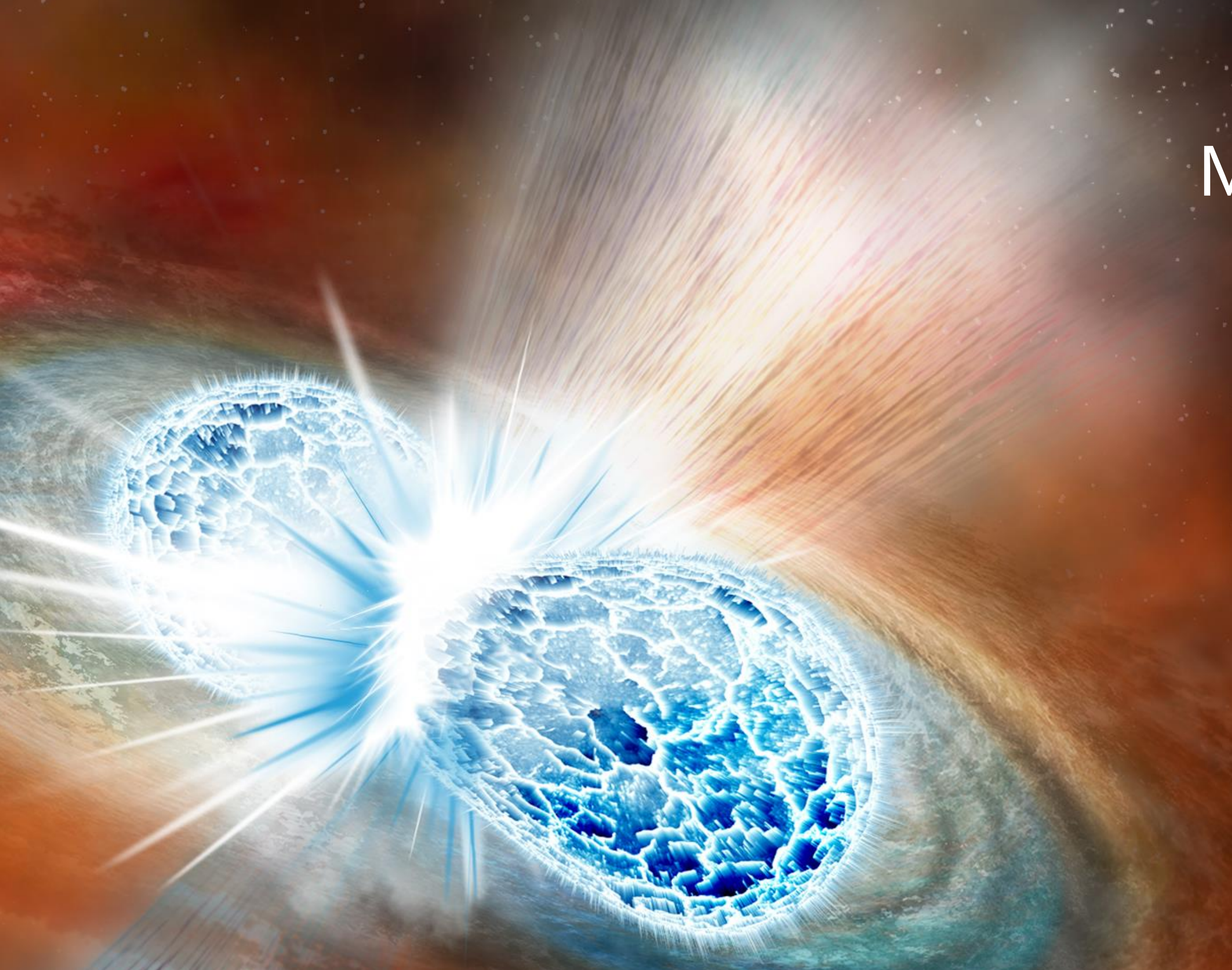

Mass ~ 3.4 M$_\odot$

19. April 2019

Second detection of a gravitational wave from a binary neutron star merger event!

GW190814 The third event ???

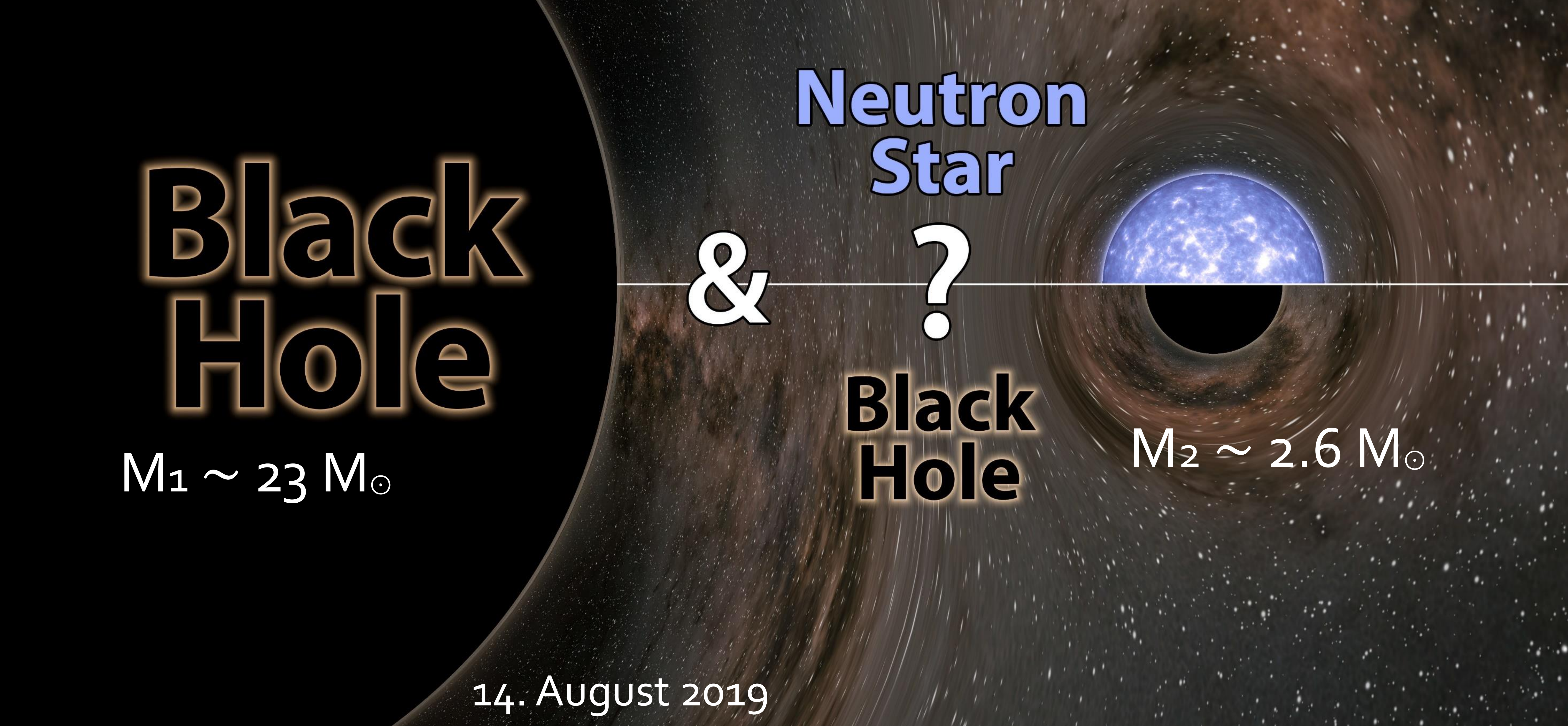

14. August 2019

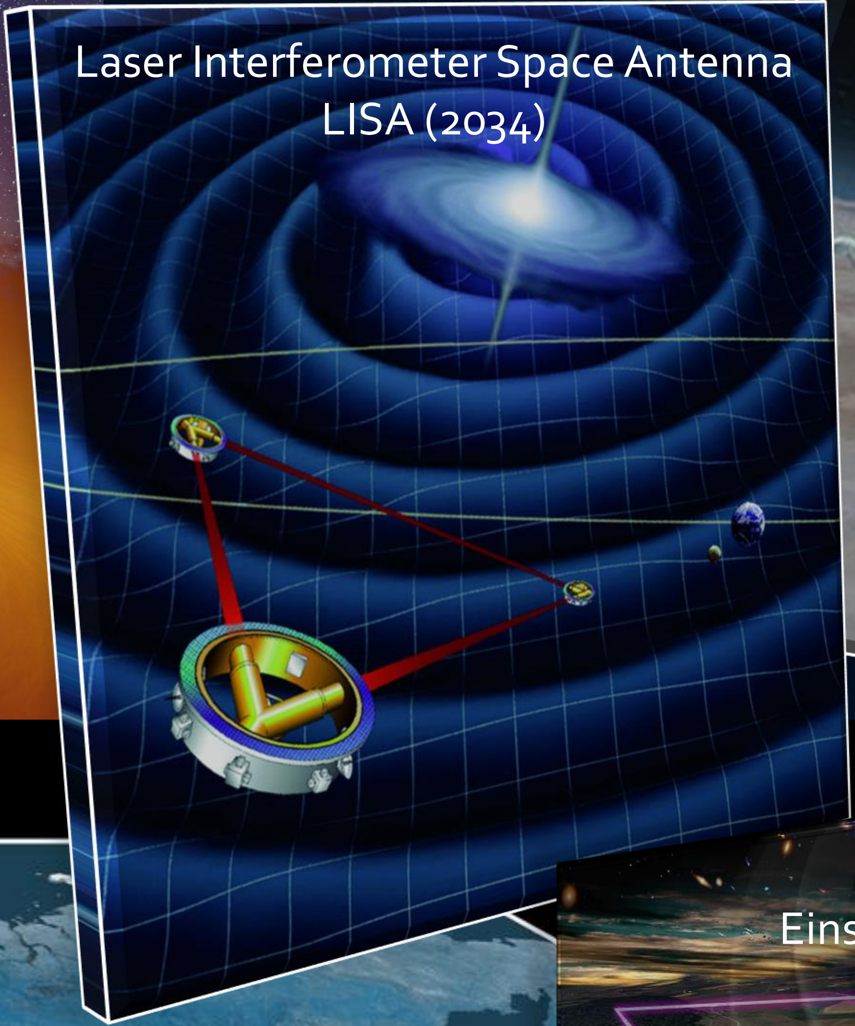

The next observing runs (O4,O5,..)

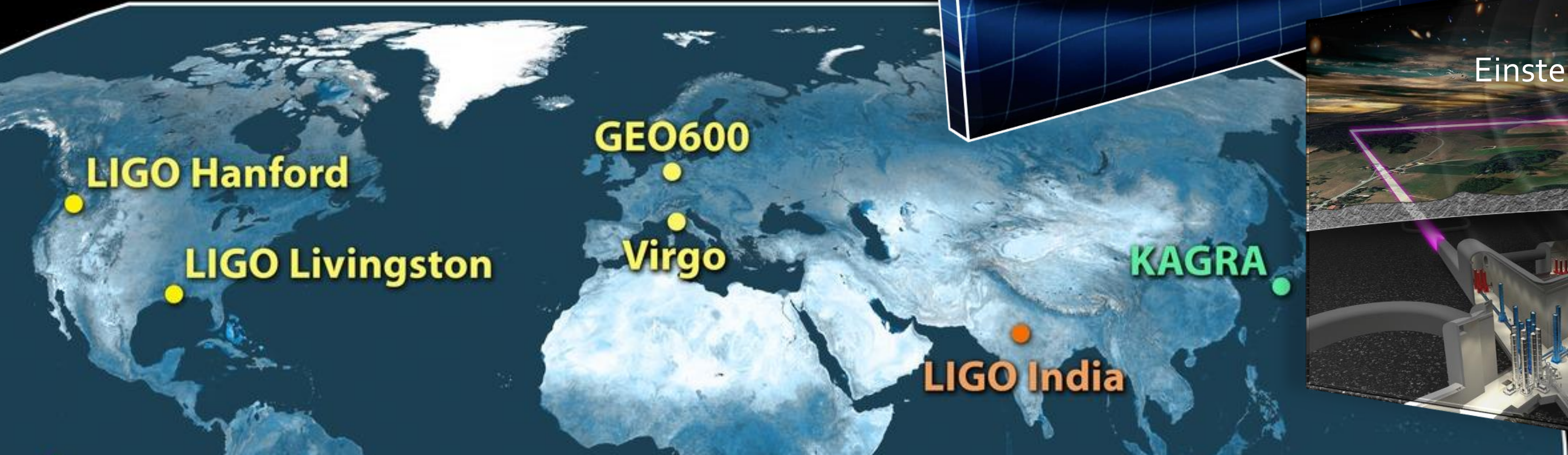

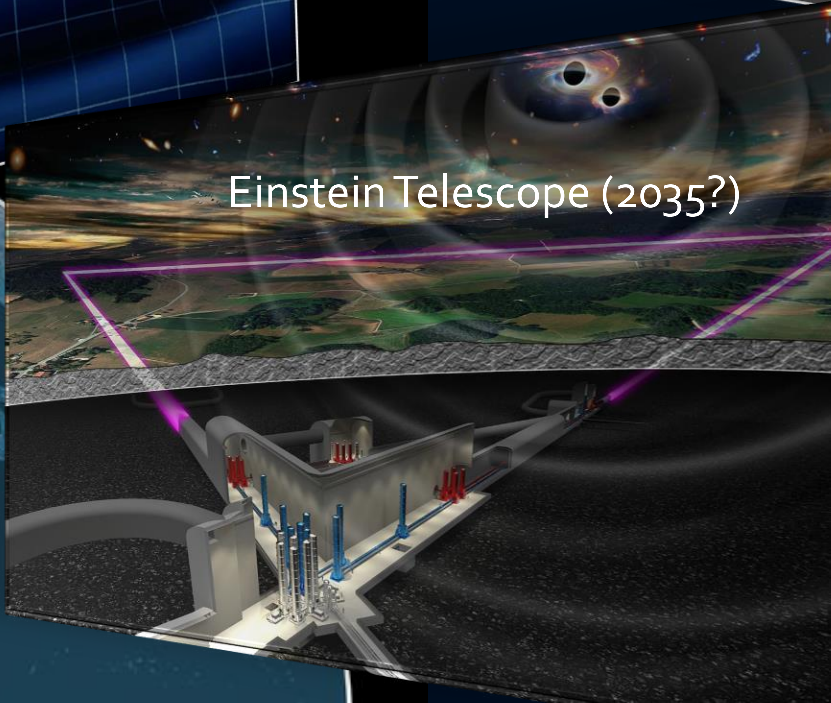

Gravitationswellen von Neutronenstern Kollisionen

Neutronenstern Kollision (Simulation)

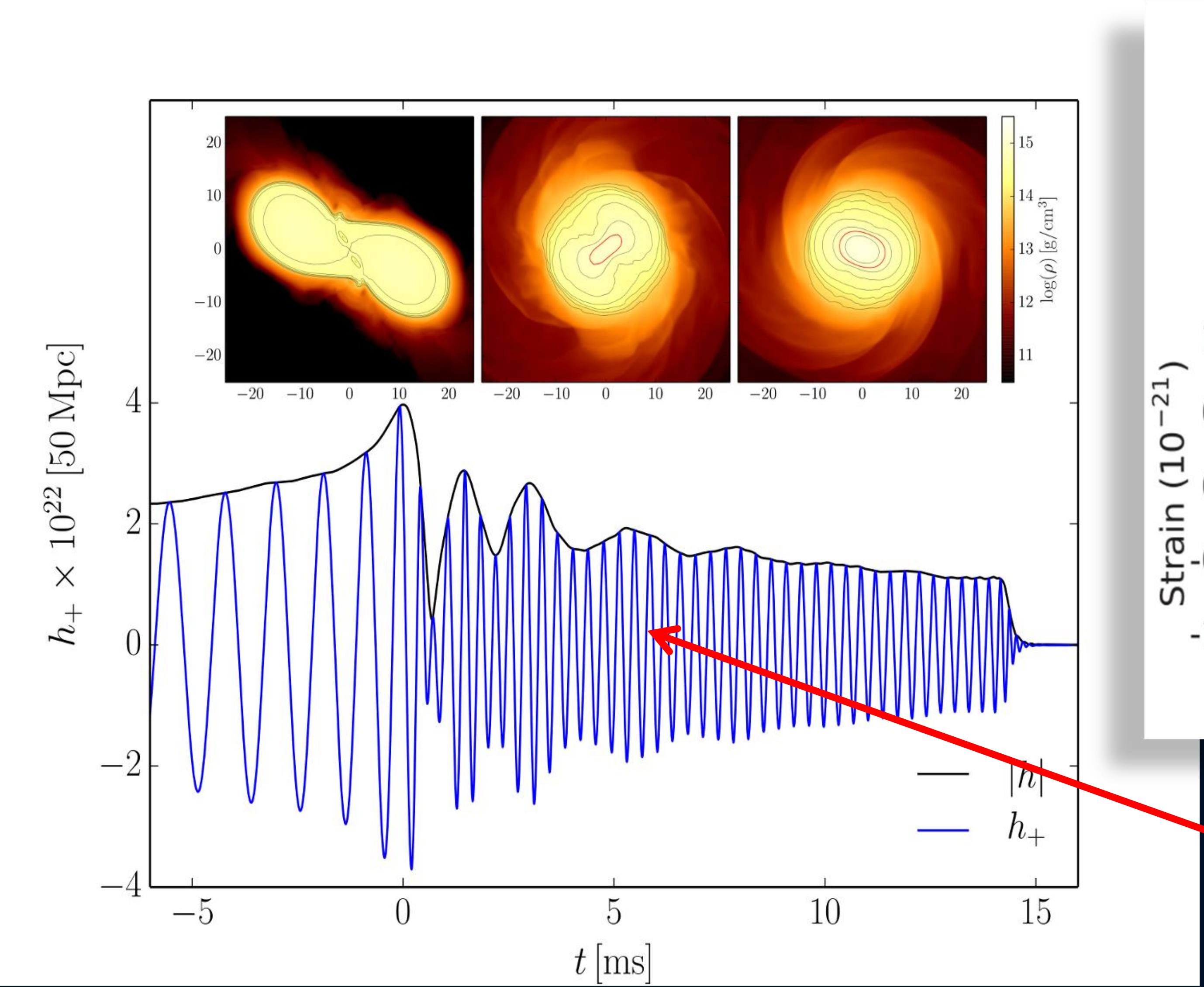

Kollision zweier schwarzer Löcher

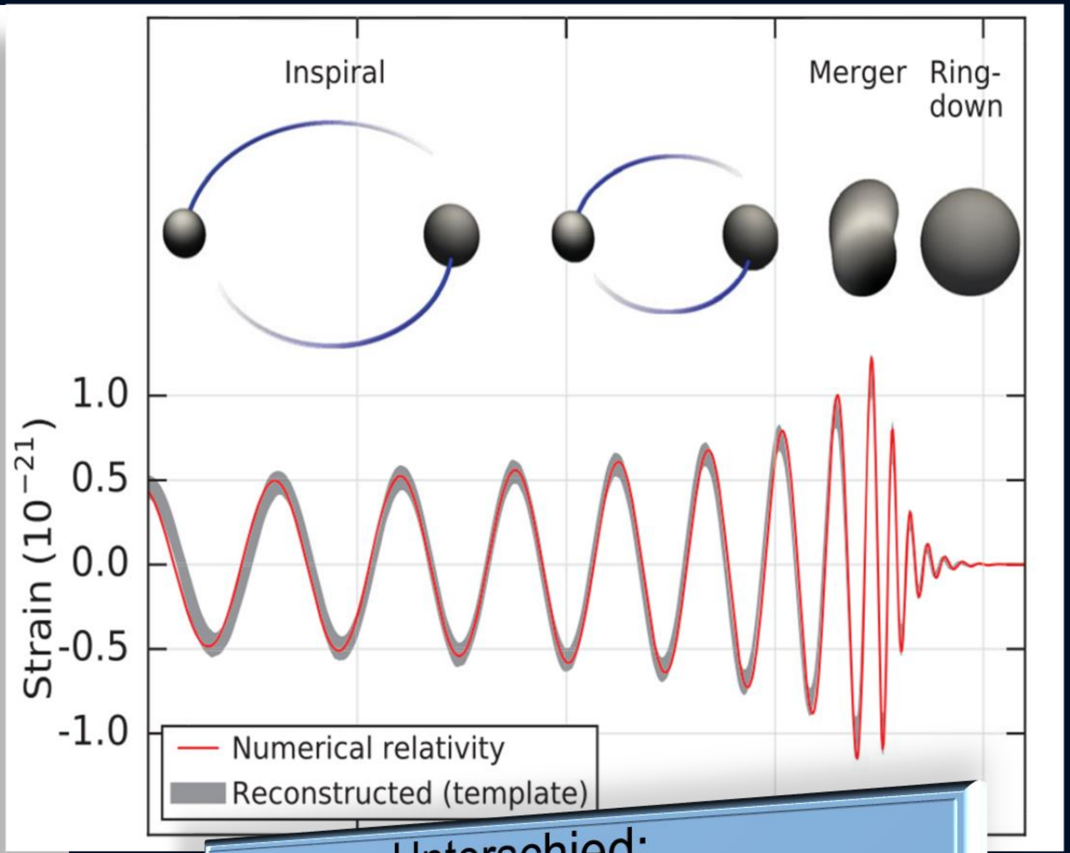

<u>Unterschied:</u>
Bei Neutronenstern Kollisionen
gibt es meistens eine
Post-Kollisionsphase

The Einstein Equation and the EOS of Compact Stars

ART	Yang-Mills-Theories
$D_\beta v^\alpha = \partial_\beta \, v^\alpha + \Gamma^\alpha_{\sigma\beta} \, v^\sigma$	$D_{\beta a}{}^{b} = \partial_\beta \, 1_a{}^{b} + ig \, A_{\beta a}{}^{b}$
$R^\delta{}_{\mu\alpha\beta} \, v^\mu = [D_\alpha, D_\beta] \, v^\delta$ $R^\delta{}_{\mu\alpha\beta} = \Gamma^\delta_{\mu\alpha\|\beta} - \Gamma^\delta_{\mu\beta\|\alpha}$ $+\Gamma^\delta_{\nu\beta}\Gamma^\nu_{\mu\alpha} + \Gamma^\delta_{\nu\alpha}\Gamma^\nu_{\mu\beta}$	$F_{\alpha\beta a}{}^{b} = \frac{1}{ig} \left[D_{\alpha a}{}^{c}, D_{\beta c}{}^{b} \right]$ $= A_{\beta a}{}^{b}{}_{\|\alpha} - A_{\alpha a}{}^{b}{}_{\|\beta}$ $+ \frac{1}{ig} \left[A_{\alpha a}{}^{c}, A_{\beta c}{}^{b} \right]$
$\mathcal{L}_G = R + \underbrace{(c_1 \, R_{\mu\nu} R^{\mu\nu} + \ldots)}_{\equiv 0 \text{ for ART}}$	$\mathcal{L}_{YM} = \frac{1}{4} F_{\mu\nu a}{}^{b} \, F^{\mu\nu}{}_{a}{}^{b}$

QuantumCromoDynamic:

$(SU(3)_{(c)}$- Color Yang-Mills-Gauge Theory)

$$D_{\beta A}{}^{B} = \partial_\beta \, 1_A{}^{B} + ig \, G_{\beta A}{}^{B}$$

$A, {}^{B}$ =red, green, blue

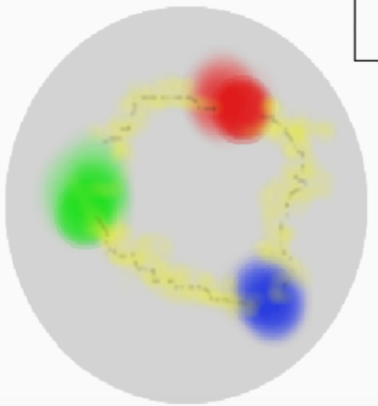

$$\psi^f_A = \begin{pmatrix} \psi^f_r \\ \psi^f_g \\ \psi^f_b \end{pmatrix}$$

Confinement

chiral symmetry, ...

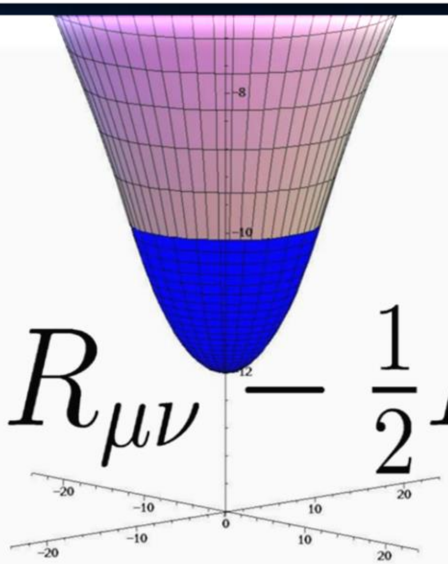

$$R_{\mu\nu} - \frac{1}{2} R \, g_{\mu\nu} = \frac{8\pi G}{c^4} \, T_{\mu\nu}$$

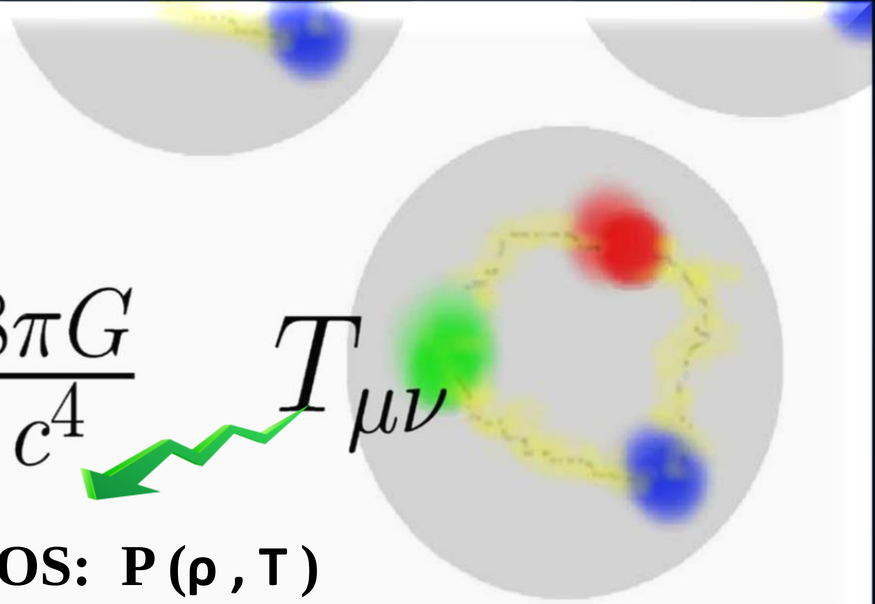

EOS: P (ρ , T)

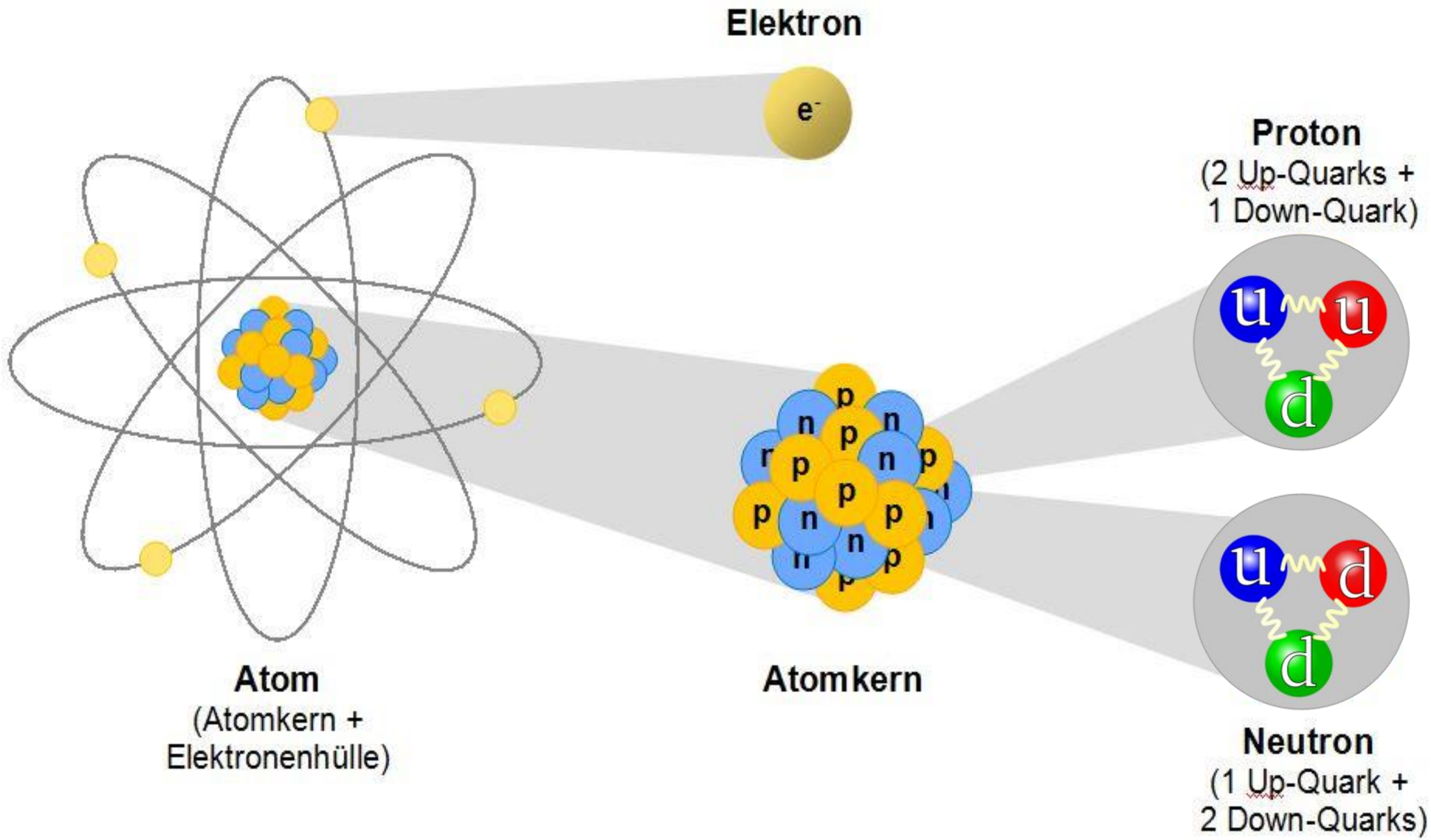
Elektron
e⁻
Proton
(2 Up-Quarks +
1 Down-Quark)
u
u
d
Atom
(Atomkern +
Elektronenhülle)
Atomkern
Neutron
(1 Up-Quark +
2 Down-Quarks)

Die experimentelle Untersuchung
der Eigenschaften der elementaren Materie

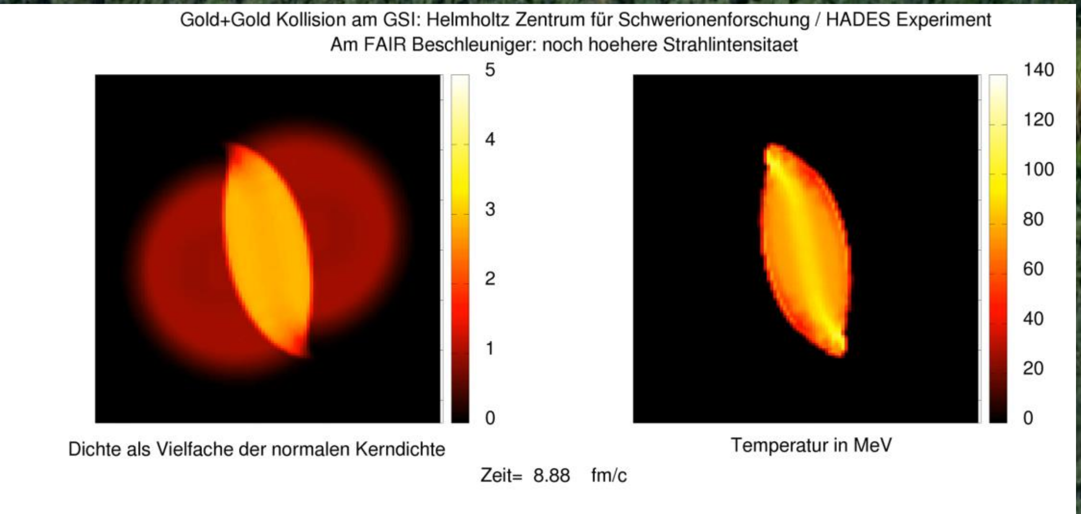

FAIR - Das Universum im Labor

Zurzeit entsteht in Darmstadt das neue internationale Beschleunigerzentrum FAIR, eines der größten Forschungsvorhaben weltweit

Mit FAIR wird Materie im Labor erzeugt und erforscht werden, wie sie sonst nur im Universum vorkommt

Der Hadron-Quark Phasenübergang

Temperatur vs. Dichte

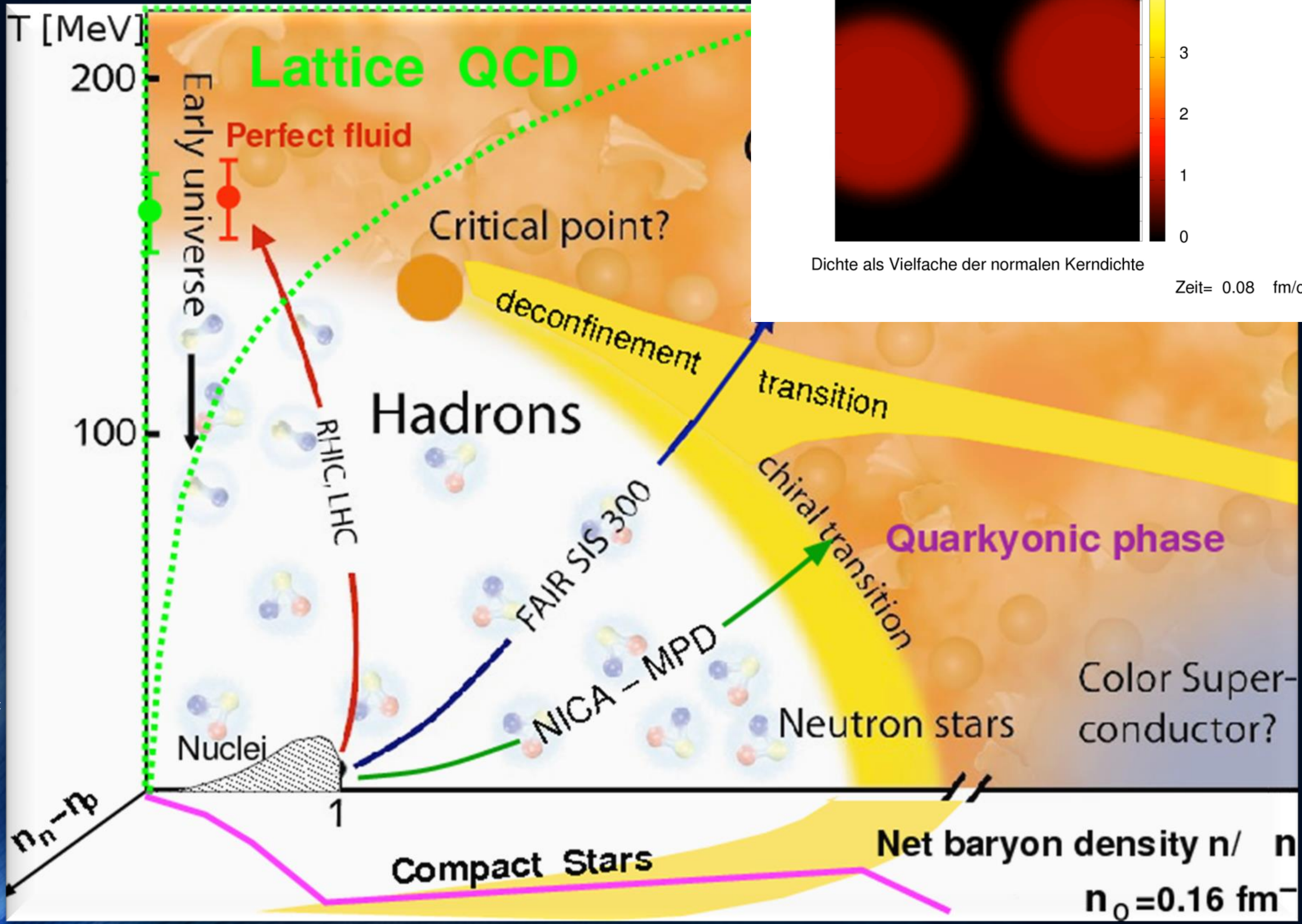

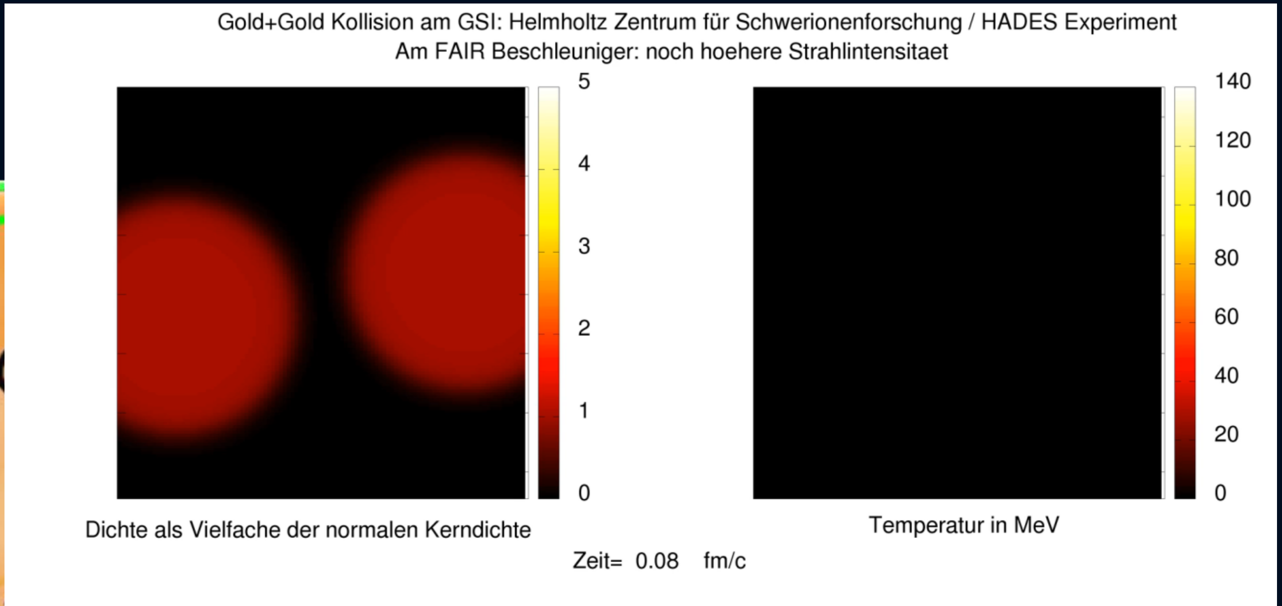

1 MeV≈ 10^{10} Grad ≈ 10000 heißer als im Inneren der Sonne

Hadronische Teilchen

Neutron Proton

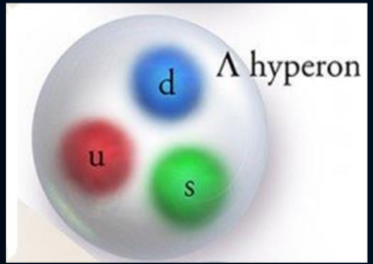

Das Innere von hybriden Sternen

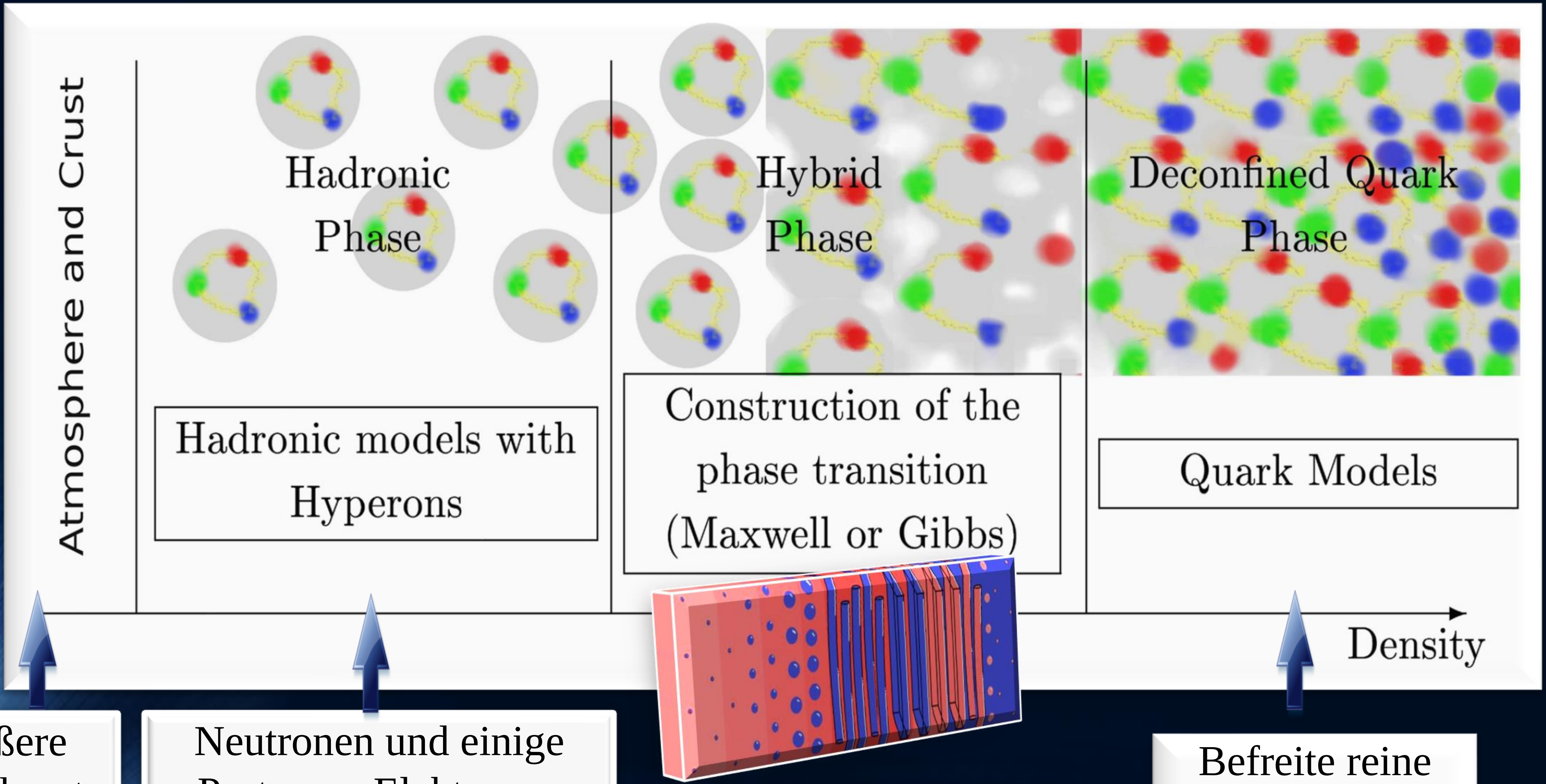

Äußere Eisenkruste

Neutronen und einige Protonen, Elektronen vielleicht auch Hyperonen

Phasenübergang vielleicht Pasta-Struktur

Befreite reine Quarkphase

Neutronensterne, Quarksterne und schwarze Löcher

Bei welcher Dichte der Phasenübergang zum Quark-Gluon-Plasma einsetzt und welche Eigenschaften dieser Übergang im Detail hat ist weitgehend unbekannt. Theoretische Modellierung mittels unterschiedlicher effektiver Elementarteilchenmodelle.

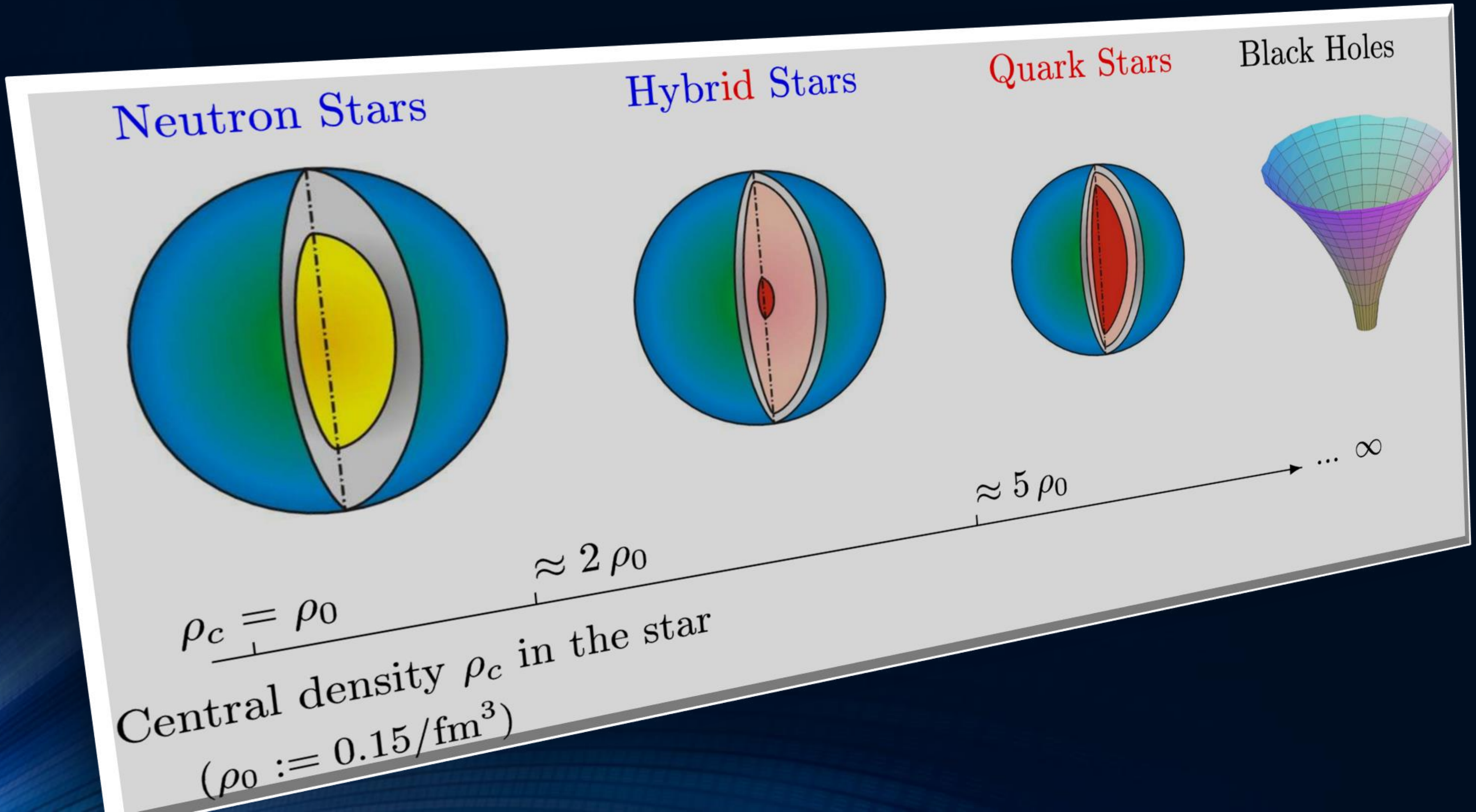

Numerical Relativity and Relativistic Hydrodynamics of Binary Neutron Star Mergers

A realistic numerical simulation of a twin star collapse, a merger of two compact stars or a collapse to a black hole needs to go beyond a static, spherically symmetric TOV-solution of the Einstein- and hydrodynamical equations.

$$R_{\mu\nu} - \frac{1}{2} g_{\mu\nu} R = 8\pi T_{\mu\nu}$$

$$\nabla_\mu (\rho u^\mu) = 0\,, \qquad \nabla_\nu T^{\mu\nu} = 0\,.$$

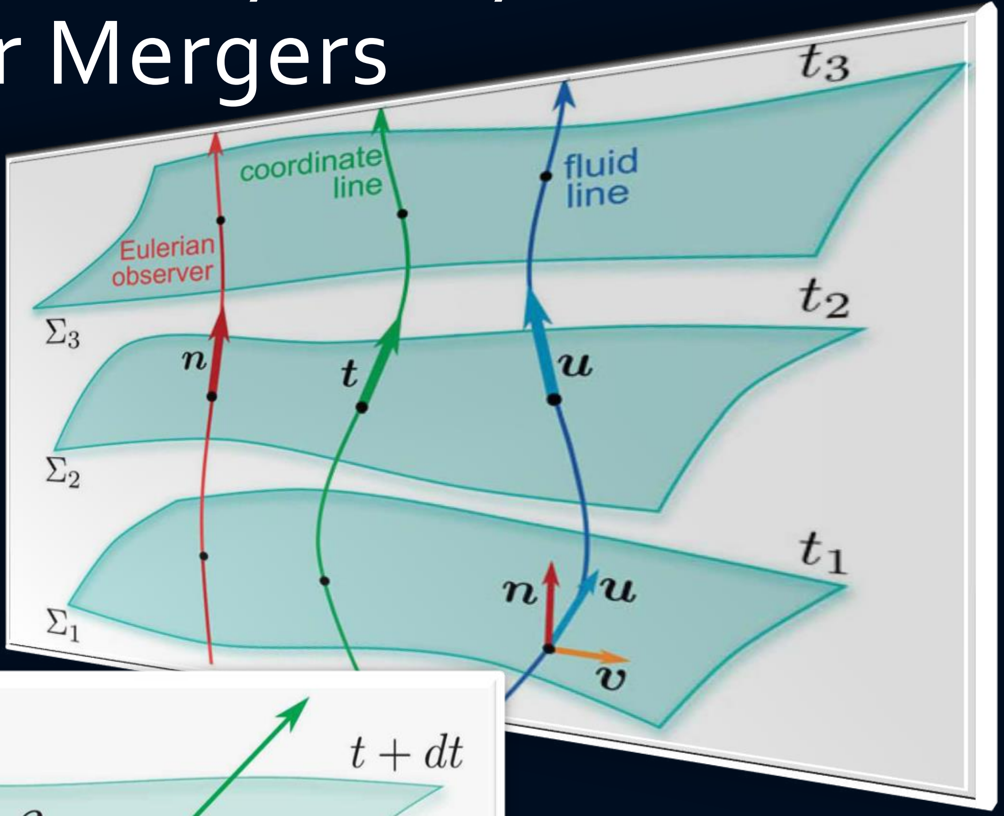

(3+1) decomposition of spacetime

$$g_{\mu\nu} = \begin{pmatrix} -\alpha^2 + \beta_i \beta^i & \beta_i \\ \beta_i & \gamma_{ij} \end{pmatrix}$$

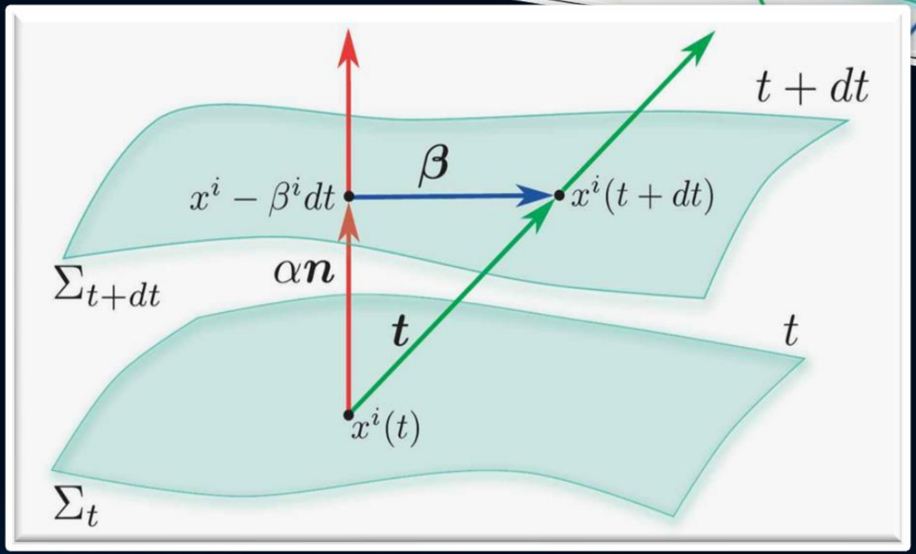

$$d\tau^2 = \alpha^2(t, x^j) dt^2 \qquad x^i_{t+dt} = x^i_t - \beta^i(t, x^j) dt$$

All figures and equations from: Luciano Rezzolla, Olindo Zanotti: Relativistic Hydrodynamics, Oxford Univ. Press, Oxford (2013)

The late inspiral phase (density, lapse and shift)

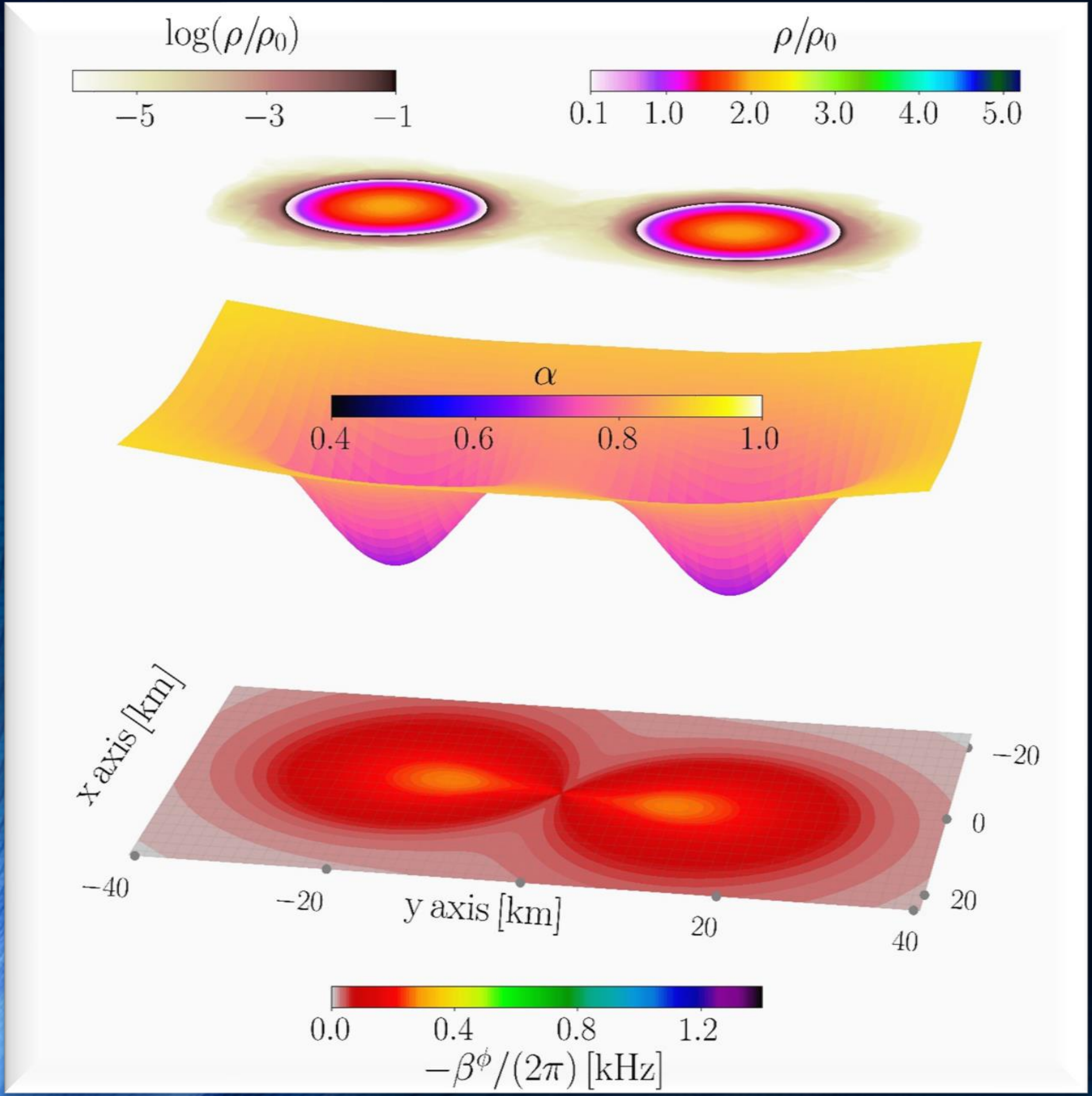

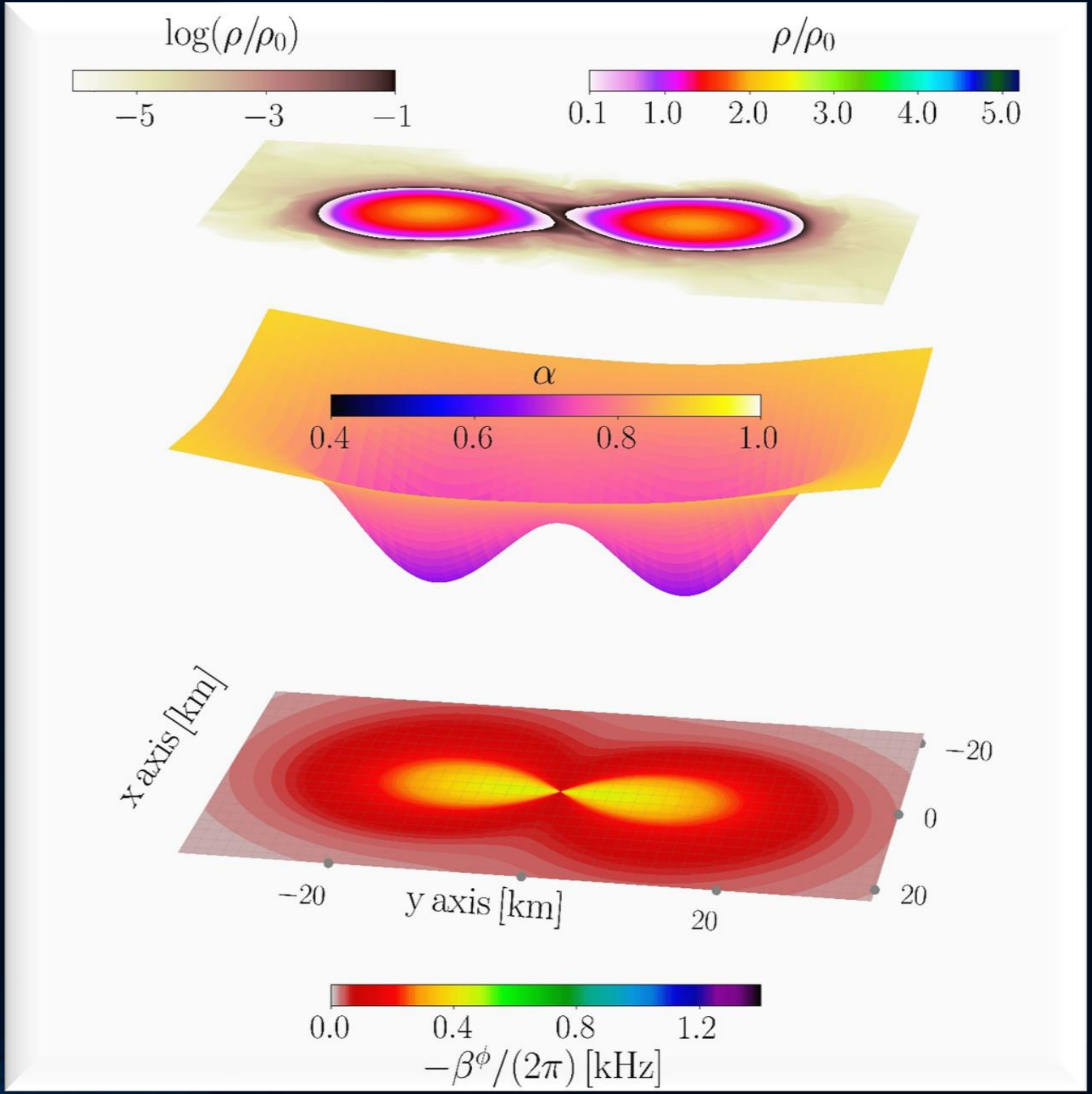

Broadbrush picture

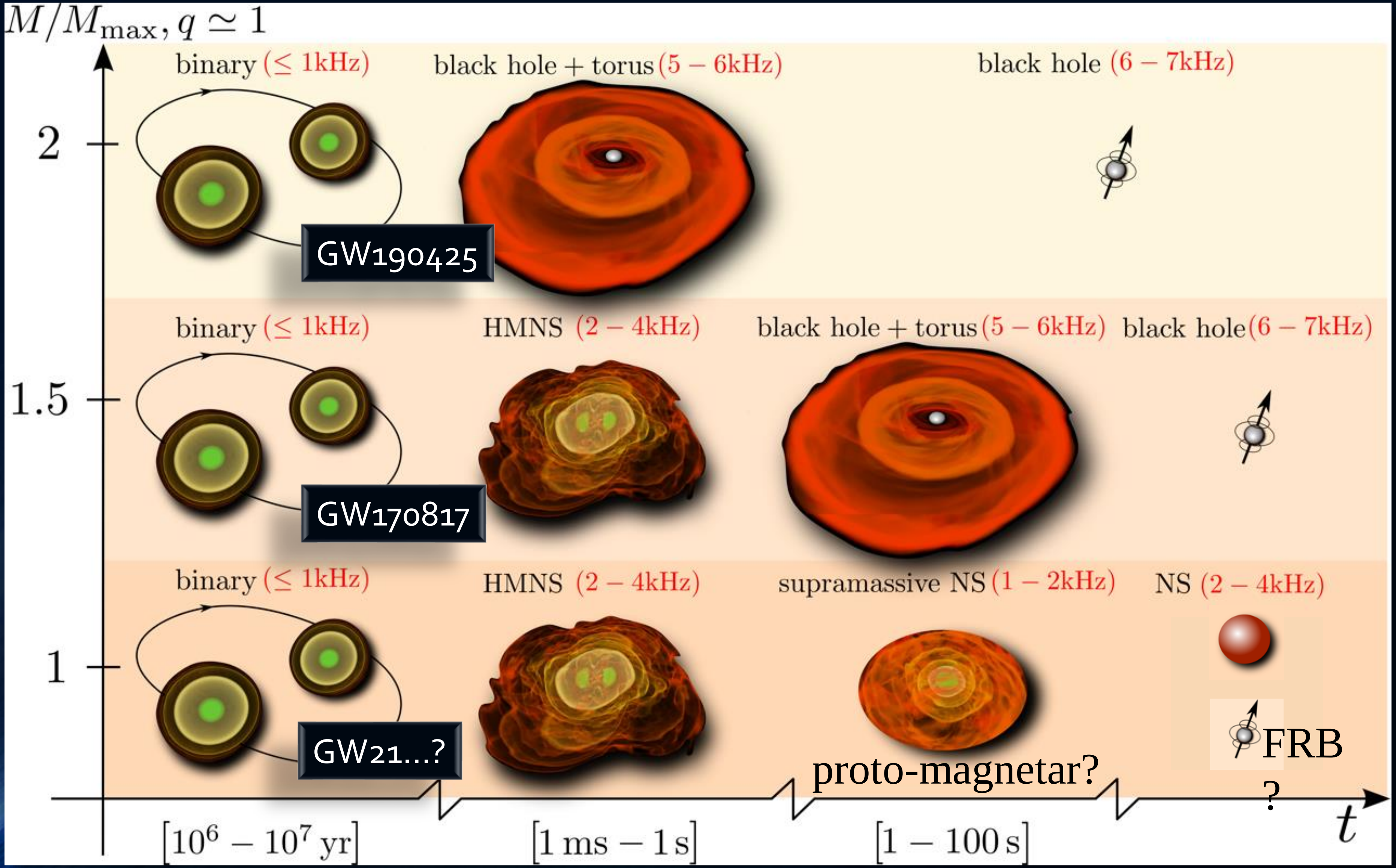

Gravitational Waves and Hypermassive Hybrid Stars

ALF2-EOS: Mixed phase region starts at $3\rho_0$ (see red curve), initial NS mass: 1.35 M_{solar}

Hanauske, et.al. PRD, 96(4), 043004 (2017)

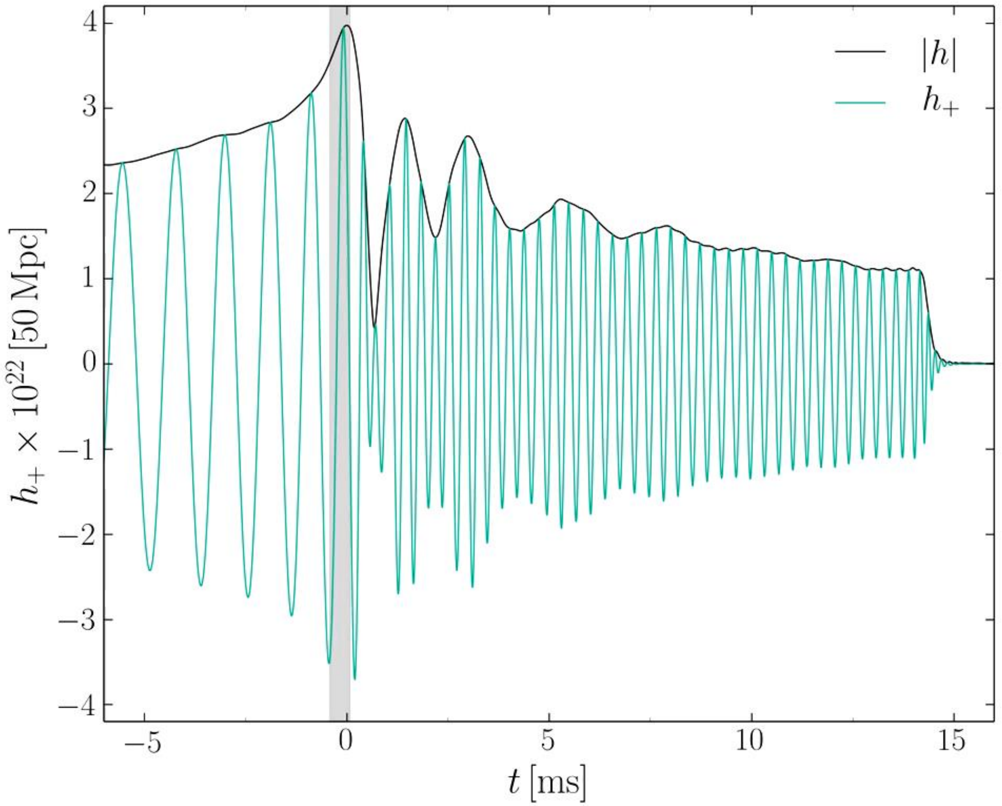

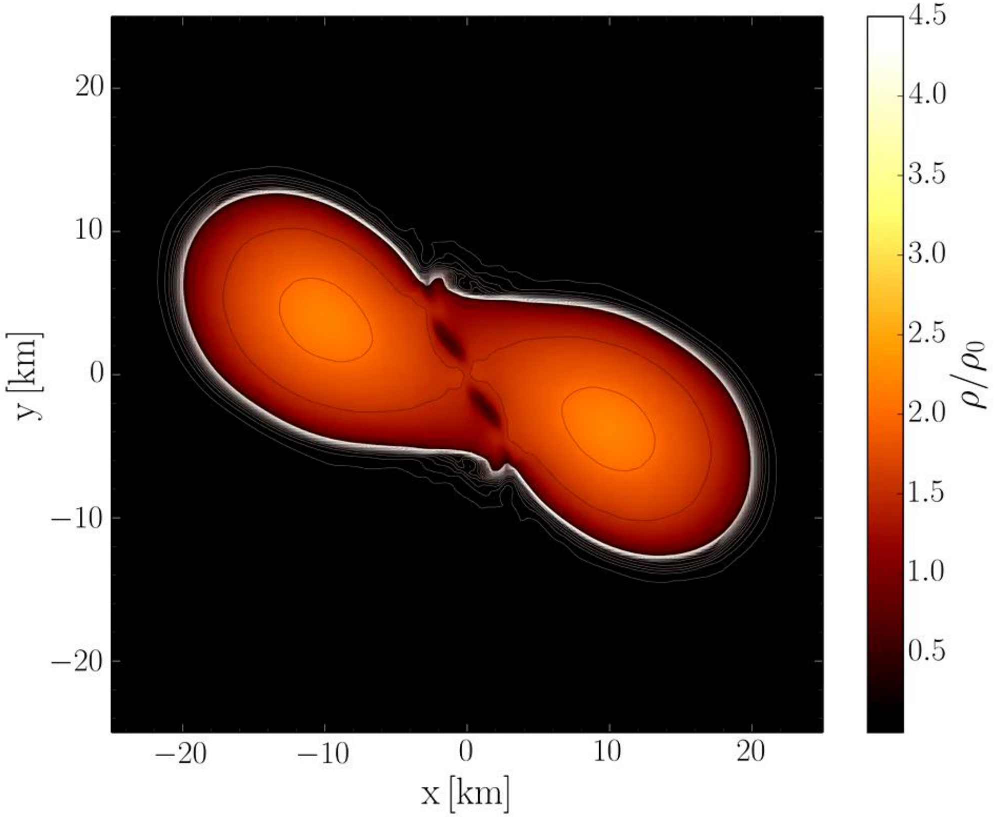

Gravitational wave amplitude at a distance of 50 Mpc

Rest mass density distribution ρ(x,y) in the equatorial plane

in units of the nuclear matter density ρ_0

GW170817: Tidal Deformability Restrictions on the Equation of State (EOS) (for high and low spin assumption)

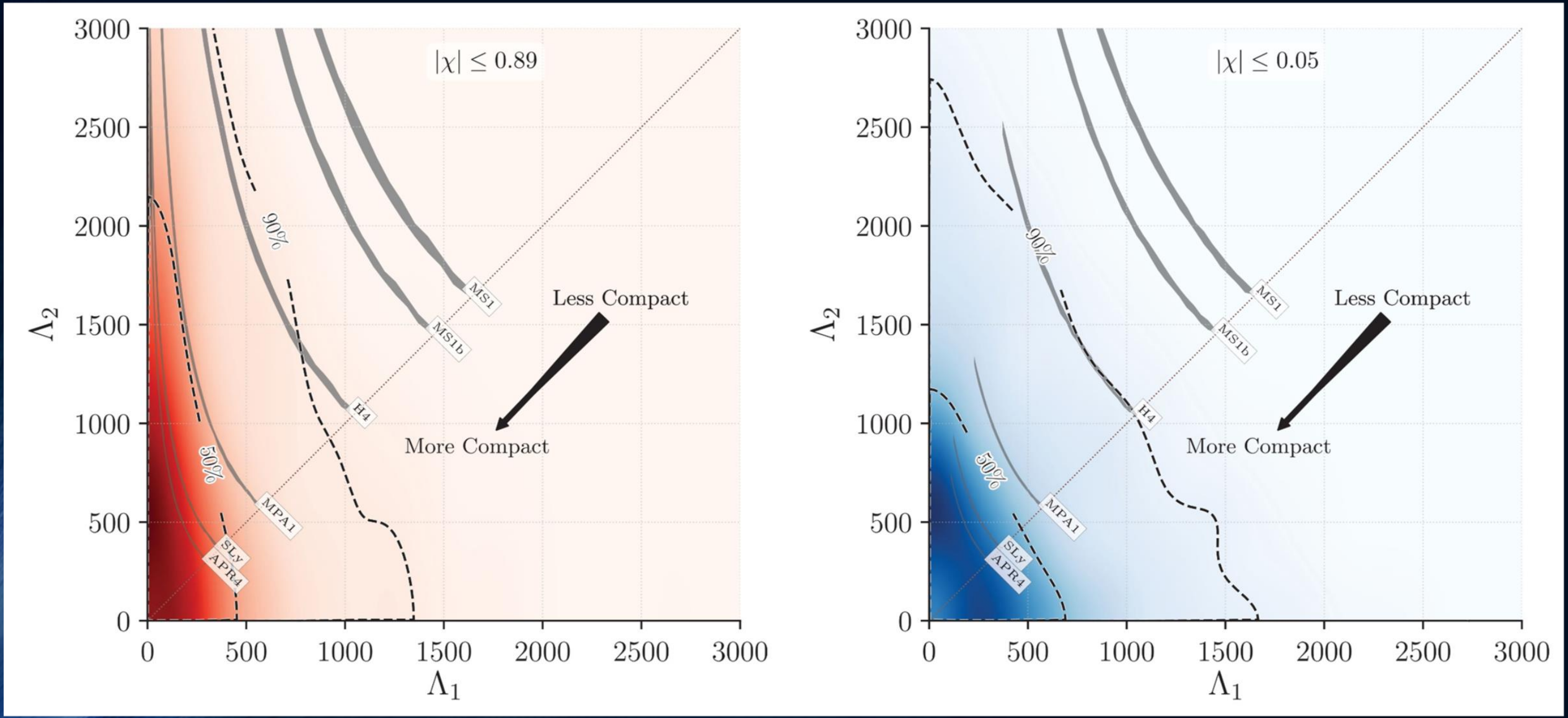

GW170817: Constraining the Neutron Star Radius and EOS

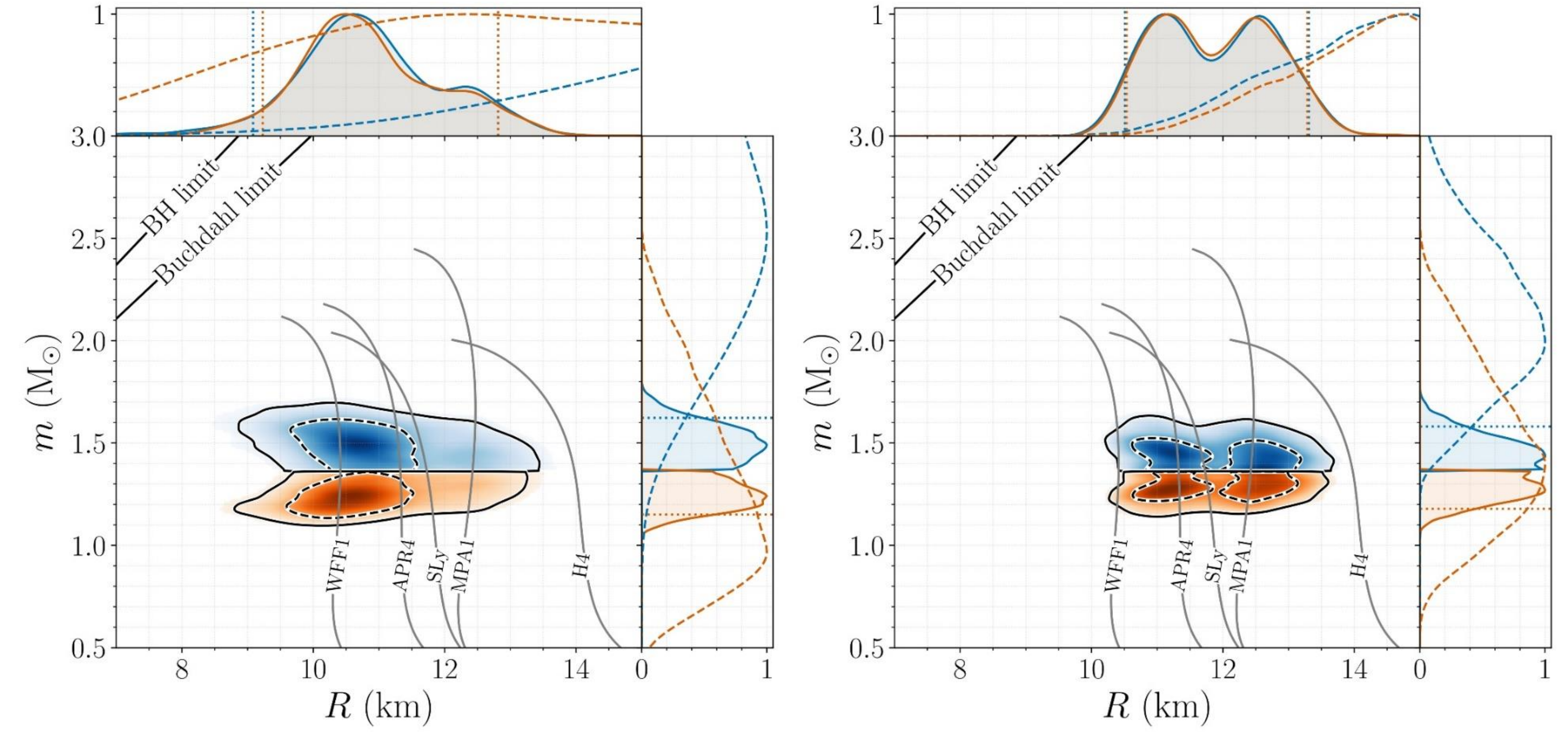

FIG. 3. Marginalized posterior for the mass m and areal radius R of each binary component using EOS-insensitive relations (left panel) and a parametrized EOS where we impose a lower limit on the maximum mass of $1.97\,M_\odot$ (right panel). The top blue (bottom orange) posterior corresponds to the heavier (lighter) NS. Example mass-radius curves for selected EOSs are overplotted in grey. The lines in the top left denote the Schwarzschild BH ($R = 2m$) and Buchdahl ($R = 9m/4$) limits. In the one-dimensional plots, solid lines are used for the posteriors, while dashed lines are used for the corresponding parameter priors. Dotted vertical lines are used for the bounds of the 90% credible intervals.

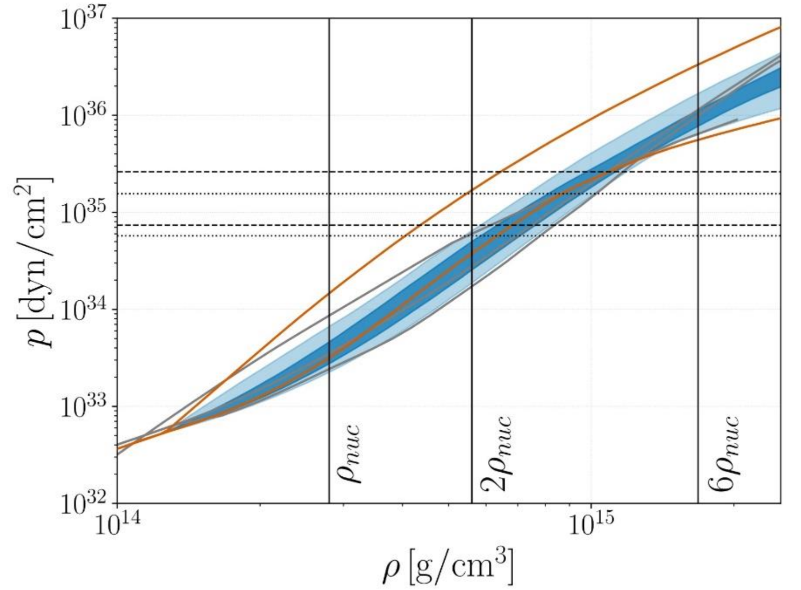

FIG. 2. Marginalized posterior (blue) and prior (orange) for the pressure p as a function of the rest-mass density ρ of the NS interior using the spectral EOS parametrization and imposing a lower limit on the maximum NS mass supported by the EOS of $1.97\,M_\odot$. The dark (light) blue shaded region corresponds to the 50% (90%) posterior credible level and the orange lines show the 90% prior credible interval. Horizontal lines denote the 90% credible interval for the central pressure of the heavier (dashed) and the lighter (dotted) binary components. Vertical lines correspond to once, twice, and six times the nuclear saturation density. Overplotted in grey are representative EOS models [121, 122, 124], using data taken from [19]; from top to bottom at $2\rho_{\rm nuc}$ we show H4, APR4, and WFF1.

GW170817: Measurements of neutron star radii and equation of state, *The LIGO /Virgo Collaboration*, arXiv:1805.11581v1

GW170817: Constraining the Neutron Star Radius and EOS

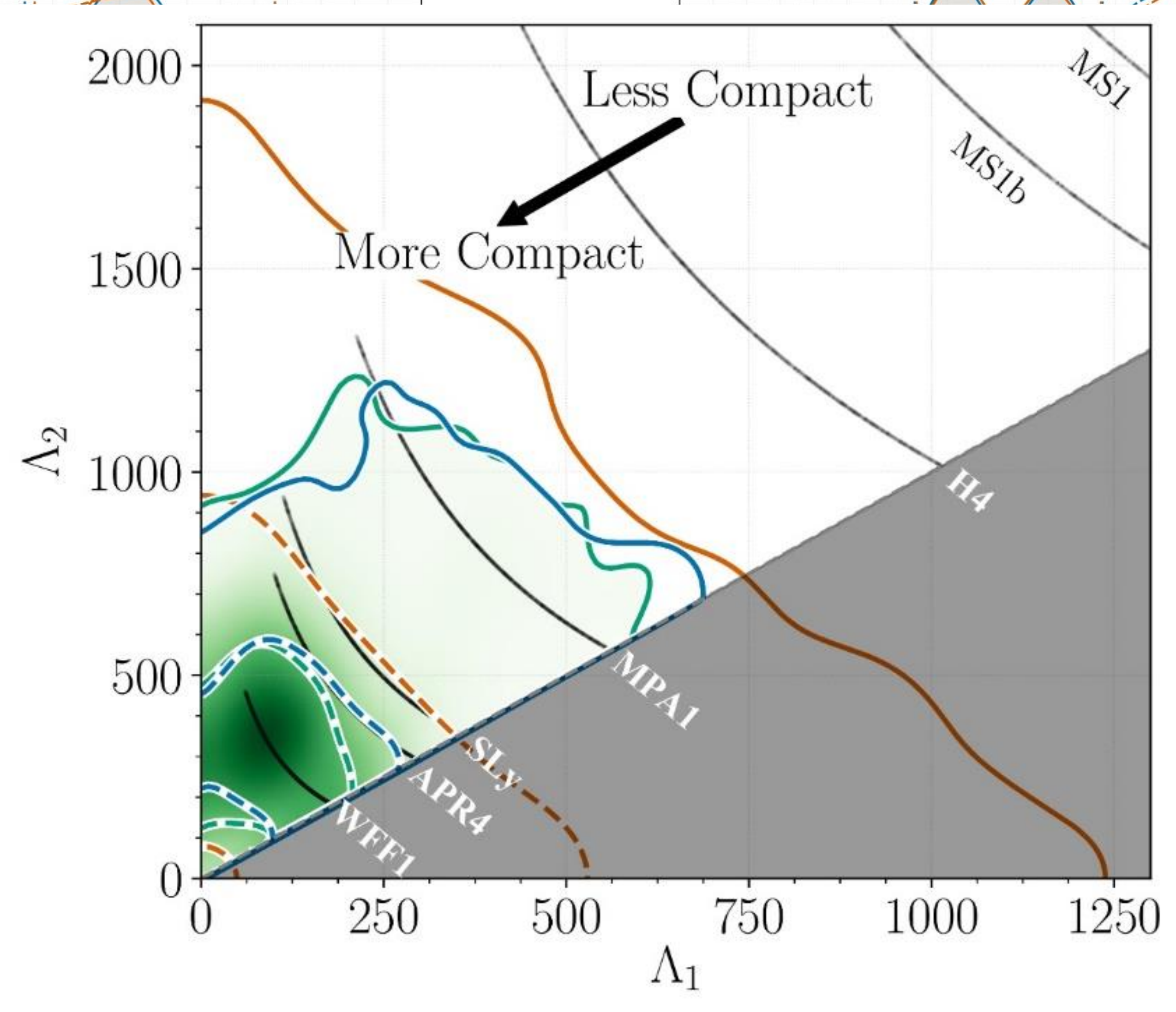

FIG. 3. Marginaliz
and a parametrized
posterior correspor
the top left denote
used for the posteri
of the 90% credibl

ions (left panel)
(bottom orange)
ey. The lines in
, solid lines are
d for the bounds

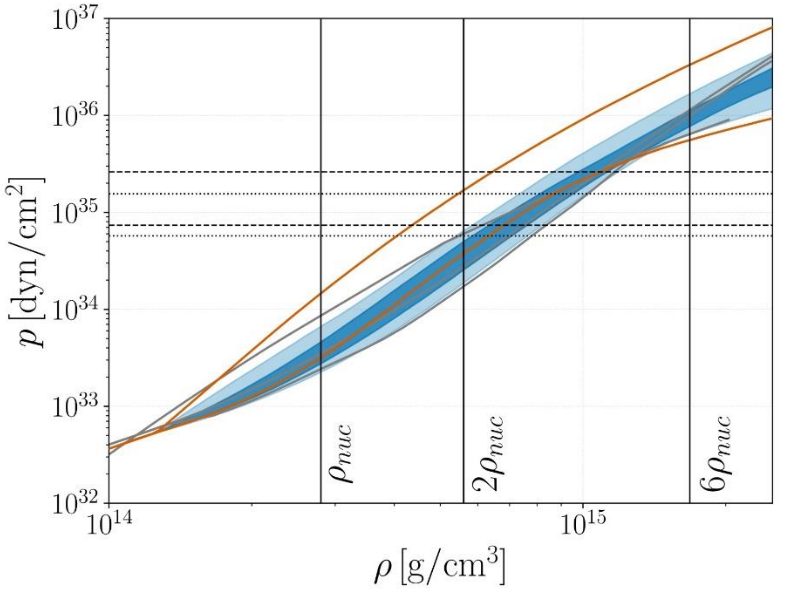

FIG. 2. Marginalized posterior (blue) and prior (orange) for the pressure p as a function of the rest-mass density ρ of the NS interior using the spectral EOS parametrization and imposing a lower limit on the maximum NS mass supported by the EOS of $1.97\,\mathrm{M_\odot}$. The dark (light) blue shaded region corresponds to the 50% (90%) posterior credible level and the orange lines show the 90% prior credible interval. Horizontal lines denote the 90% credible interval for the central pressure of the heavier (dashed) and the lighter (dotted) binary components. Vertical lines correspond to once, twice, and six times the nuclear saturation density. Overplotted in grey are representative EOS models [121, 122, 124], using data taken from [19]; from top to bottom at $2\rho_{\rm nuc}$ we show H4, APR4, and WFF1.

GW170817: Measurements of neutron star radii and equation of state, *The LIGO /Virgo Collaboration*, arXiv:1805.11581v1

GW170817: Constraining the Neutron Star Radius

Impact of Phase Transitions

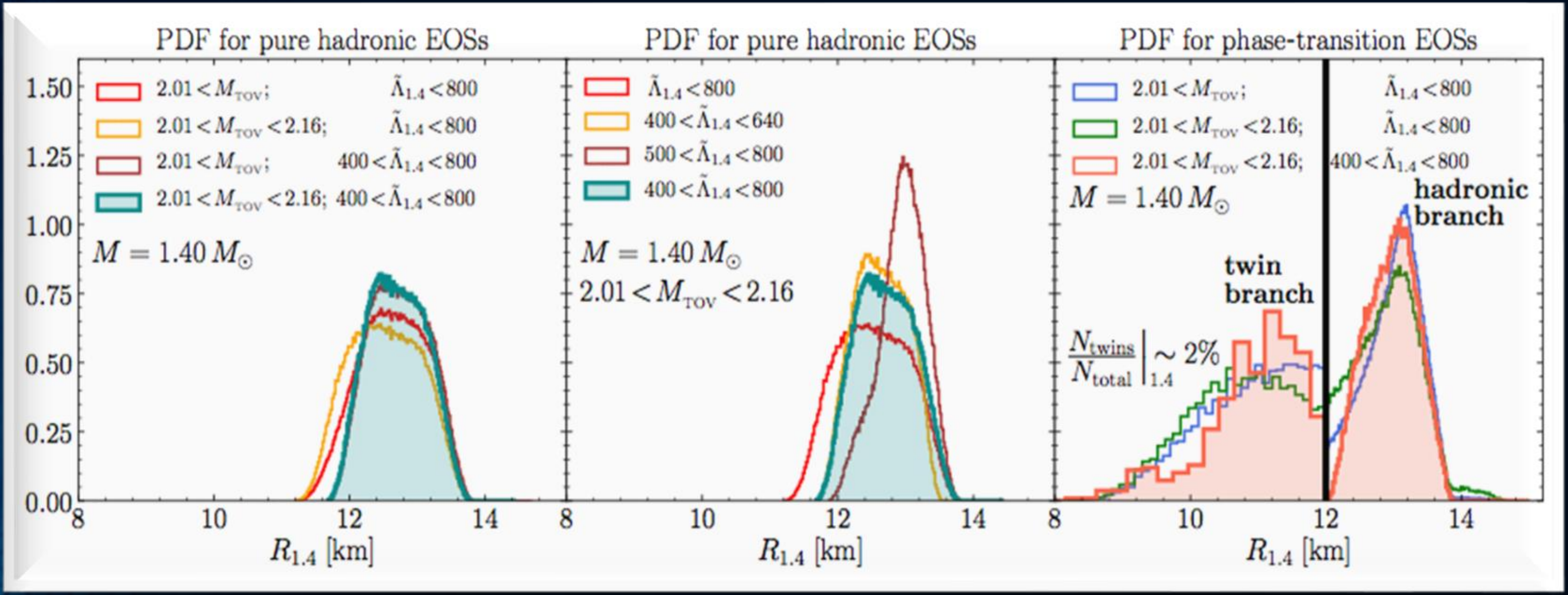

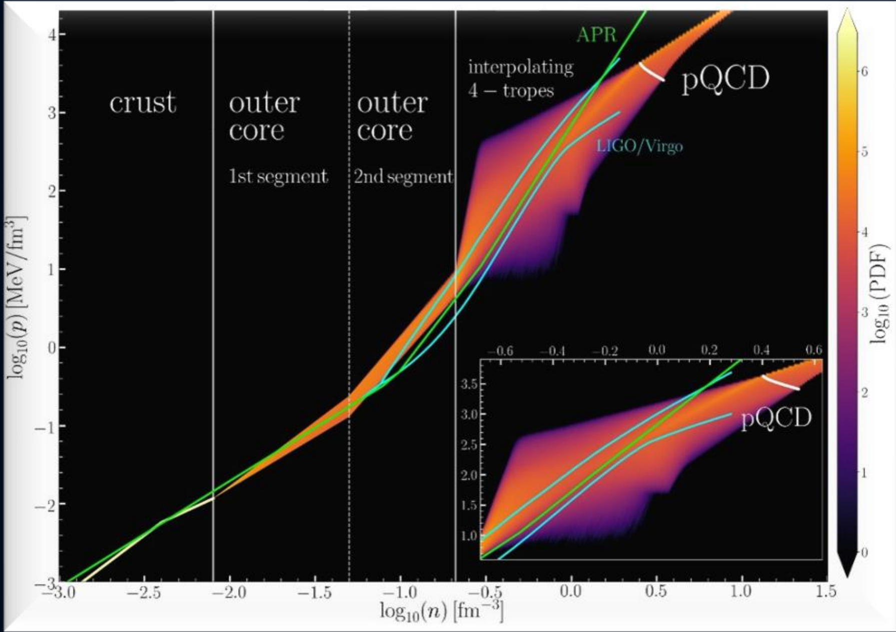

$$12.00 < R_{1.4}/\mathrm{km} < 13.45 \qquad \bar{R}_{1.4} = 12.45\,\mathrm{km}$$

EOSs without phase transitions

$$8.53 < R_{1.4}/\mathrm{km} < 13.74 \qquad \bar{R}_{1.4} = 13.06\,\mathrm{km}$$

EOSs with phase transitions

E.Most, L.Weih, L.Rezzolla, J. Schaffner-Bielich "New constraints on radii and tidal deformabilities of neutron stars from GW170817", arXiv:1803.00549, (accepted in PRL)

See also: De, Finstad, Lattimer, Brown, Berger, Biwer, (2018), arXiv:1804.08583 ; Bauswein, Just, Janka, N. Stergioulas, APJL 850, L34 (2017) ; Fattoyev, Piekarewicz, Horowitz, PRL 120, 172702 (2018) ; Nandi & Char, Astrophys. J. 857, 12 (2018) ; Paschalidis, Yagi, Alvarez-Castillo, Blaschke, Sedrakian, PRD 97, 084038 ; Ruiz, Shapiro, Tsokaros, PRD 97, 021501 (2018) ; Annala, Gorda, Kurkela, Vuorinen, PRL 120, 172703 (2018) ; Raithel, Özel, Psaltis, (2018) arXiv:1803.07687

GW170817: … us

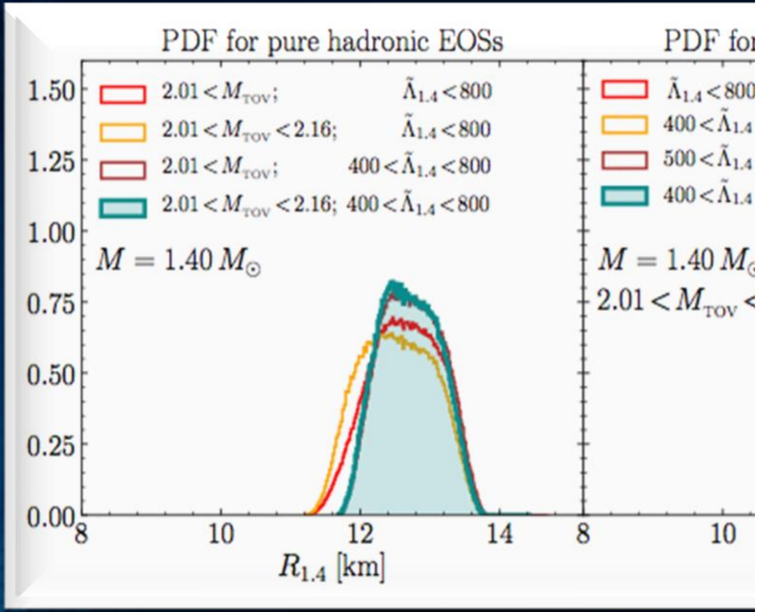

$$12.00 < R_{1.4}/\mathrm{km} < 13.45$$

$$8.53 < R_{1.4}/\mathrm{km} < 13.74 \qquad \bar{R}$$

Reference	R_i [km]
Without a phase transition	
Bauswein et al. [42]	$10.68^{+0.15}_{-0.03} \leq R_{1.6}$
Most et al. [51]	$12.00 \leq R_{1.4} \leq 13.45$
Burgio et al. [54]	$11.8 \leq R_{1.5} \leq 13.1$
Tews et al. [55]	$11.3 \leq R_{1.4} \leq 13.6$
De et al. [56]	$8.9 \leq R_{1.4} \leq 13.2$
LIGO/Virgo [57]	$10.5 \leq R_{1.4} \leq 13.3$
With a phase transition	
Annala et al. [46]	$R_{1.4} \leq 13.6$
Most et al. [51]	$8.53 \leq R_{1.4} \leq 13.74$
Burgio et al. [54]	$R_{1.5} = 10.7$
Tews et al. [55]	$9.0 \leq R_{1.4} \leq 13.6$
This work	
NS	$R_{1.4} = 13.11$
HS `Model-2`	$12.9 \leq R_{1.4} \leq 13.11$
HS_T `Model-1`	$10.1 \leq R_{1.4} \leq 12.9$
HS_T `Model-2`	$10.4 \leq R_{1.4} \leq 11.9$

TABLE II. Constraints on the radius of neutron stars from GW170817 for models without a phase transition (top), works considering the possibility of a transition to quark matter (middle) and for EOSs of *Category III* in the present work (bottom).

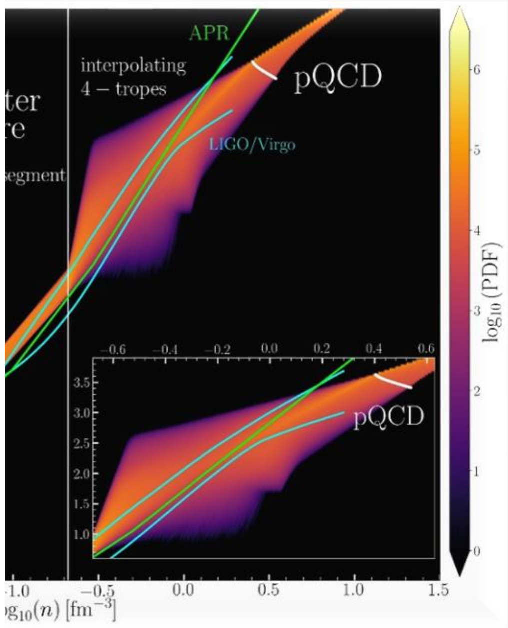

…t, L.Weih, L.Rezzolla, J. …fner-Bielich "New …aints on radii and tidal …mabilities of neutron …rom GW170817", …1803.00549, …pted in PRL)

See also: De, Finstad, Lattimer, Brown, Berger, Biwe… …v, Piekarewicz, Horowitz, PRL 120, 172702 (2018) ; Nandi & Char, Astrophys. J. 857, 12 (201… …ros, PRD 97, 021501 (2018) ; Annala, Gorda, Kurkela, Vuorinen, PRL 120, 172703 (201…

GW170817: Constraining the maximum mass of Neutron Stars

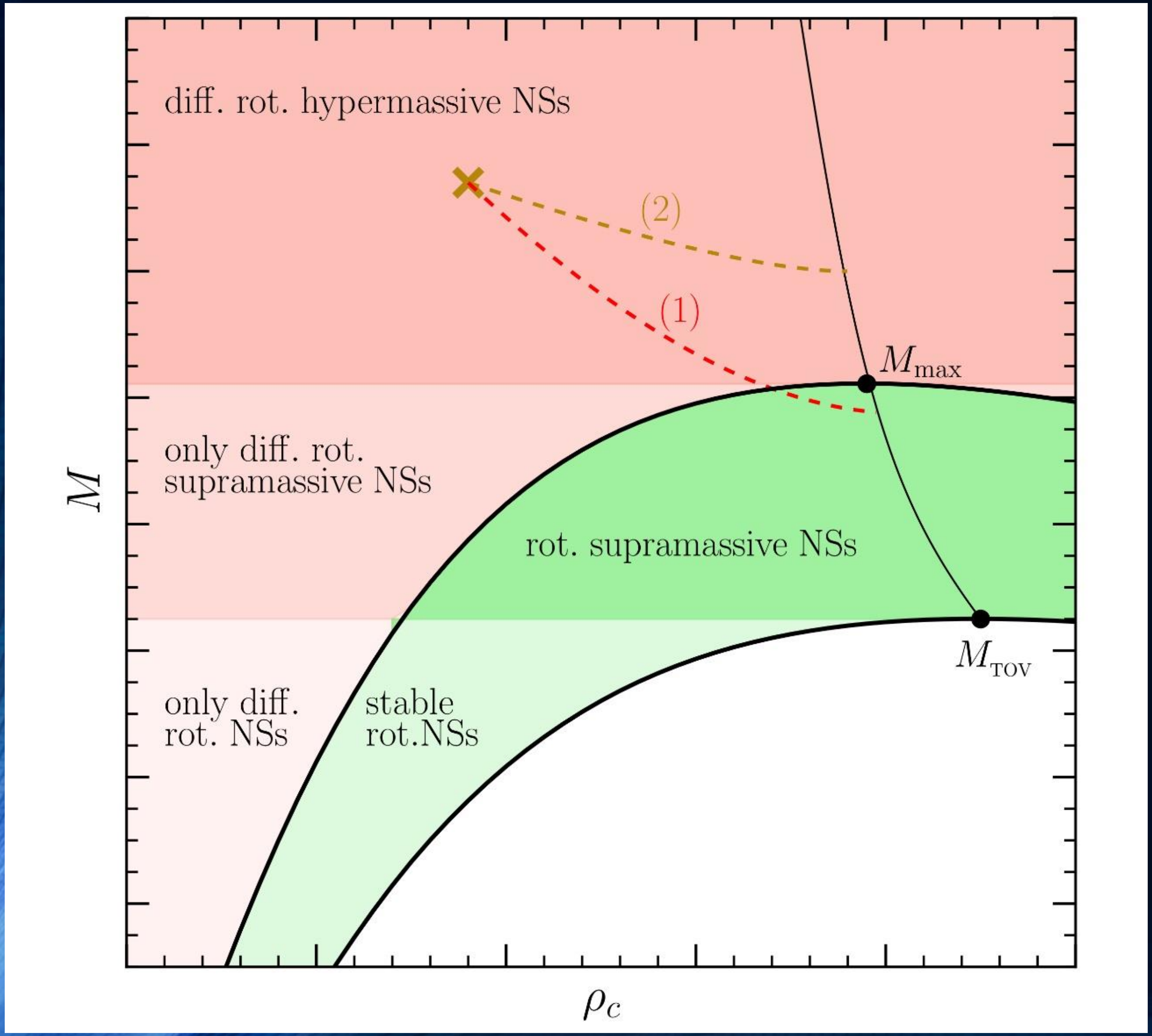

The highly differentially rotating hypermassive/supramassive neutron star will spin down and redistribute its angular momentum (e.g. due to viscosity effects, magnetic braking). After ~1 second it will cross the stability line as a uniformly rotating supramassive neutron star (close to M_{max}) and collapse to a black hole. Parts of the ejected matter will fall back into the black hole producing the gamma-ray burst.

L.Rezzolla, E.Most, L.Weih, "Using Gravitational Wave Observations and Quasi-Universal Relations to constrain the maximum Mass of Neutron Stars",The Astrophysical Journal Letters 852, L25 (2018):
$2.01 \pm 0.04 < M_{TOV} < 2.16 \pm 0.17$

See also: S.Lawrence et al. ,APJ808,186, 2015
Margalit & Metzger, The Astrophysical Journal Letters 850, L19 (2017): $M_{TOV} < 2.17$ (90%)
Zhou, Zhou, Li, PRD 97, 083015 (2018)
Ruiz, Shapiro, Tsokaros, PRD 97,021501 (2018)

Was geschieht zwischen der Kollision und dem Kollaps zum schwarzen Loch?

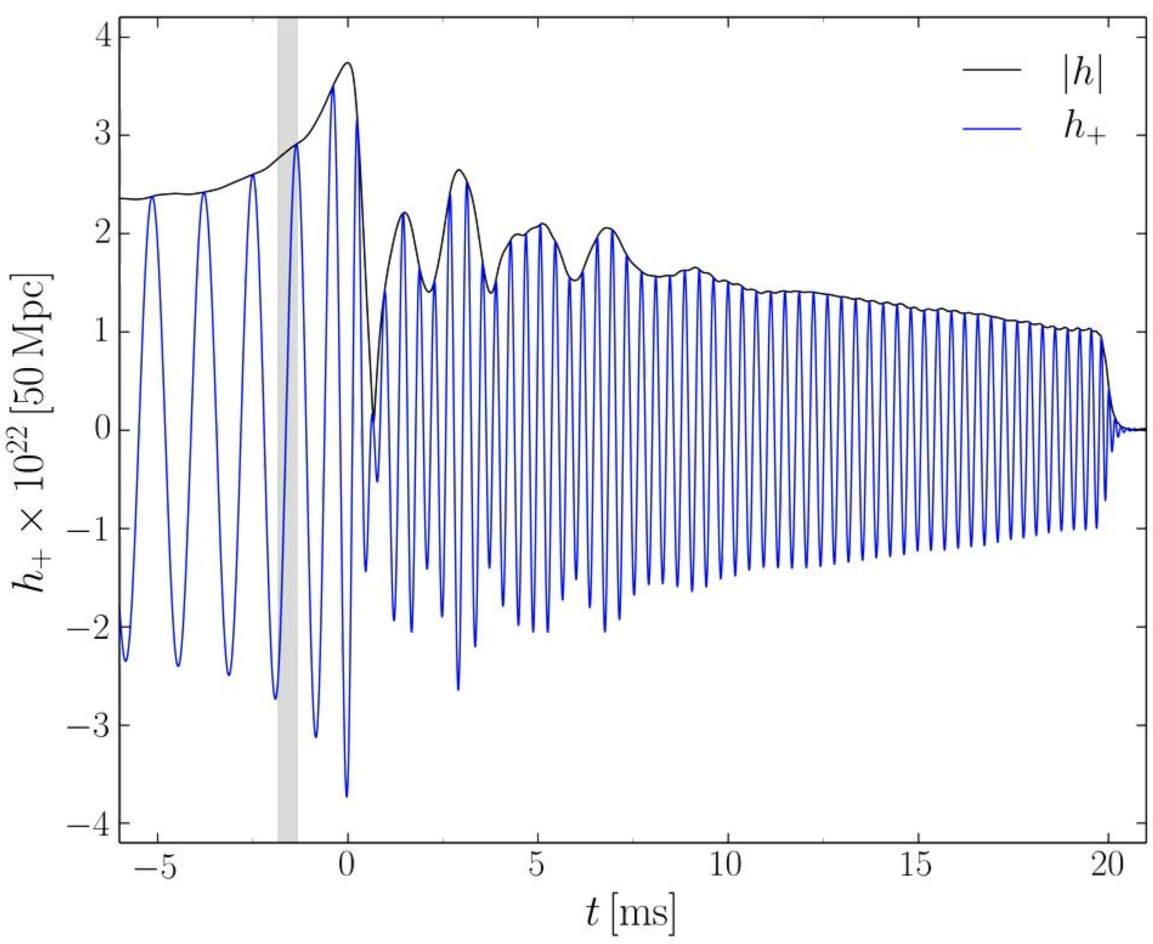

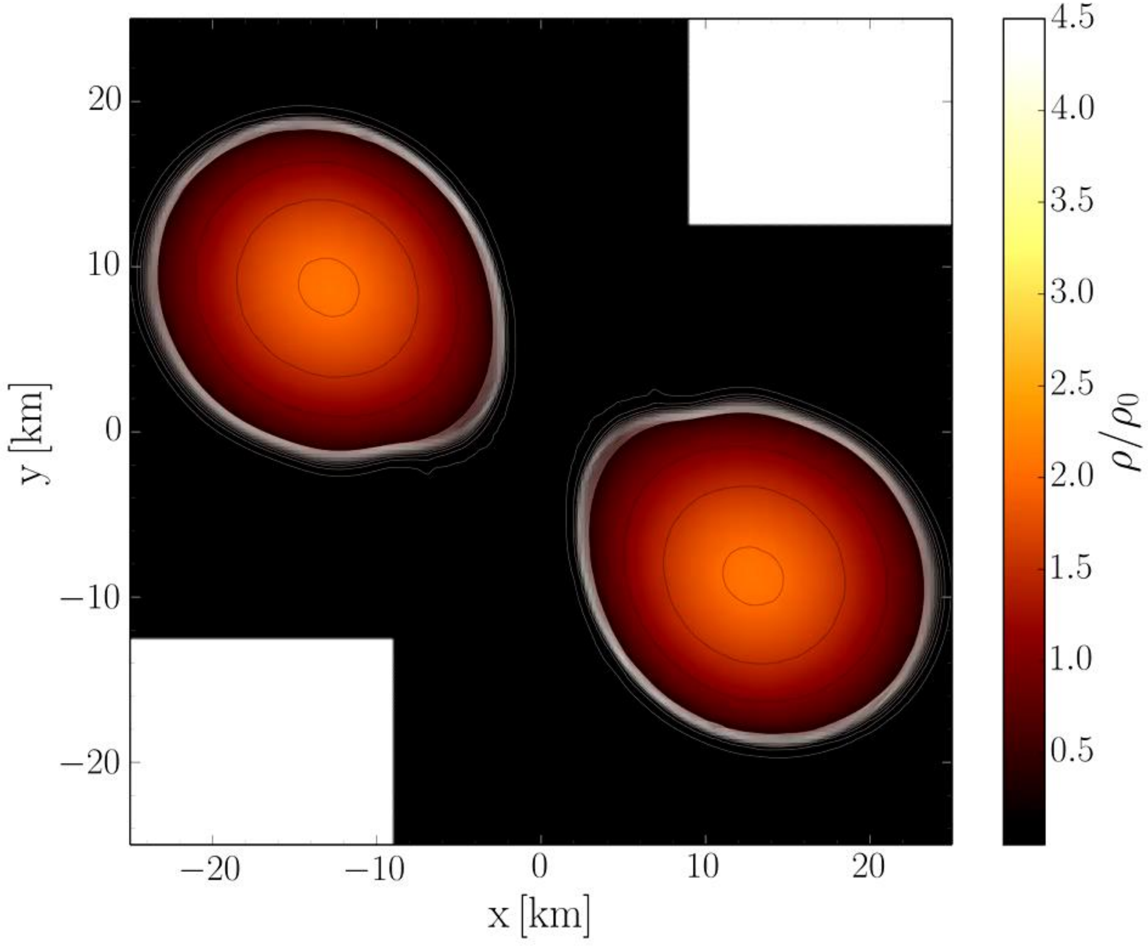

Amplitude der emittierten Gravitationswelle

Dichteprofil in der äquatorialen Ebene

The different Phases of a Binary Compact Star Merger Event

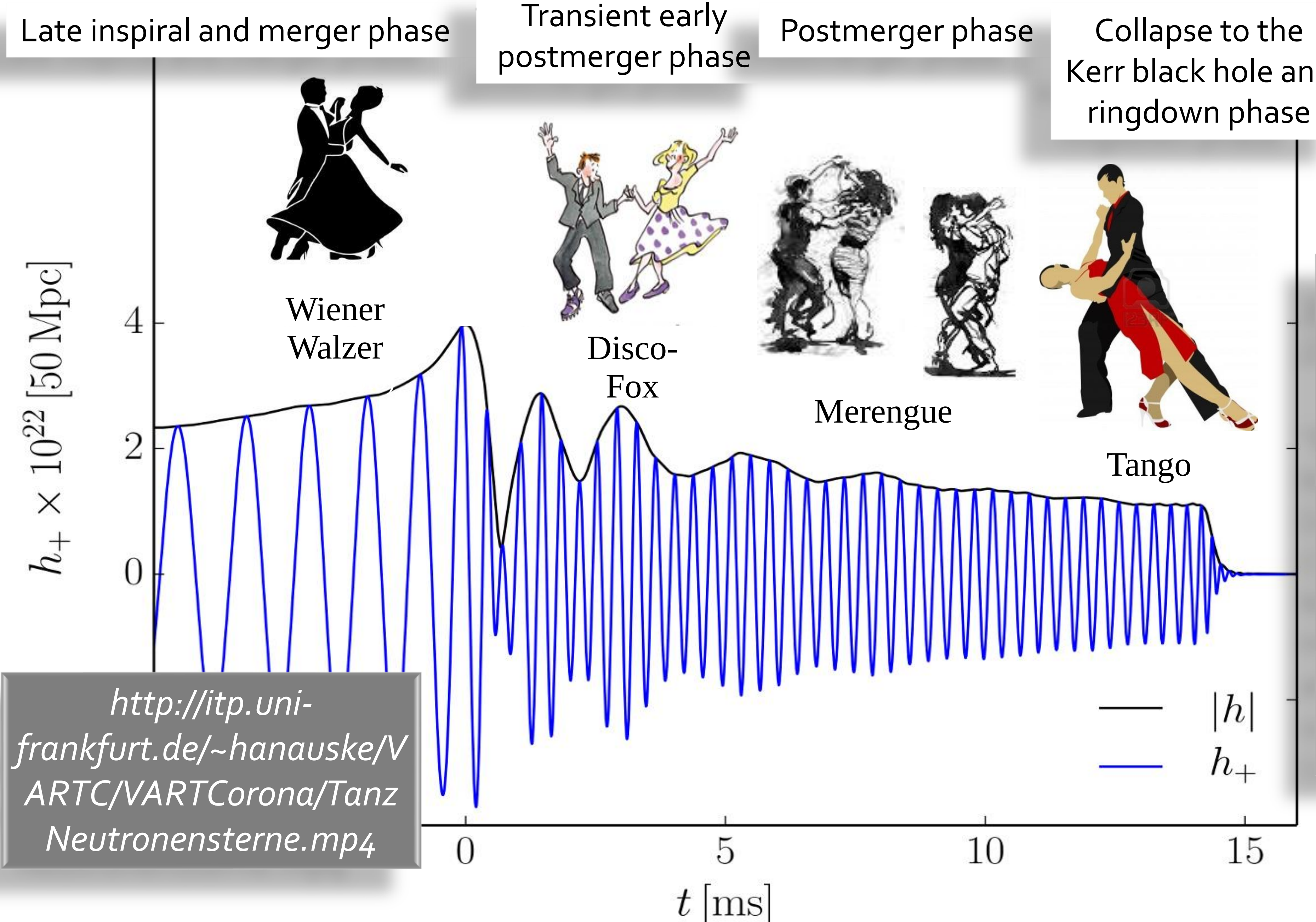

http://itp.uni-frankfurt.de/~hanauske/VARTC/VARTCorona/TanzNeutronensterne.mp4

Wy exactly these dances?
Details in

"Binary Compact Star Mergers and the Phase Diagram of Quantum Chromodynamics", Matthias Hanauske and Horst Stöcker, Discoveries at the Frontiers of Science, 107-132; Springer, Cham (2020)

The different Phases during the Postmergerphase of the HMNS

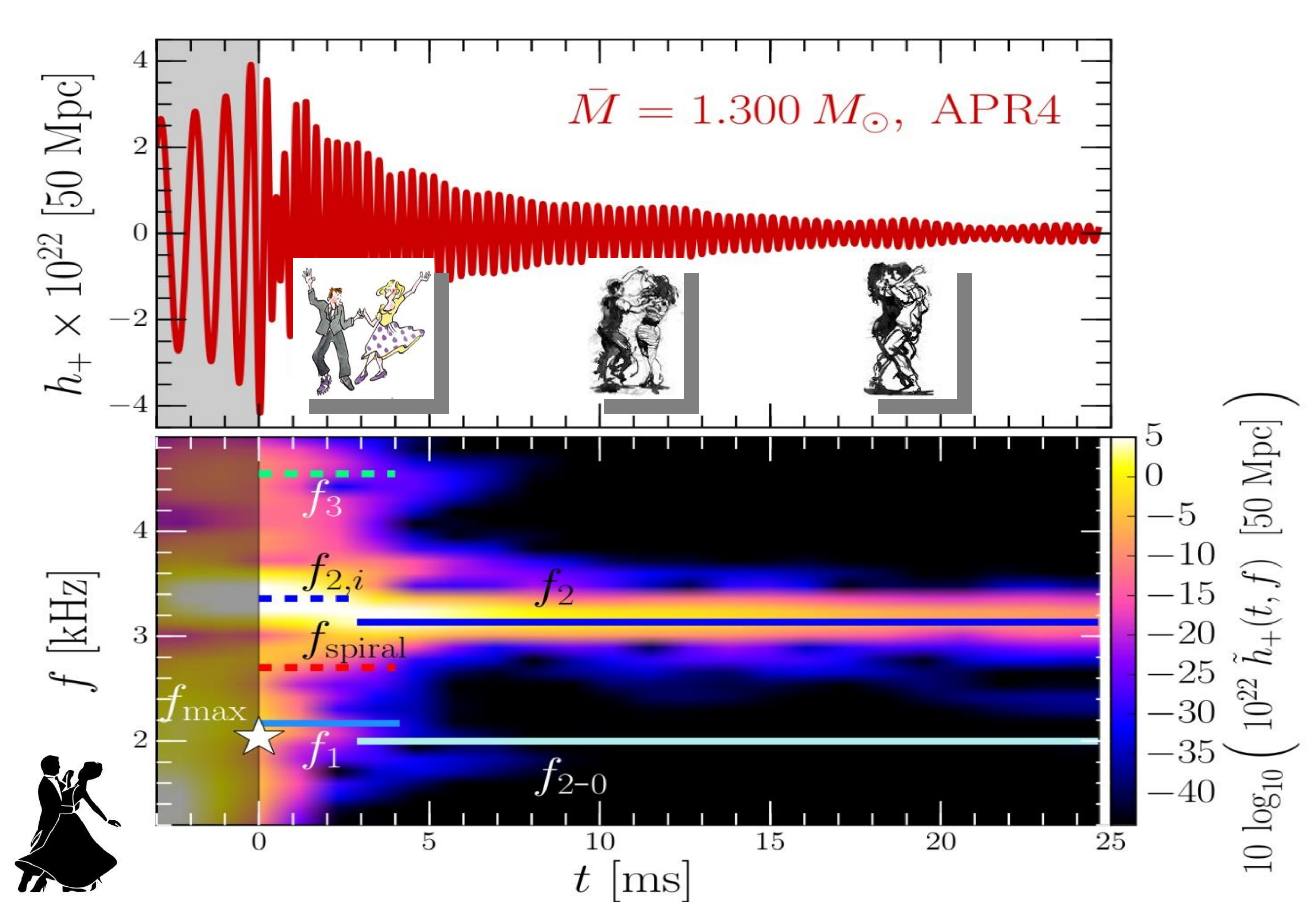

Pulsare :=
Rotierende Neutronensterne mit starkem Magnetfeld

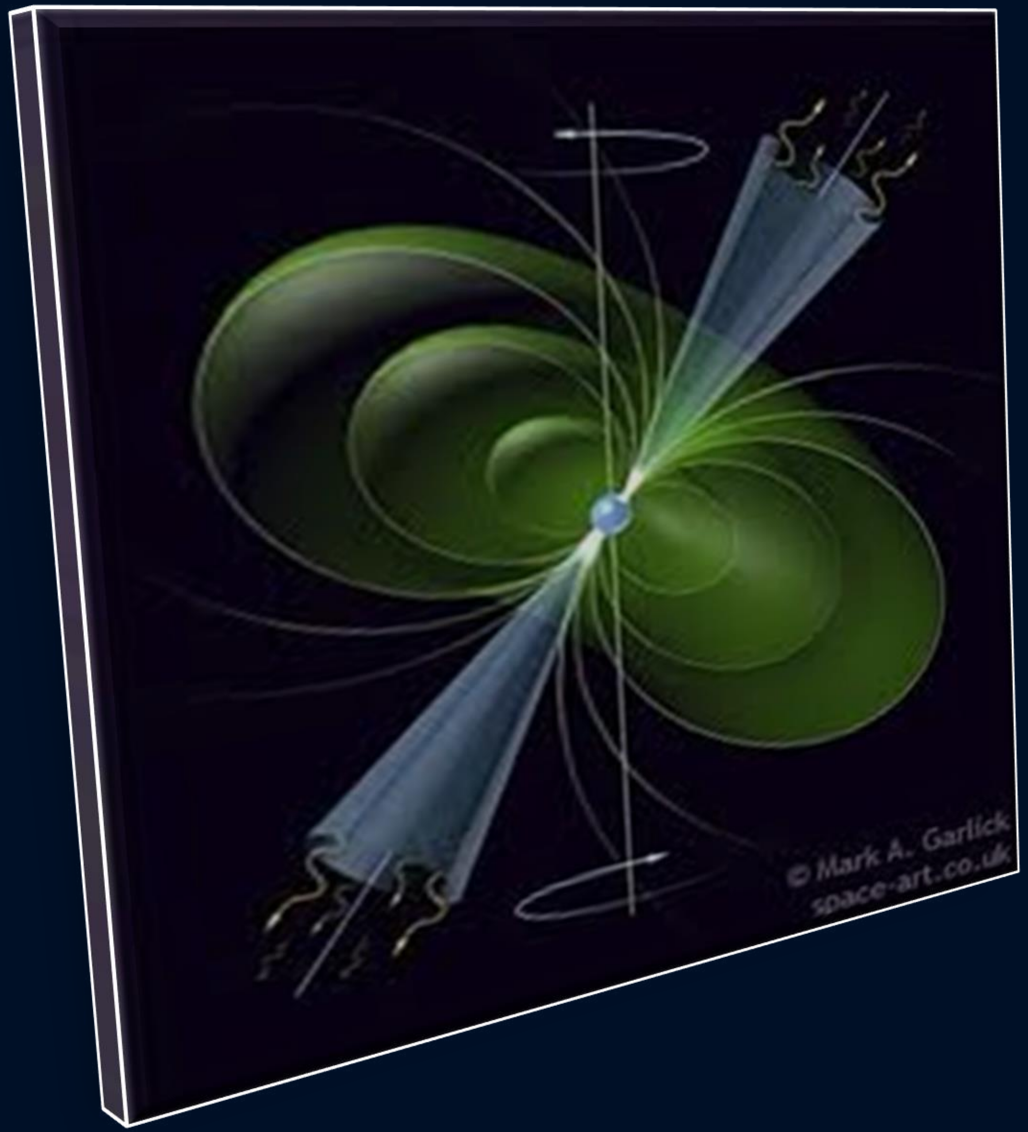

In den letzten 50 Jahren konnten mittels Radioteleskopen ca. 3000 rotierende Neutronensterne (Pulsare) gefunden werden.

Der erste Pulsar wurde im Jahre 1967 entdeckt (PSR 1919+21, Bell)

Man unterscheidet Sekundenpulsare und Millisekunden-Pulsare

PSR B0329+54 (0.715 s)

PSR B0531+21 (33.5 ms)

PSR B1937+21 (1.56 ms)

Binäre Neutronenstern Systeme

Zurzeit kennt man ca. 25 binäre Neutronenstern Systeme

Beispiel:
Der **Double Pulsar**
(PSR J0737-3039A/B):
Entdeckt im Jahre 2003
Eccentricity: 0.088
Pulsar A: P=23 ms, M=1.3381(7)
Pulsar B: P=2.7 s, M=1.2489(7)

Abstand zwischen den Sternen nur 800,000 km
Orbitale Periode: 147 Minuten

Abstand verkleinert sich langsam aufgrund der Abstrahlung von Gravitationswellen

Die beiden Neutronensterne werden erst in 85 Millionen Jahren kollidieren

Kramer, Wex, Class. Quantum Grav. 2009

McGill NCS Multimedia Services Animation by Daniel Cantin, DarwinDimensions)

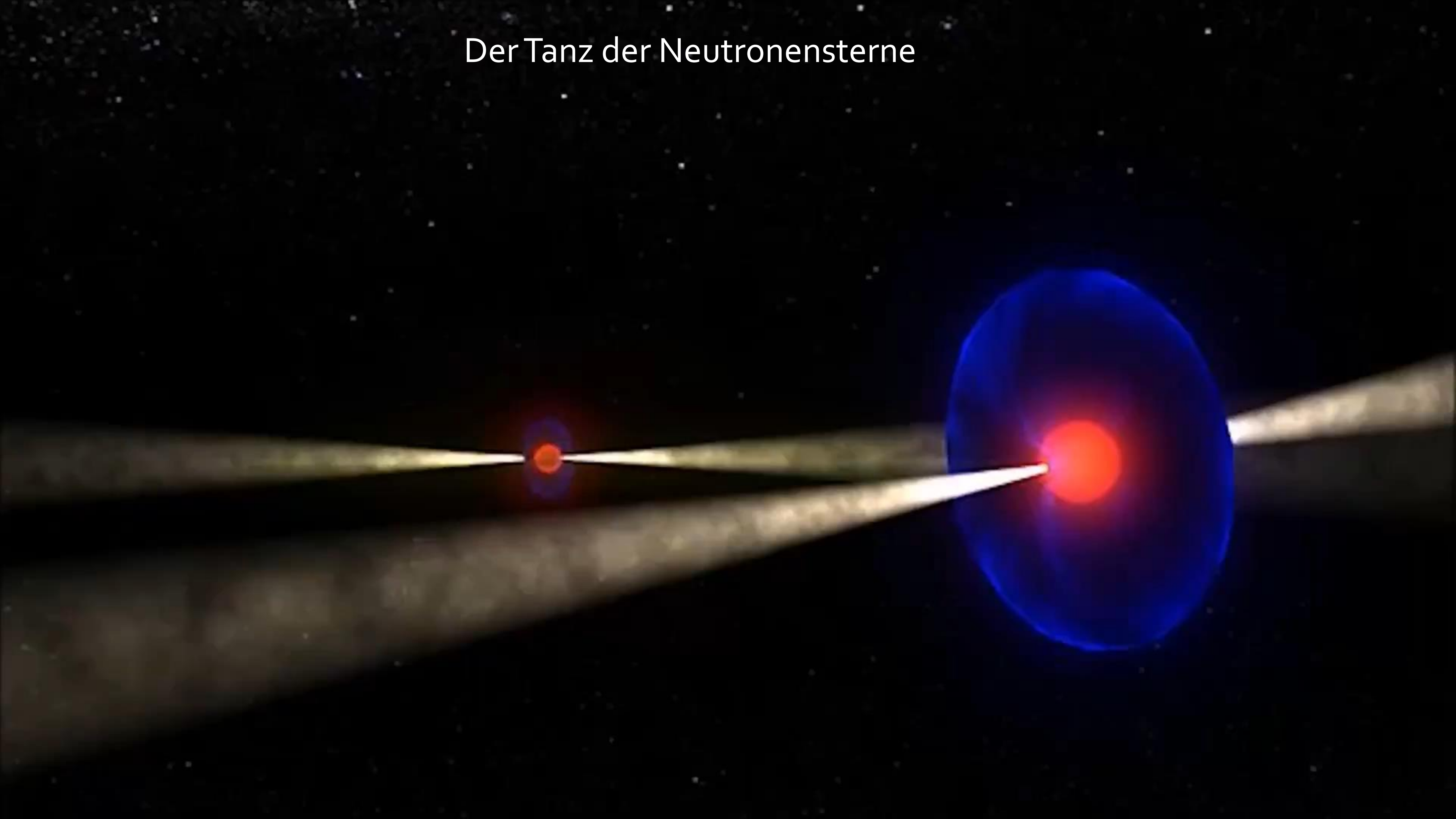
Der Tanz der Neutronensterne

Der Tanz der Neutronensterne in VR
(siehe Link auf der Homepage)

Tanz der Neutronensterne

The Co-Rotating Frame

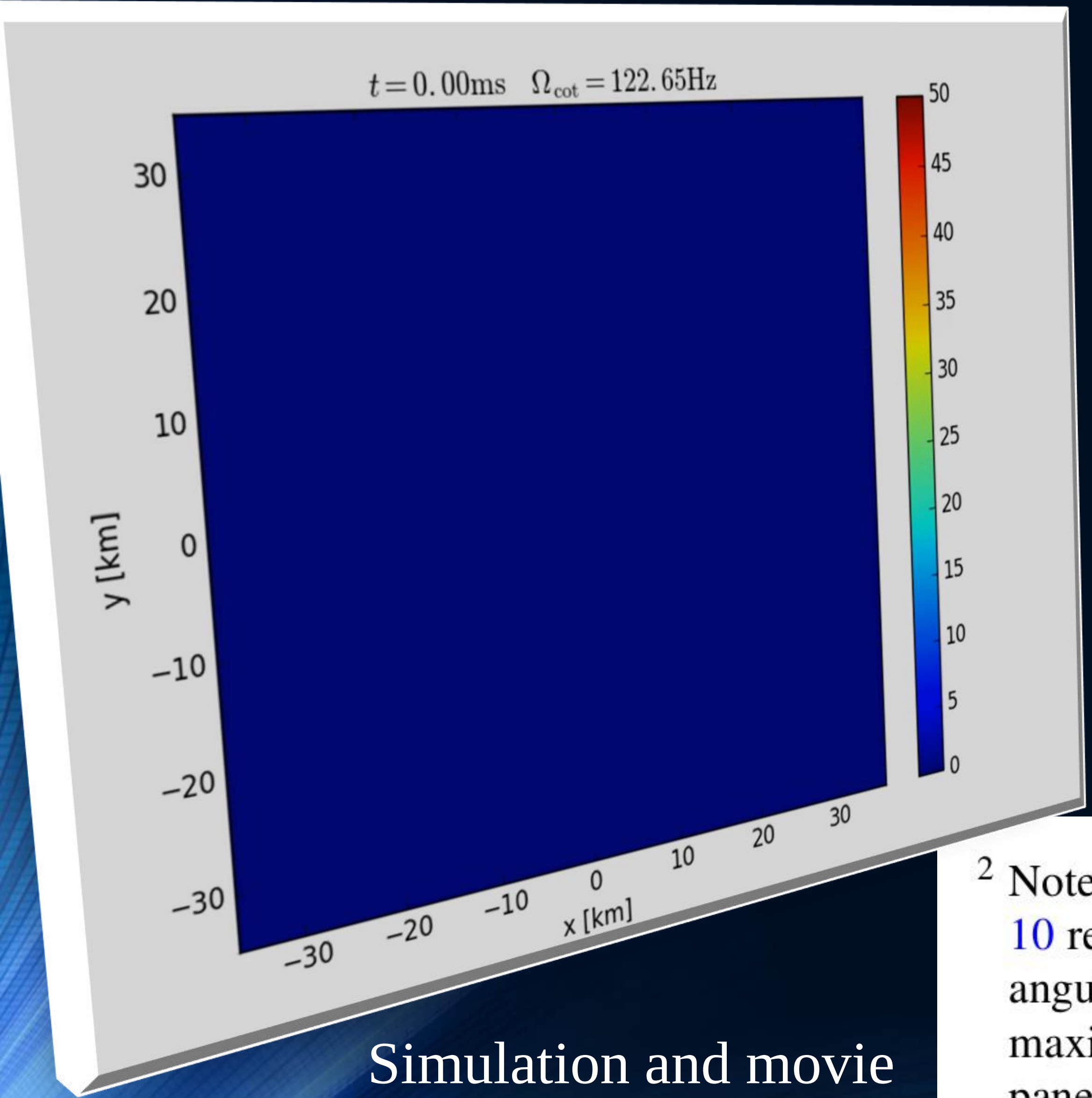

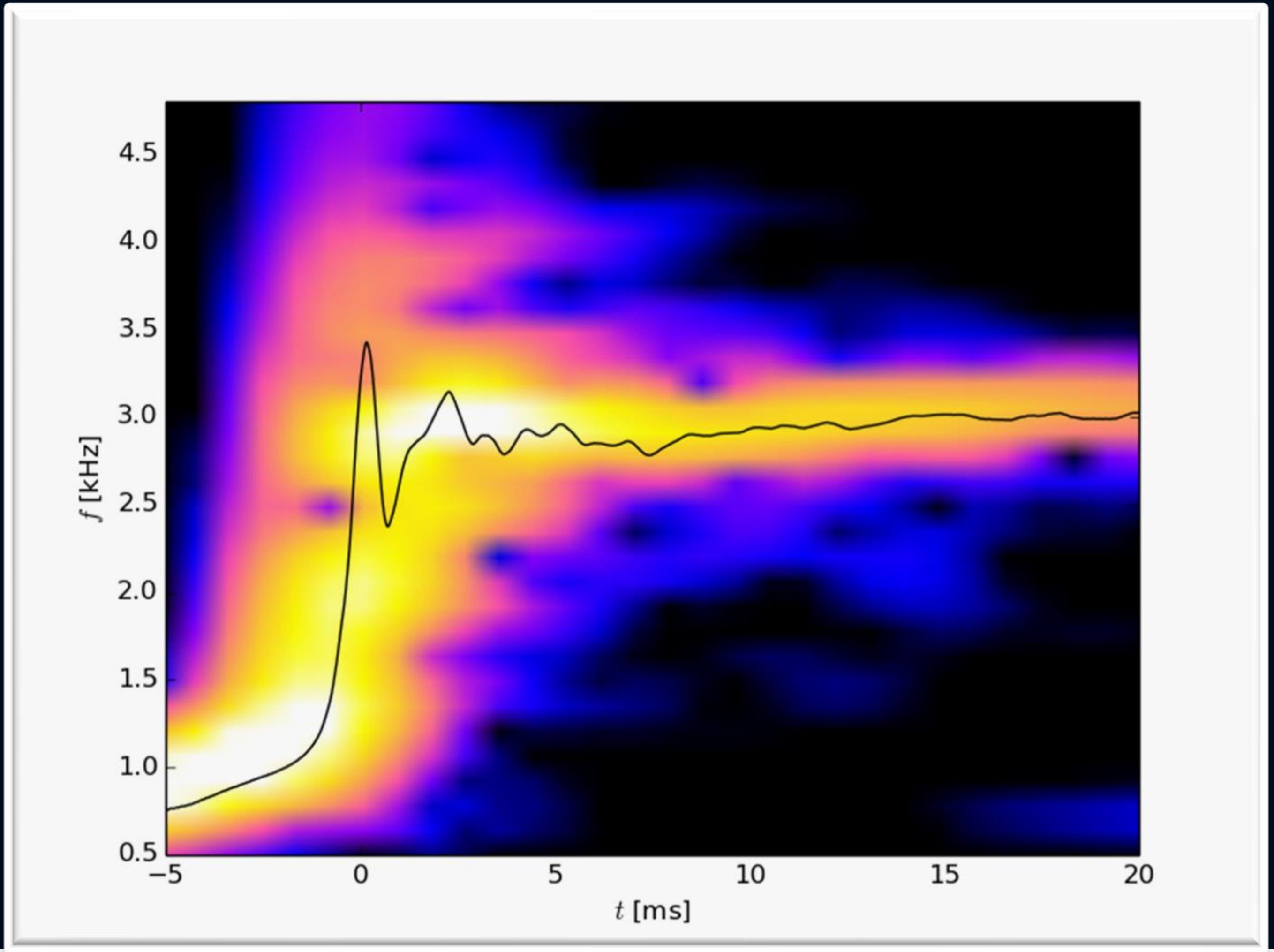

Simulation and movie
has been produced by Luke Bovard

[2] Note that the angular-velocity distribution in the lower central panel of Fig. 10 refers to the corotating frame and that this frame is rotating at half the angular frequency of the emitted gravitational waves, $\Omega_{\rm GW}$. Because the maximum of the angular velocity $\Omega_{\rm max}$ is of the order of $\Omega_{\rm GW}/2$ (cf. left panel of Fig. 12), the ring structure in this panel is approximately at zero angular velocity.

Density and Temperature Evolution inside the HMNS

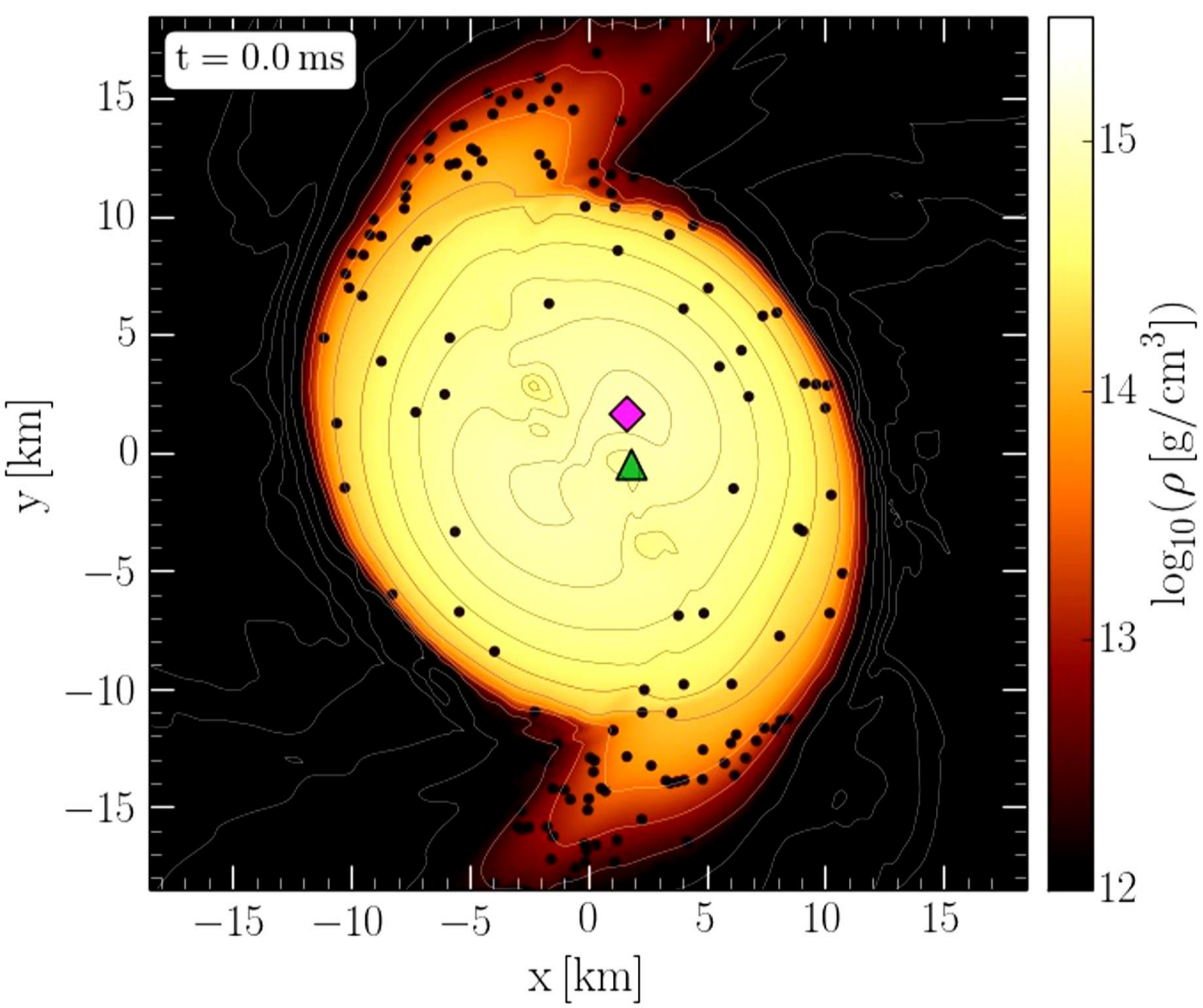

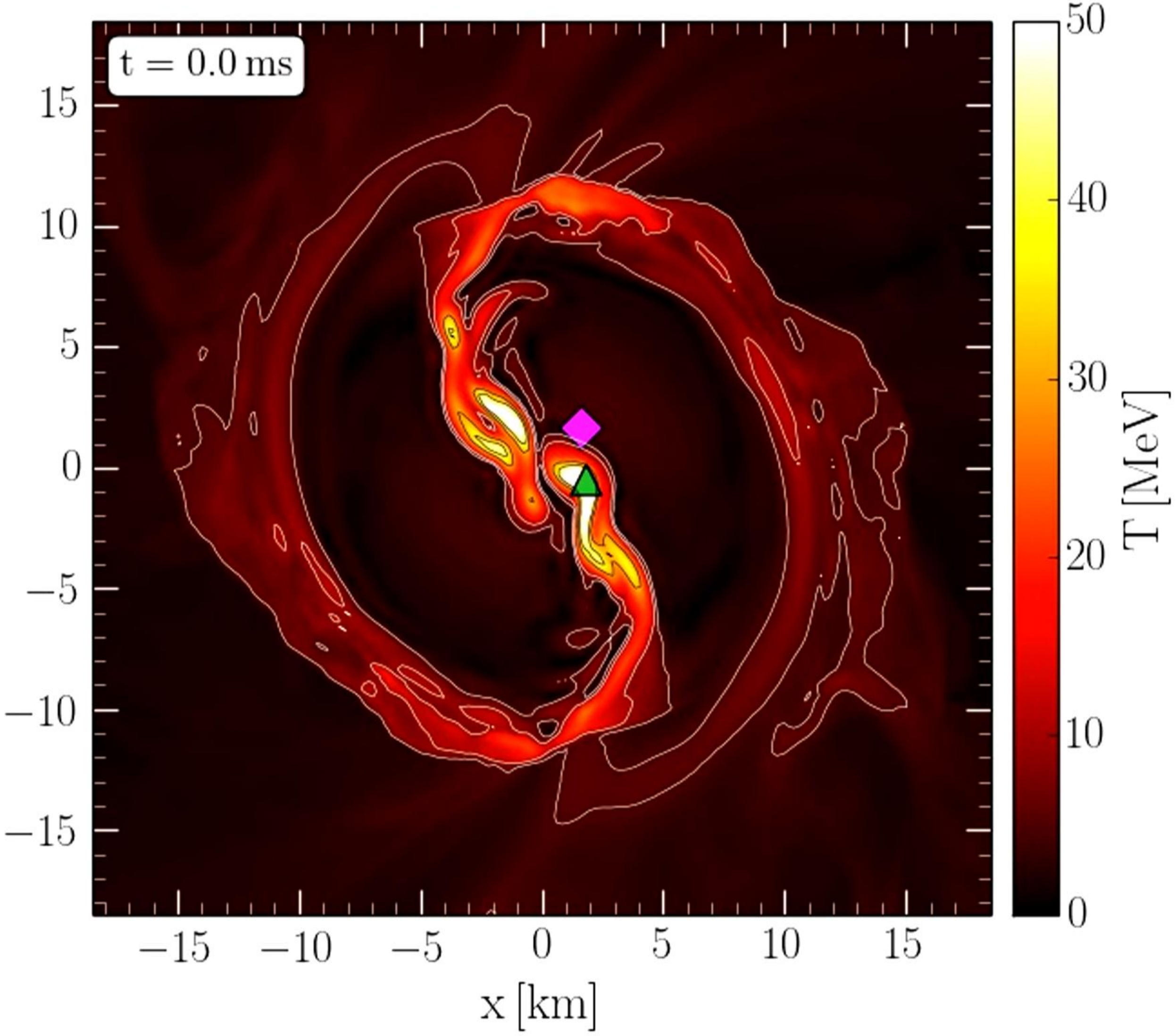

Rest mass density on the equatorial plane

Temperature on the equatorial plane

Binary Neutron Star Mergers in the QCD Phase Diagram

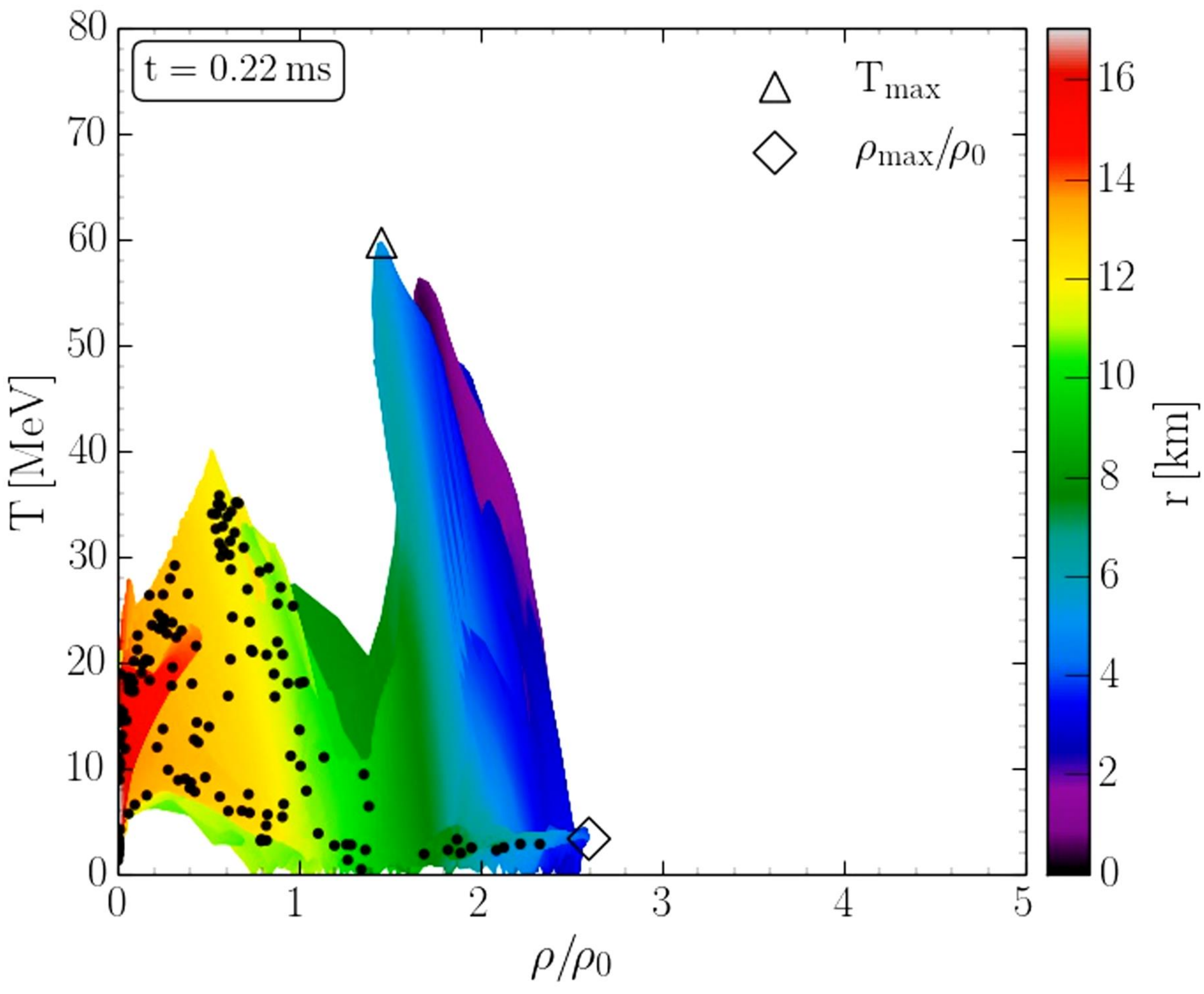

Evolution of hot and dense matter inside the inner area of a hypermassive neutron star simulated within the LS220 EOS with a total mass of M_{total}=2.7 M_{solar} in the style of a (T- ρ) QCD phase diagram plot

The color-coding indicate the radial position r of the corresponding (T- ρ) fluid element measured from the origin of the simulation (x , y) = (0 , 0) on the equatorial plane at z = 0.

The open triangle marks the maximum value of the temperature while the open diamond indicates the maximum of the density.

The Angular Velocity in the (3+1)-Split

The angular velocity Ω in the (3+1)-Split is a combination of the lapse function α , the ϕ-component of the shift vector β^{ϕ} and the 3-velocity v^{ϕ} of the fluid (spatial projection of the 4-velocity **u**):

(3+1)-decomposition of spacetime:

$$g_{\mu\nu} = \begin{pmatrix} -\alpha^2 + \beta_i \beta^i & \beta_i \\ \beta_i & \gamma_{ij} \end{pmatrix}$$

$$\Omega(x, y, z, t) = \frac{u^{\phi}}{u^{t}} = \alpha\, v^{\phi} - \beta^{\phi}$$

Angular velocity Ω

Lapse function α

Φ-component of 3-velocity v^{φ}

Frame-dragging β^{φ}

Focus: Inner core of the differentially rotating HMNS

M. Shibata, K. Taniguchi, and K. Uryu, Phys. Rev. D 71, 084021 (2005)
M. Shibata and K. Taniguchi, Phys. Rev. D 73, 064027 (2006)
F. Galeazzi, S. Yoshida and Y. Eriguchi, A&A 541, p. A156 (2012)
W. Kastaun and F. Galeazzi, Phys. Rev. D 91, p. 064027 (2015)

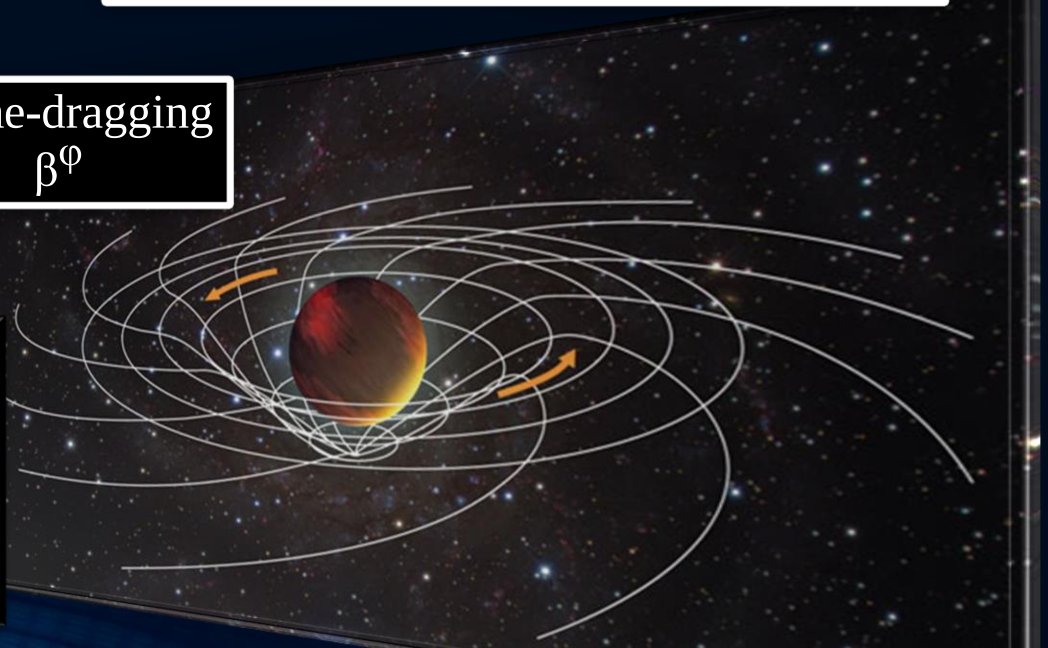

Temperature Angular Velocity

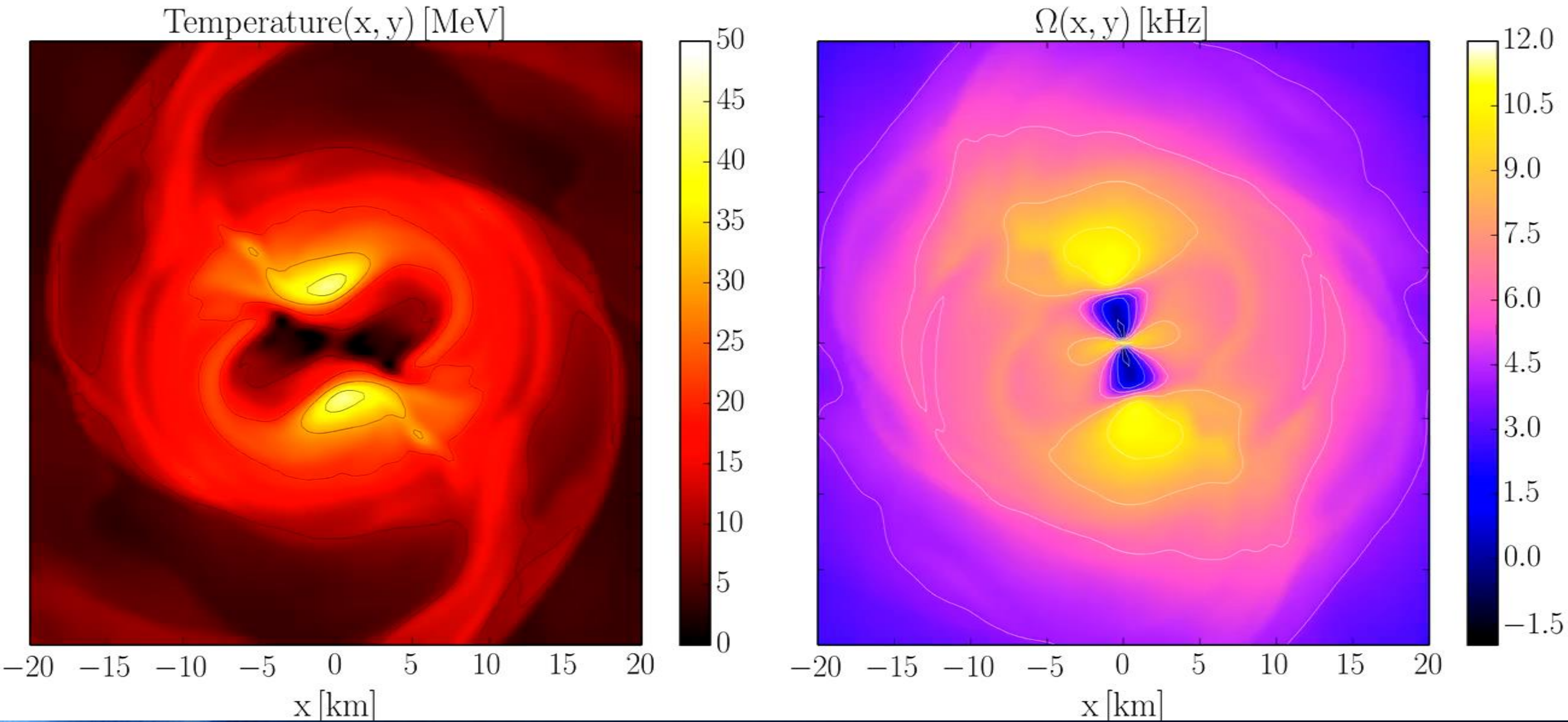

EOS: LS200 , Mass: 1.32 M_{solar} , simulation with Pi-symmetry

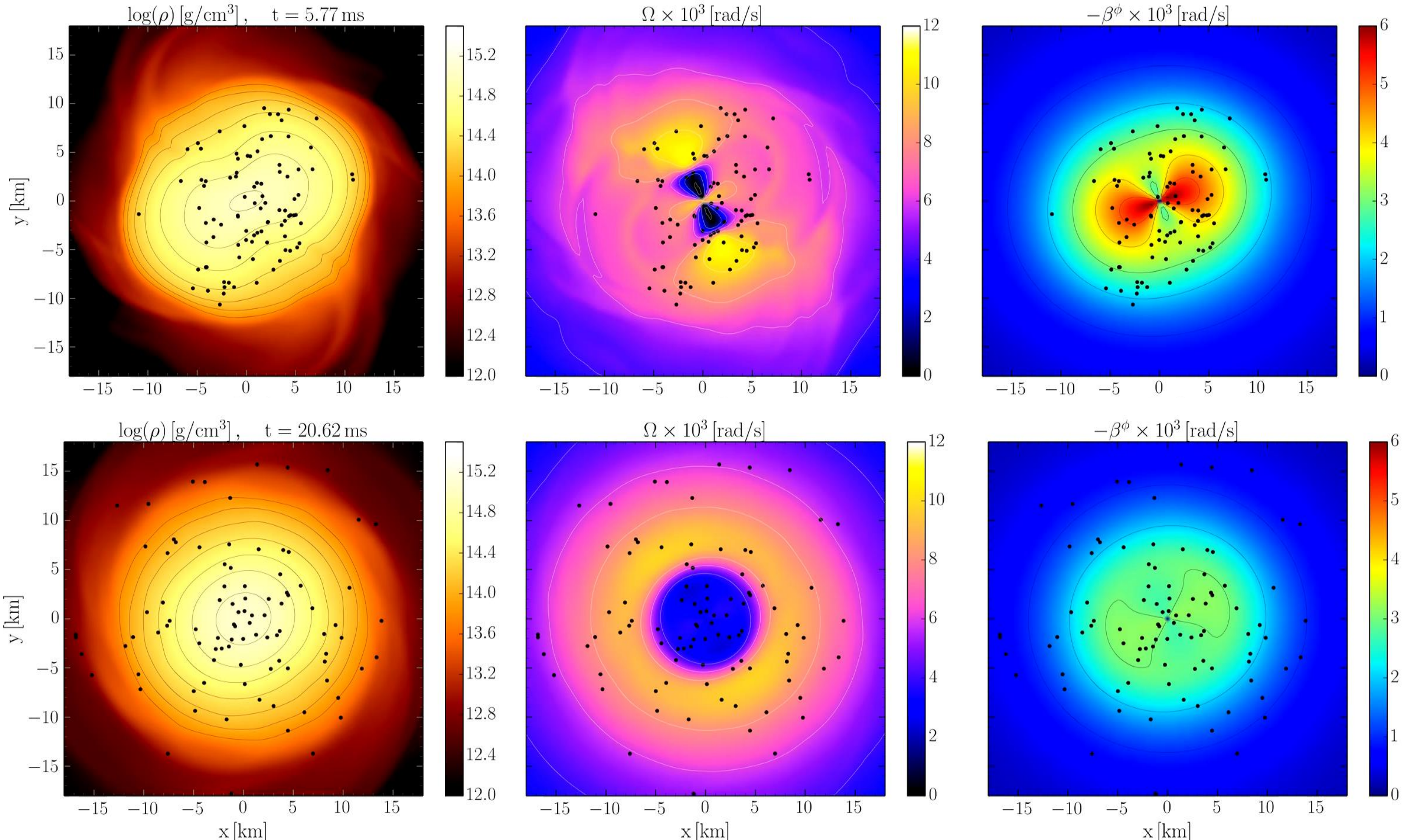

$\log(\rho)\,[\mathrm{g/cm^3}]\,, \quad t = 5.77\,\mathrm{ms}$
$\Omega \times 10^3\,[\mathrm{rad/s}]$
$-\beta^\phi \times 10^3\,[\mathrm{rad/s}]$
$\log(\rho)\,[\mathrm{g/cm^3}]\,, \quad t = 20.62\,\mathrm{ms}$
$\Omega \times 10^3\,[\mathrm{rad/s}]$
$-\beta^\phi \times 10^3\,[\mathrm{rad/s}]$
y [km]
x [km]

Time-averaged Rotation Profiles of the HMNSs

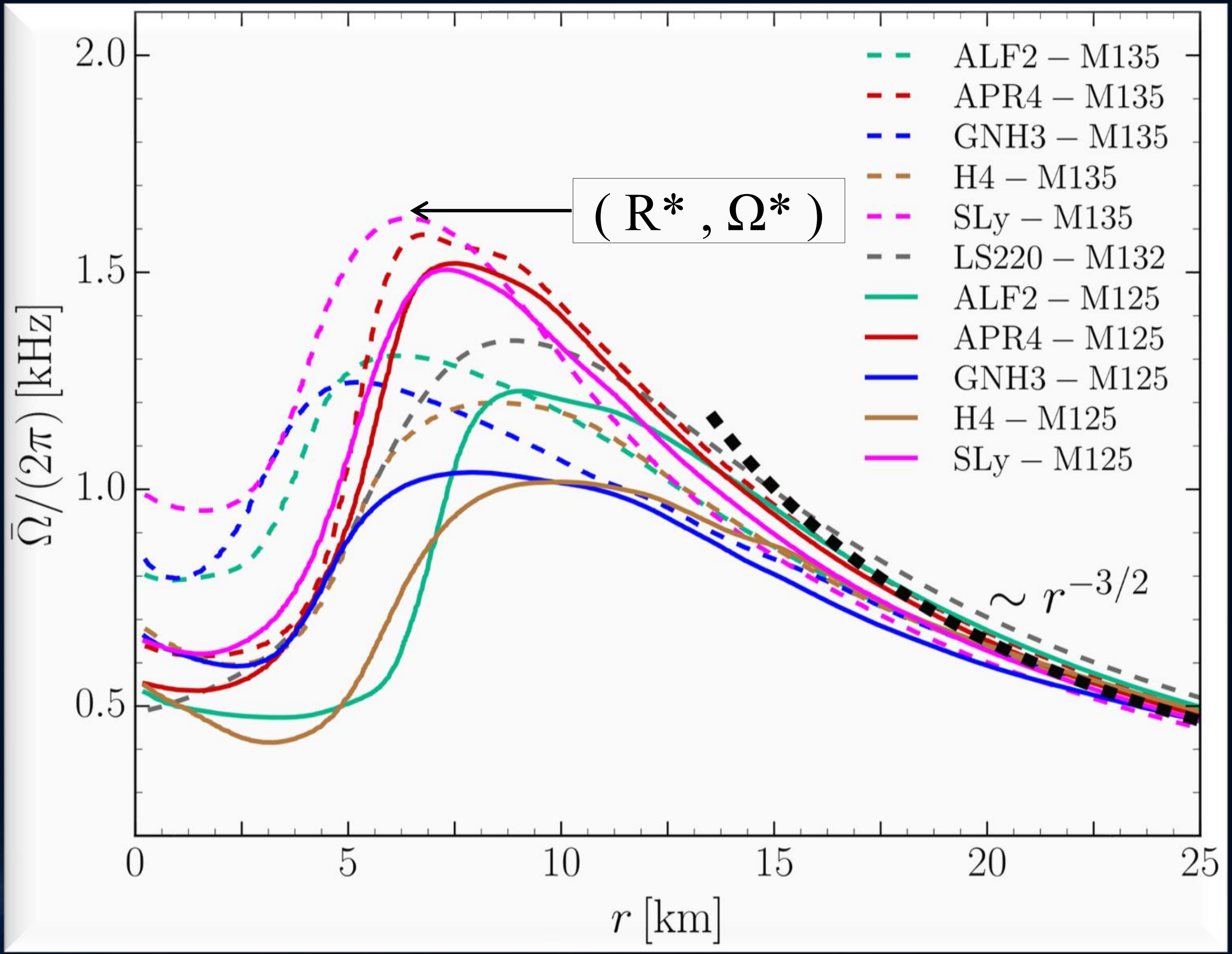

Soft EoSs:
Sly
APR4

Stiff EoSs:
GNH3
H4

Time-averaged rotation profiles for different EoS
Low mass runs (solid curves), high mass runs (dashed curves).

Hanauske, et.al. PRD, 96(4), 043004 (2017)

files of the HMNSs

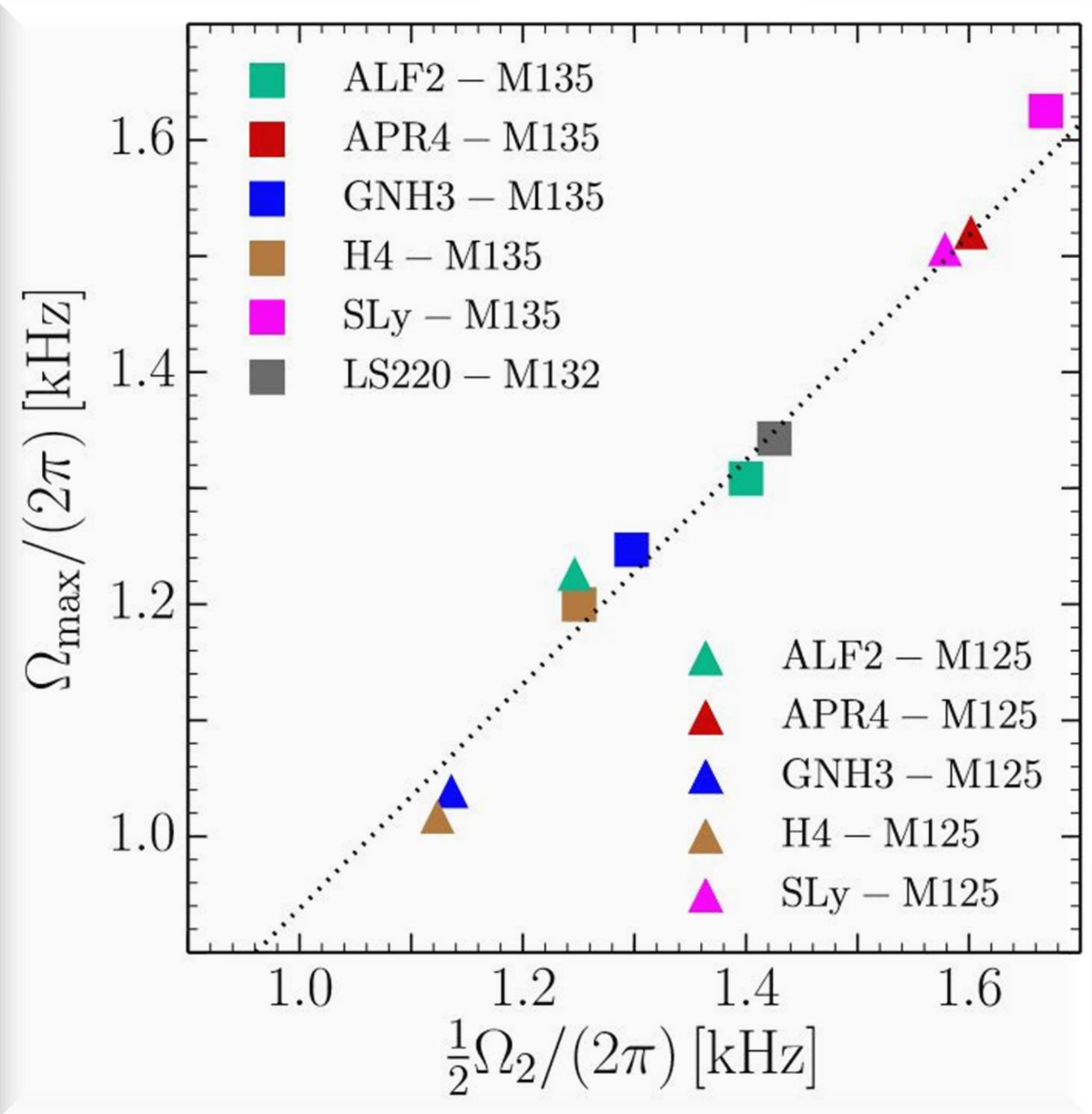

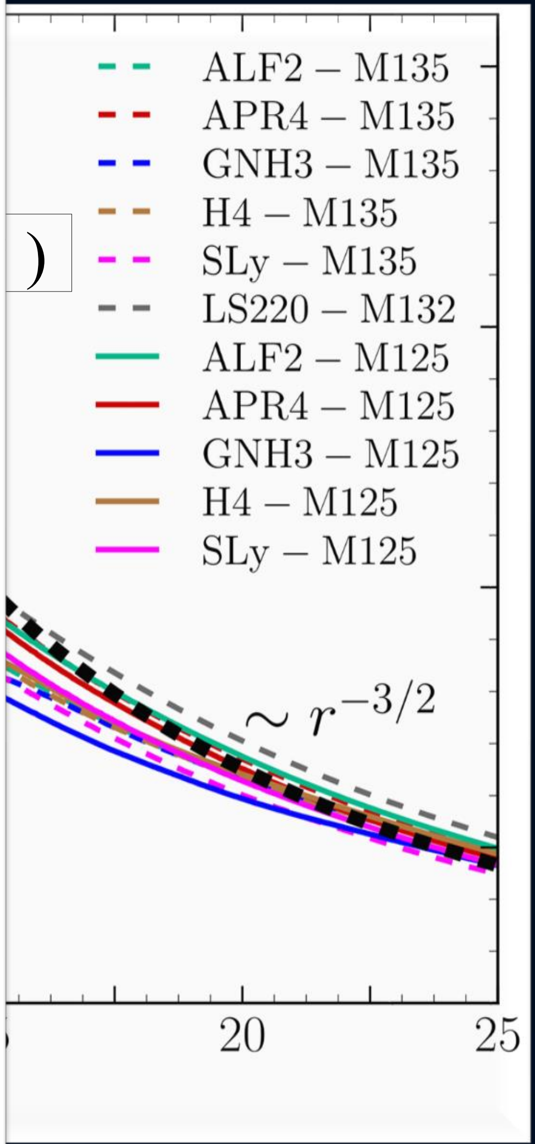

<u>Soft EoSs</u>:
Sly
APR4

<u>Stiff EoSs</u>:
GNH3
H4

S

Hanauske, et.al. PRD, 96(4), 043004 (2017)

lashed curves).

Can we detect the quark-gluon plasma with gravitational waves?

- Gravitational-wave signatures of the hadron-quark ph compact star mergers
  - *Signatures within the late inspiral phase (premerger signals)*
    - Constraining twin stars with GW170817; G Montana, L Tolós, M Han 99 (10), 103009 (2019)
  - *Signatures within the post-merger phase evolution*
    - **Phase-transition triggered collapse scenario**
      Signatures of quark-hadron phase transitions in general-relativistic neu Papenfort, V Dexheimer, M Hanauske, S Schramm, H Stöcker, L. Rezzol (2019)
    - **Delayed phase transition scenario**
      Postmerger Gravitational-Wave Signatures of Phase Transitions in Bina Rezzolla; Physical Review Letters 124 (17), 171103 (2020)
    - **Prompt phase transition scenario**
      Identifying a first-order phase transition in neutron-star mergers through gr Bastian, DB Blaschke, K Chatziioannou, JA Clark, JA Clark, T Fischer, M Oerte 061102 (2019)

Phase-transition triggered collapse scenario

Signatures of quark-hadron phase transitions in general-relativistic neutron-star mergers

ER Most, LJ Papenfort, V Dexheimer, M Hanauske, S Schramm, H Stöcker and L. Rezzolla

Physical review letters 122 (6), 061101 (2019)

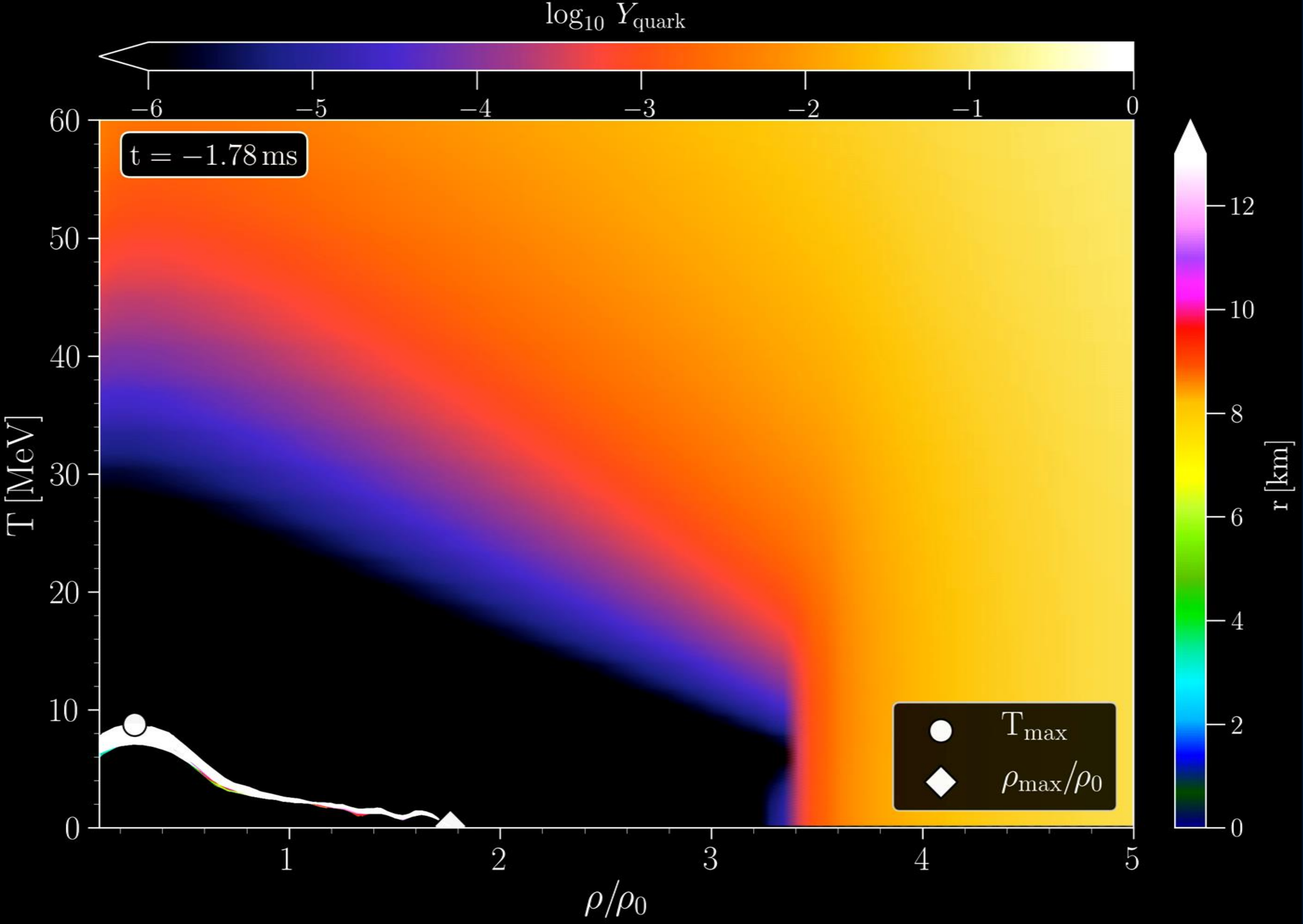

Density-Temperature-Composition dependent EOS within the CMFQ model.

The last sim... ...r (HMHS)

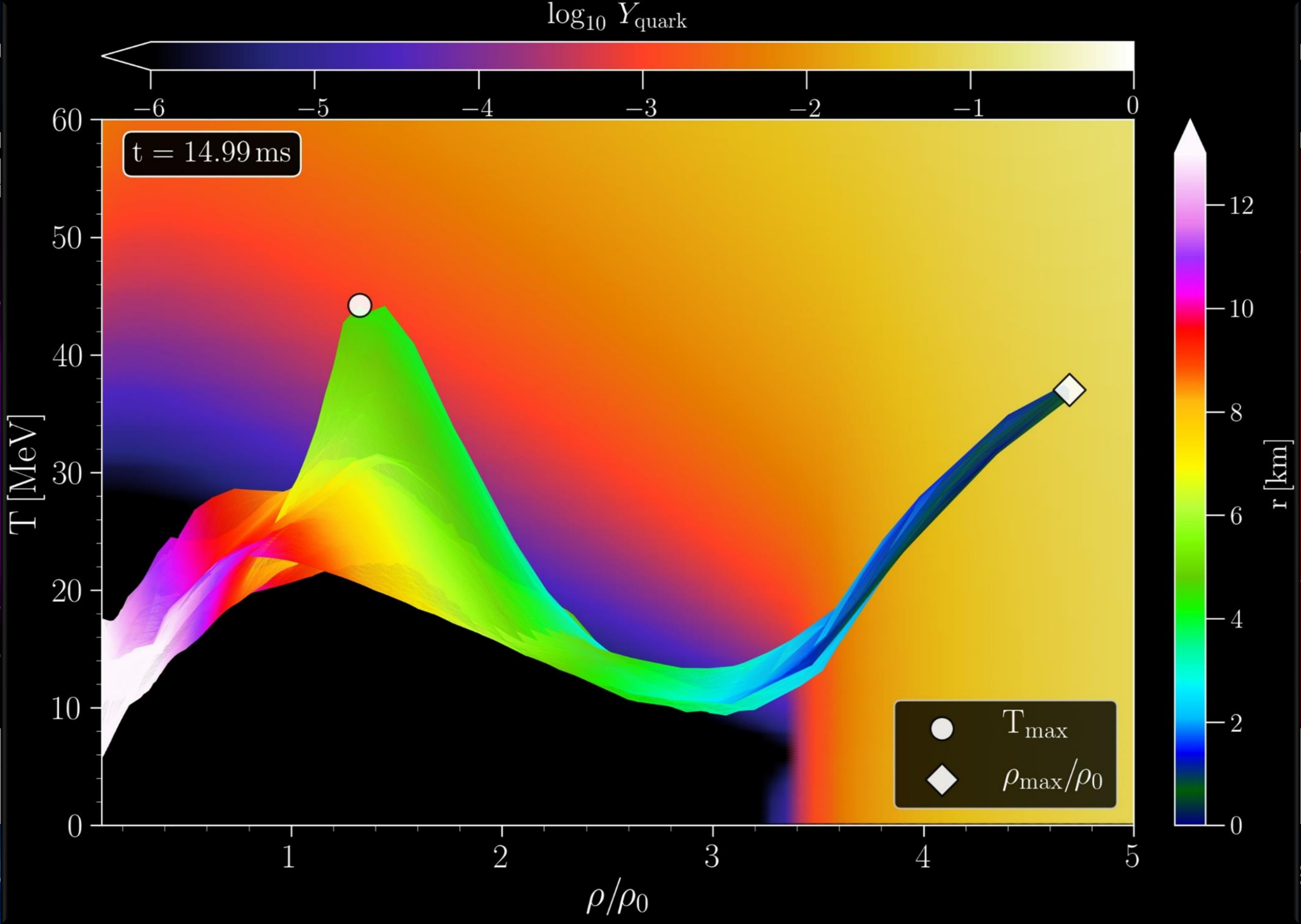

Rest mas... ...ane

The last sim (HMHS)

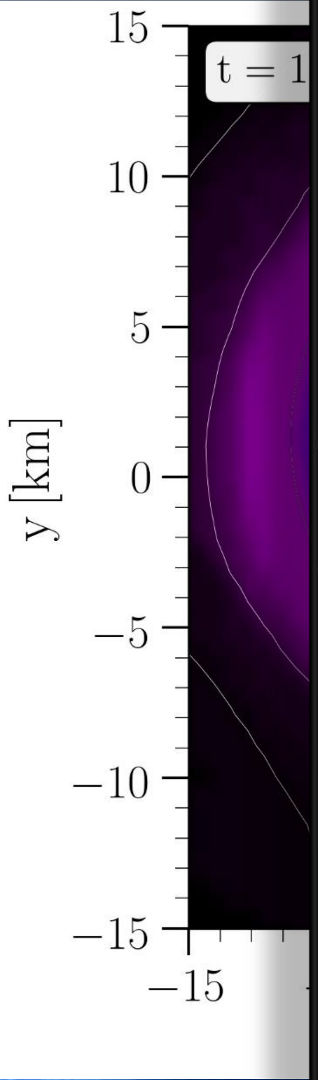

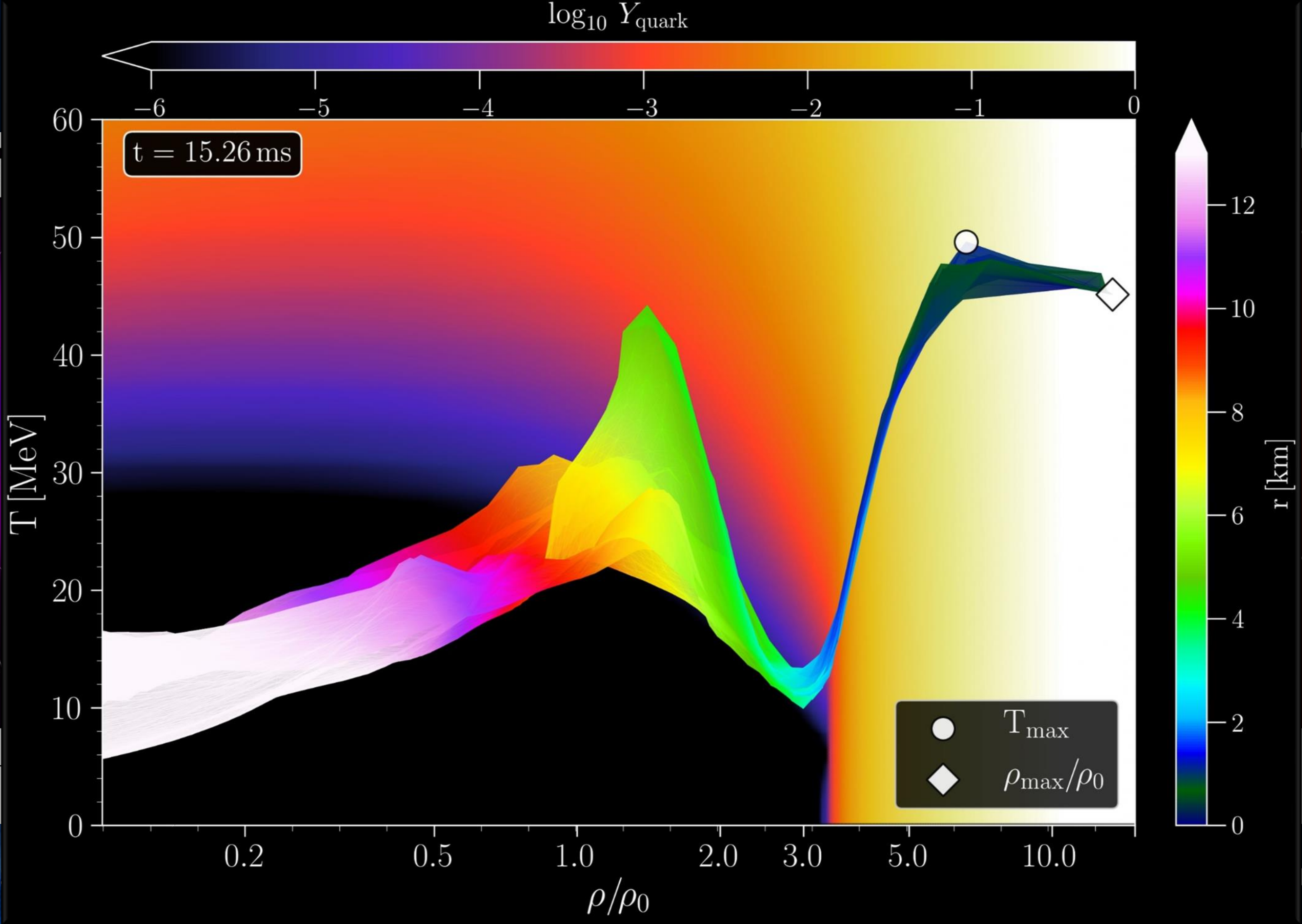

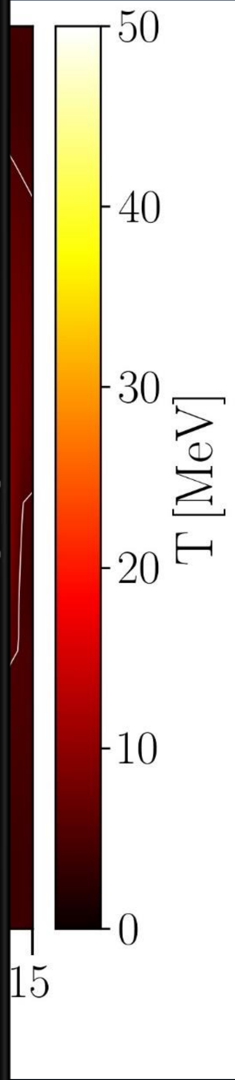

Rest mas ane

The Strange Bird Plot

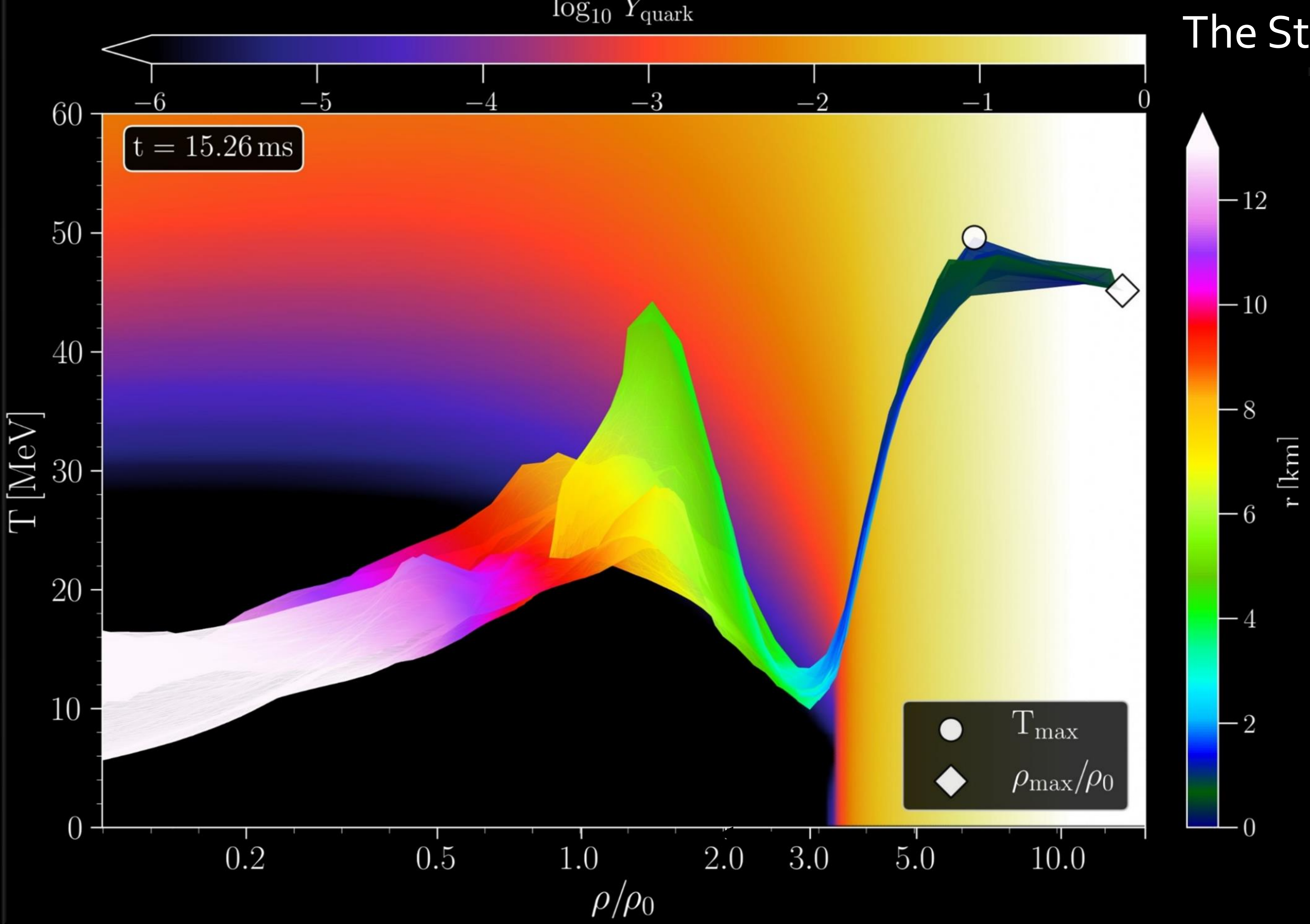

Während sich im Kopf des seltsamen Vogels die Quarks bereits aus ihrem Confinement Käfig befreit haben, besteht sein Körper noch maßgeblich aus hadronischen Teilchen. Gerade zu diesem Zeitpunkt bildet sich der Ereignishorizont um den dichten und heißen Vogelkopf und die befreite, seltsame Quarkmaterie wird durch die Bildung des schwarzen Loches makroskopisch confined.

GRAVITATIONAL COLLAPSE AND SPACE- TIME SINGULARITIES

Nobel Price 2020: R.Penrose, PRL Vol.14 No.3 (1965)

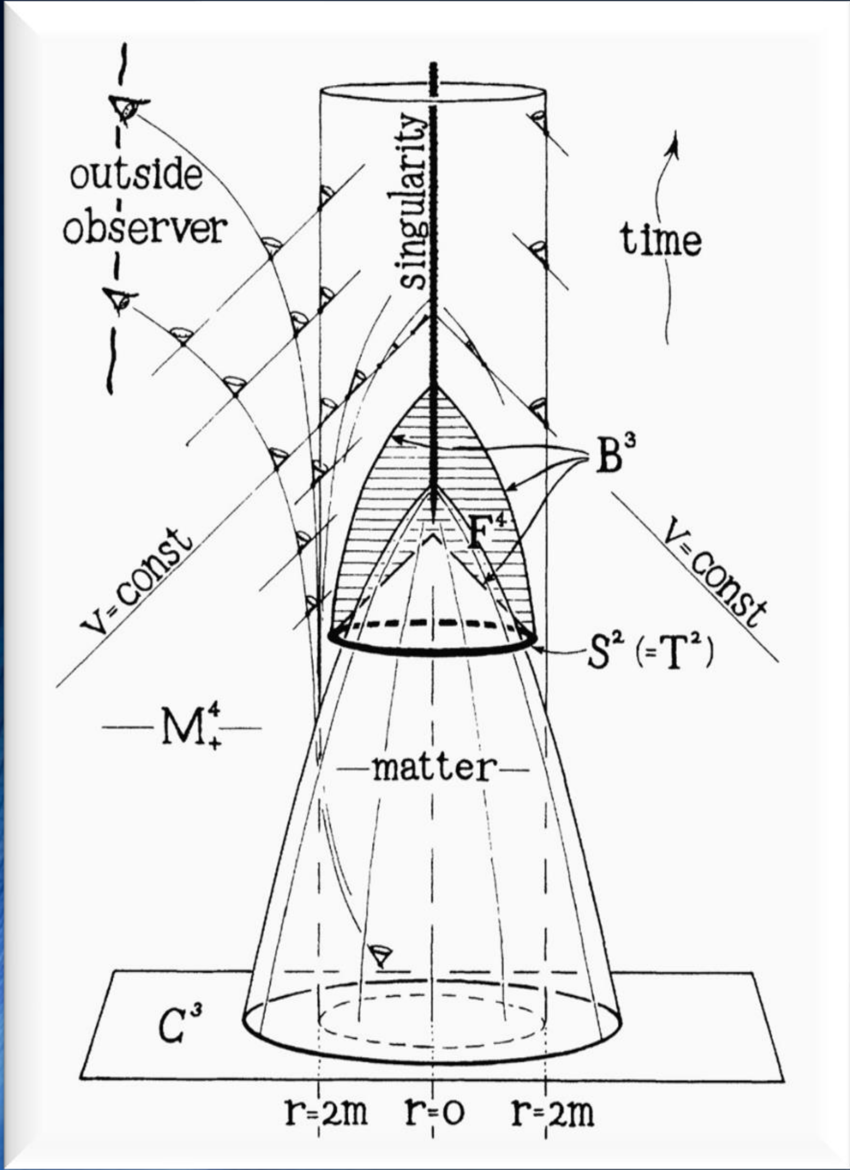

Self-drawn space-time diagram by R.Penrose (1965)

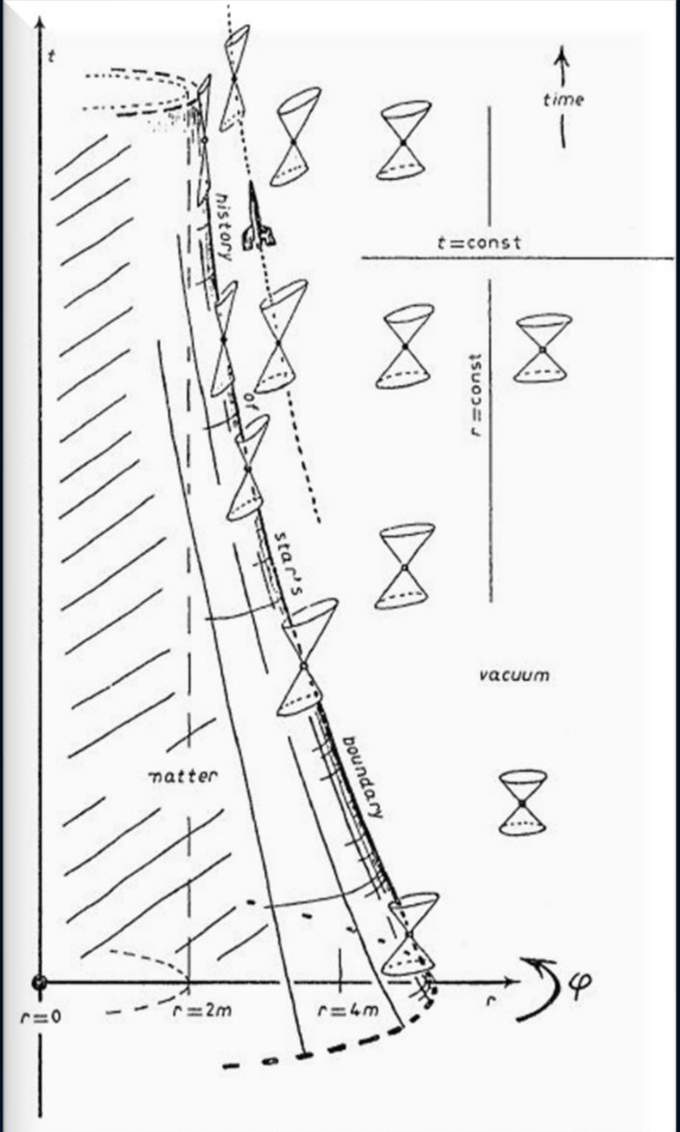

Figure 1. Spherically symmetrical collapse in the usual Schwarzschild co-ordinates.

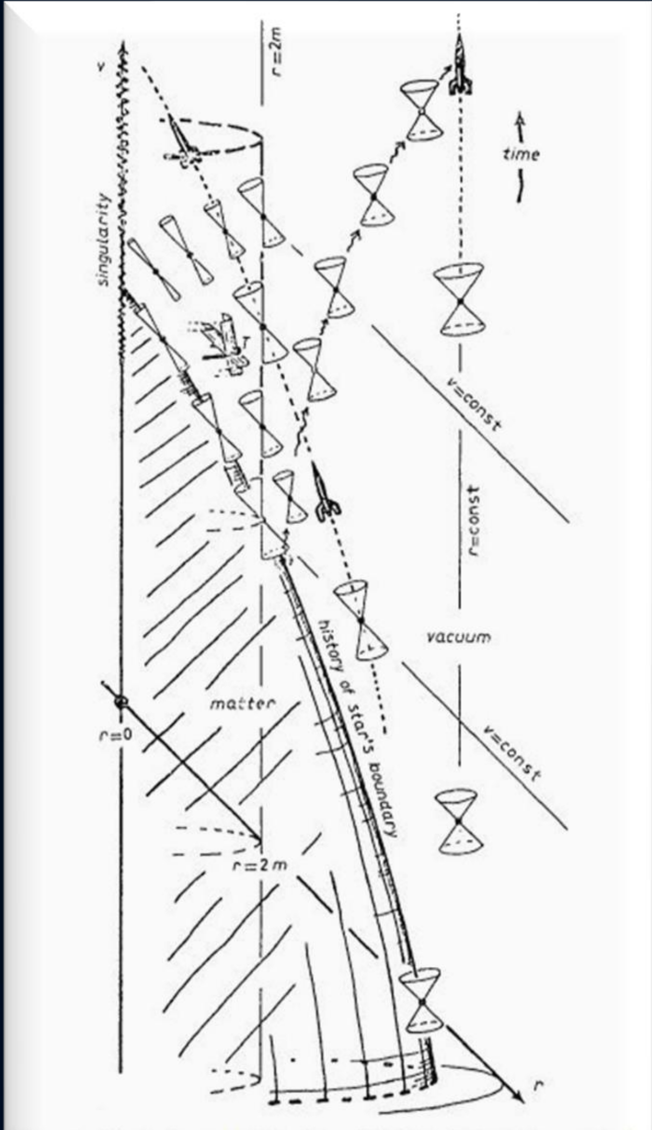

Figure 2. Spherically symmetrical collapse in Eddington-Finkelstein co-ordinates.

R.Penrose in Rivista del Nuovo Cimento, Num.Spez. I, 257 (1969)

GRAVITATIONAL COLLAPSE AND SPACE- TIME S

Nobel Price 2020: R.Penrose, PRL Vol.14 No.3

On the deconfinement phase transition in neutron-star mergers

Autoren	Elias R Most, L Jens Papenfort, Veronica Dexheimer, Matthias Hanauske, Horst Stoecker, Luciano Rezzolla
Publikationsdatum	2020/2
Zeitschrift	The European Physical Journal A
Band	56
Ausgabe	2
Seiten	1-11

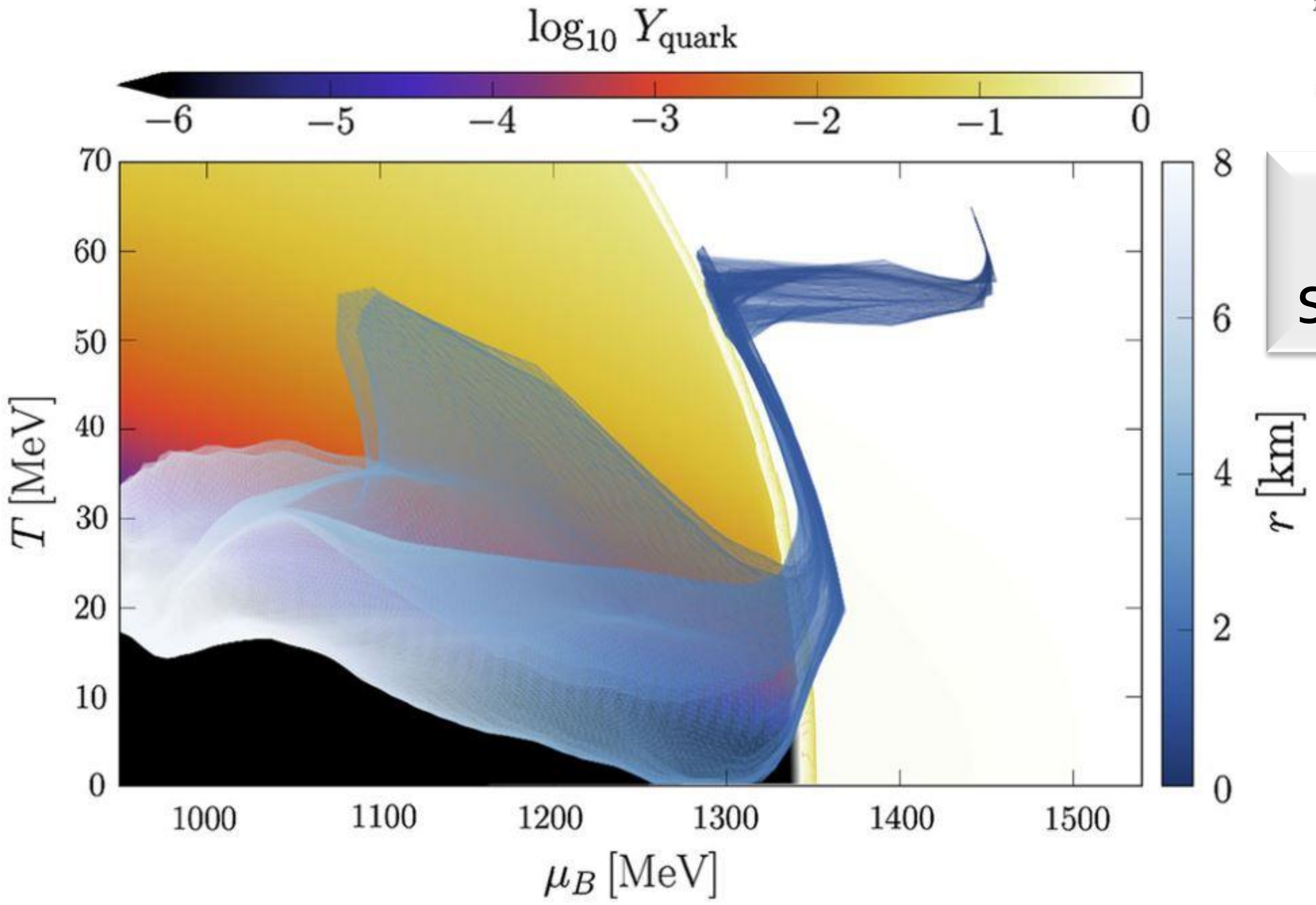

Das letzte Bild des sterbenden Schwans

co-ordinates.

Figure 2. Spherically symmetrical collapse in Eddington-Finkelstein co-ordinates.

Self-drawn space-time diagram by R.Penrose (1965)

R.Penrose in Rivista del Nuovo Cimento, Num.Spez. I, 257 (1969)

Signatures within the post-merger phase

Phase-transition triggered collapse scenario

ER Most et.al., PRL 122 (6), 061101 (2019)

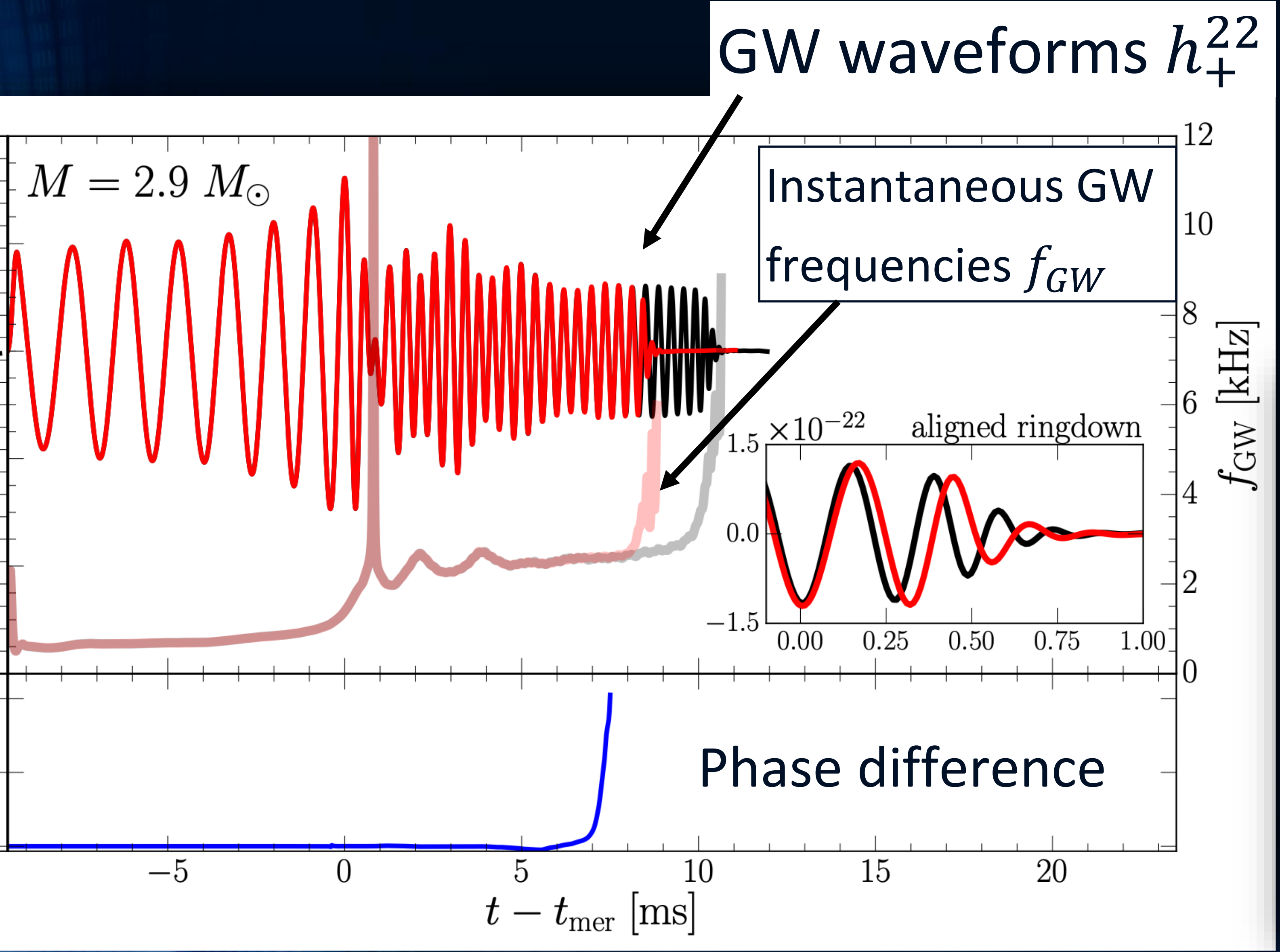

EOS based on Chiral Mean Field (CMF) model, based on a nonlinear SU(3) sigma model with (red) and without (black) phase transition.

Phase transition leads to a very hot and dense quark core that, when it collapses to a black hole, produces a ringdown signal different from the hadronic one.

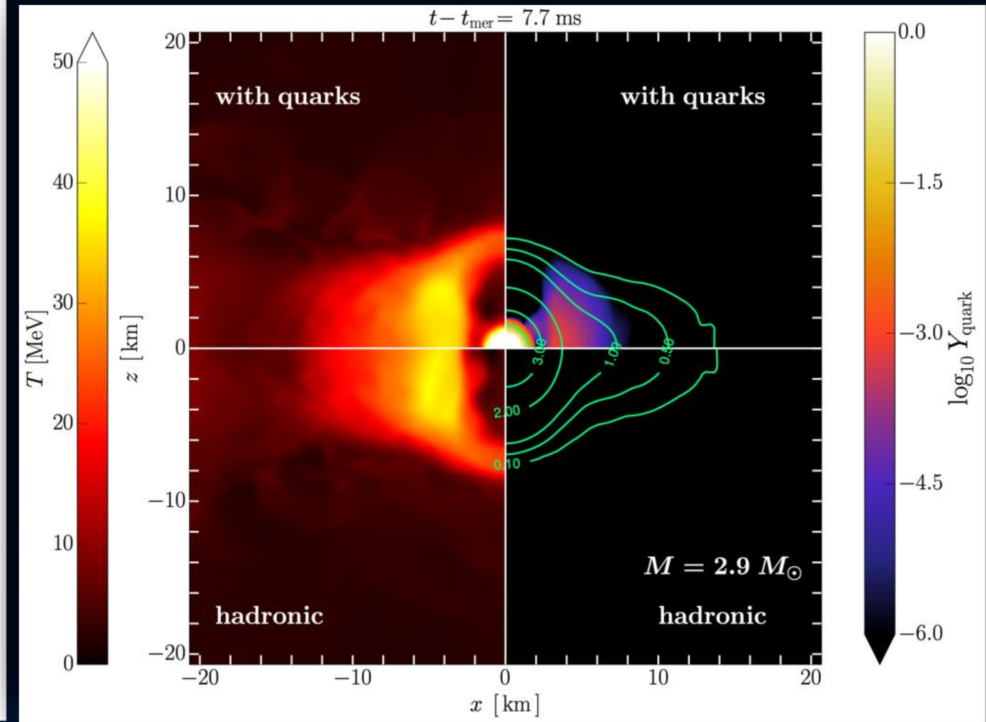

Signatures within the post-merger phase

Phase-transition triggered collapse scenario

ER Most et.al., PRL 122 (6), 061101 (2019)

EOS based on Chiral Mean Field (CMF) model, based on a nonlinear SU(3) sigma

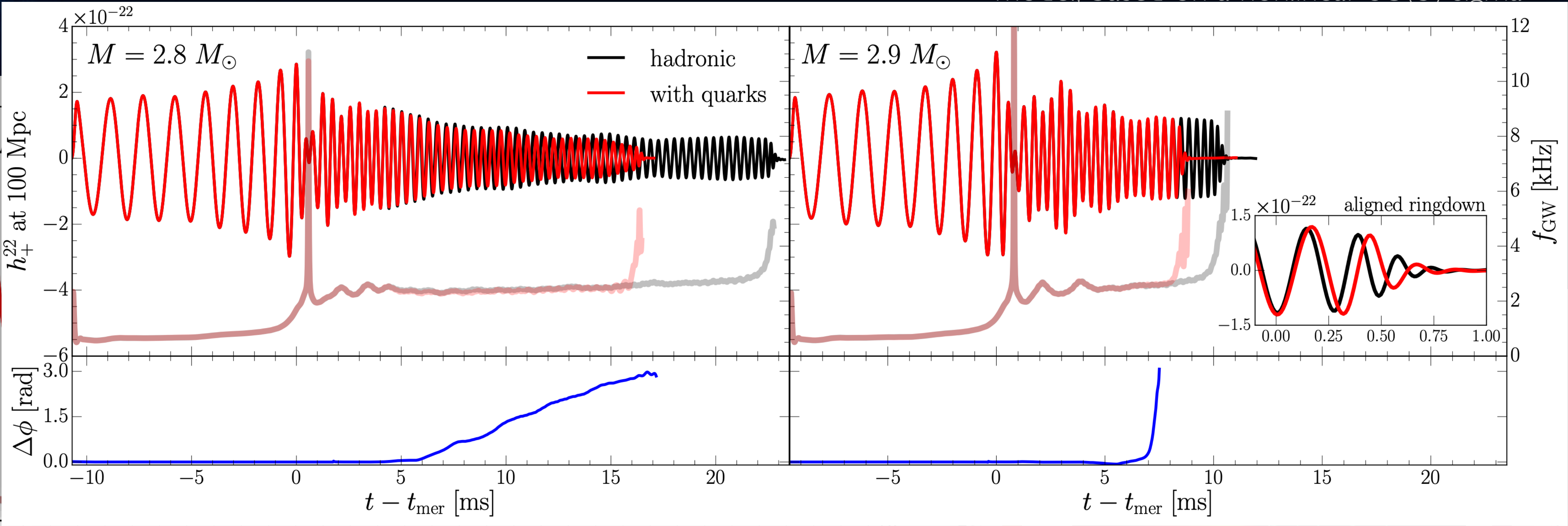

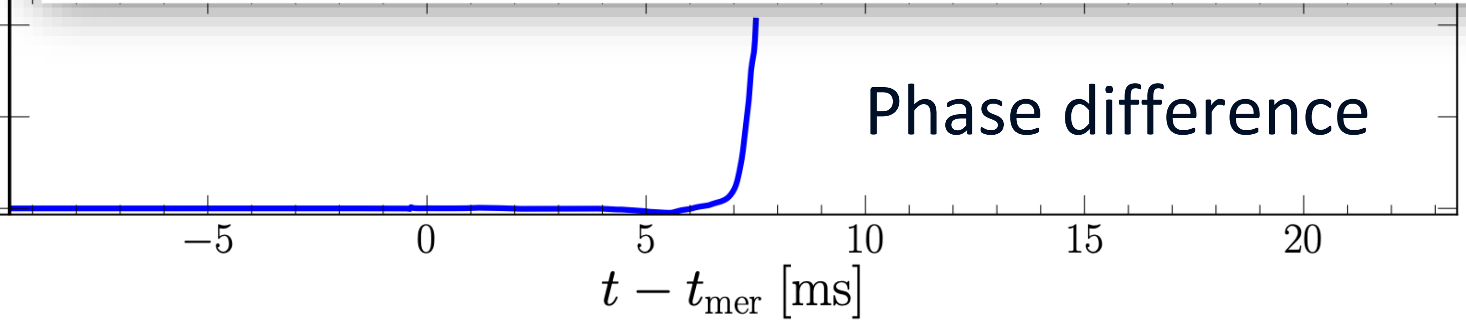

Phase difference

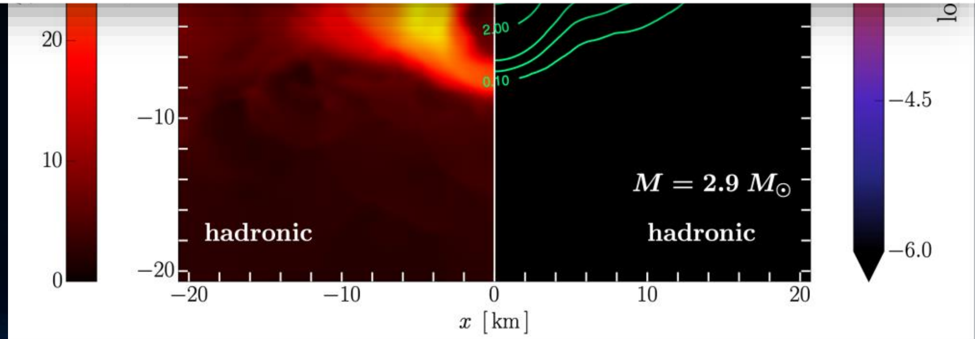

Sig…

Phas…

ER Most et al., PRL 122 (6), 061101 (2019)

CMF)

) sigma

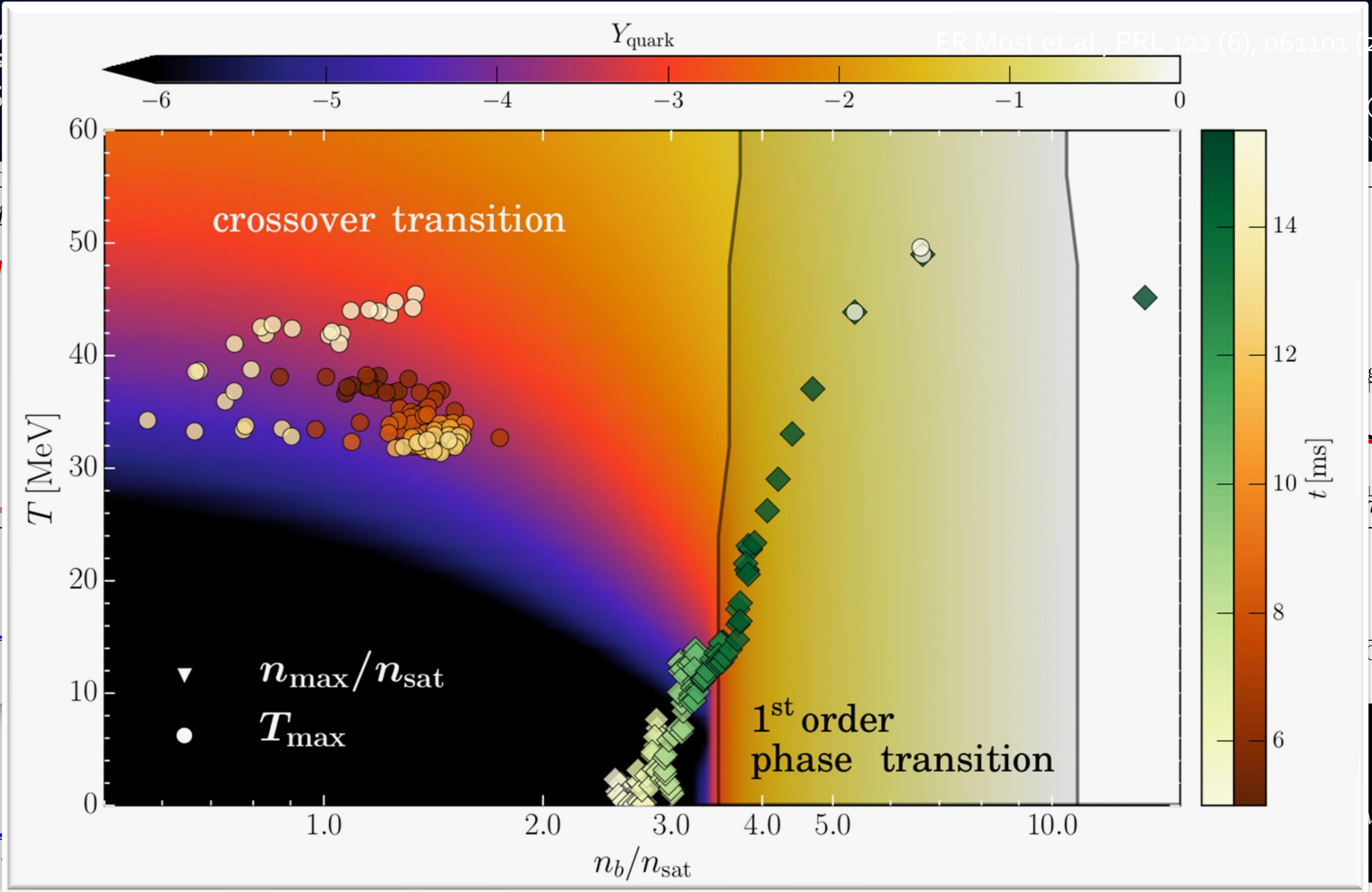

Can we detect the quark-gluon plasma with gravitational waves?

- Gravitational-wave signatures of the hadron-quark phase transition in binary compact star mergers
  - *Signatures within the late inspiral phase (premerger signals)*
    - Constraining twin stars with GW170817; G Montana, L Tolós, M Hanauske, L Rezzolla; Physical Review D 99 (10), 103009 (2019)
  - *Signatures within the post-merger phase evolution*
    - **Phase-transition triggered collapse scenario**
      Signatures of quark-hadron phase transitions in general-relativistic neutron-star mergers; ER Most, LJ Papenfort, V Dexheimer, M Hanauske, S Schramm, H Stöcker, L. Rezzolla; Physical review letters 122 (6), 061101 (2019)
    - **Delayed phase transition scenario**
      Postmerger Gravitational-Wave Signatures of Phase Transitions in Binary Mergers; LR Weih, M Hanauske, L Rezzolla; Physical Review Letters 124 (17), 171103 (2020)
    - **Prompt phase transition scenario**
      Identifying a first-order phase transition in neutron-star mergers through gravitational waves; A Bauswein, NUF Bastian, DB Blaschke, K Chatziioannou, JA Clark, JA Clark, T Fischer, M Oertel; Physical review letters 122 (6), 061102 (2019)

Signatures within the post-merger phase evolution

Delayed phase transition scenario

Postmerger Gravitational-Wave Signatures of Phase Transitions in Binary Mergers; LR Weih, M Hanauske, L Rezzolla; Physical Review Letters 124 (17), 171103 (2020)

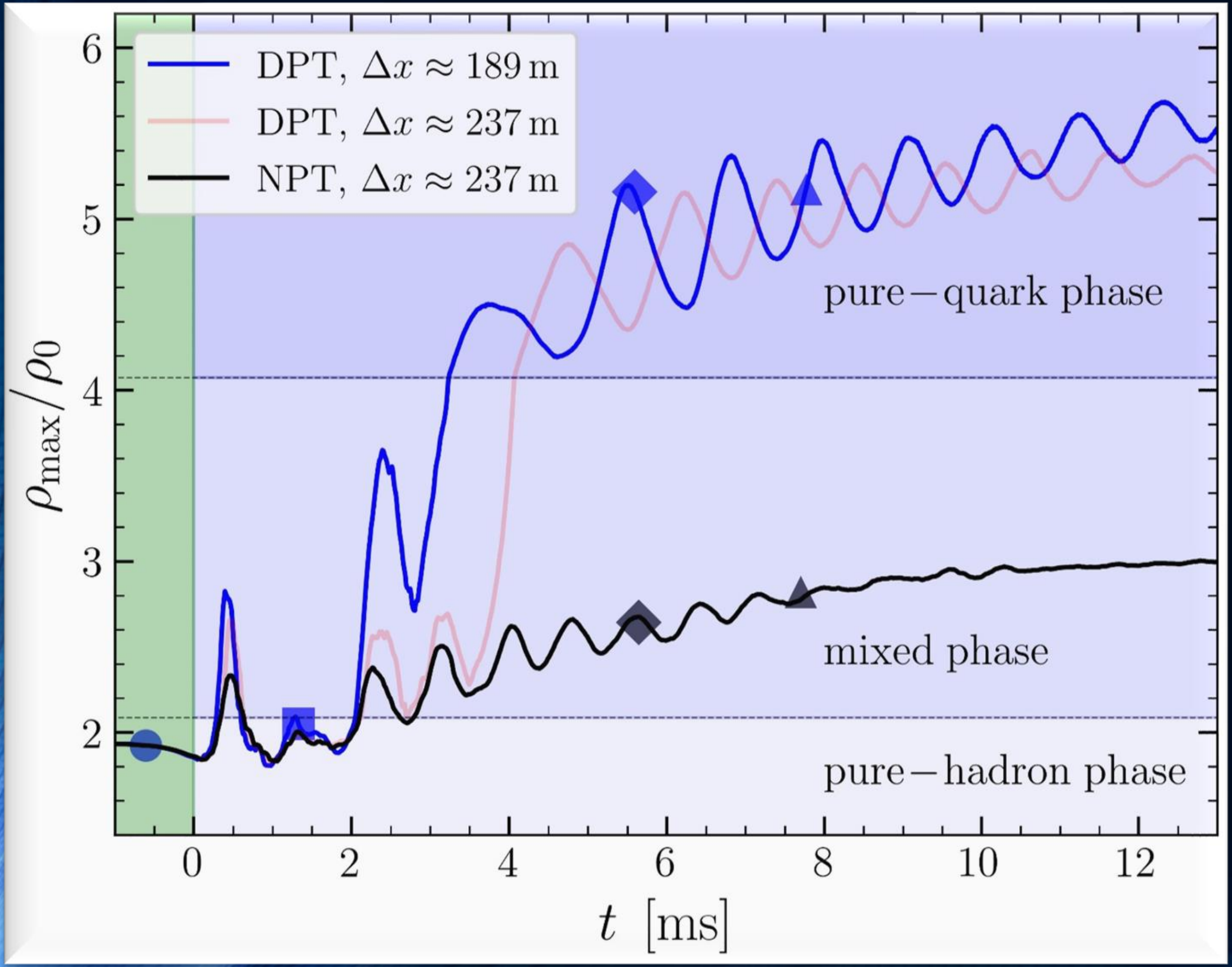

Evolution of the central rest-mass density for four binary neutron star configurations, simulated with/without a Gibbs-like hadron-quark phase transition. Blue-shaded regions mark the different phases of the EOS and apply to the DPT (Delayed phase transition) and PTTC (Phase-transition triggered collaps) scenarios only, since the NPT (No phase transition) binaries are always purely hadronic.

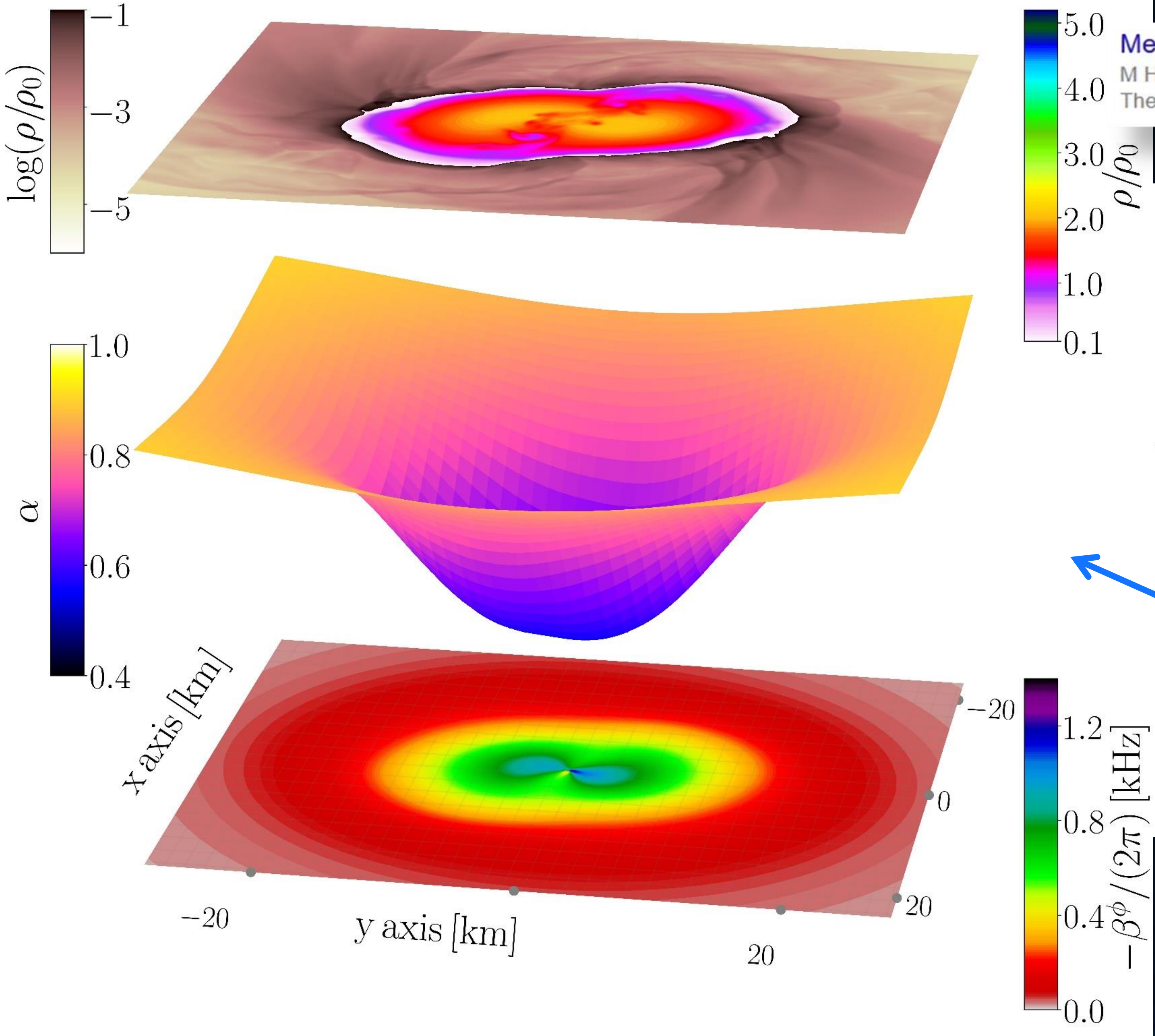

Metastable hypermassive hybrid stars as neutron-star merger remnants

M Hanauske, LR Weih, H Stöcker, L Rezzolla

The European Physical Journal Special Topics, 1-8

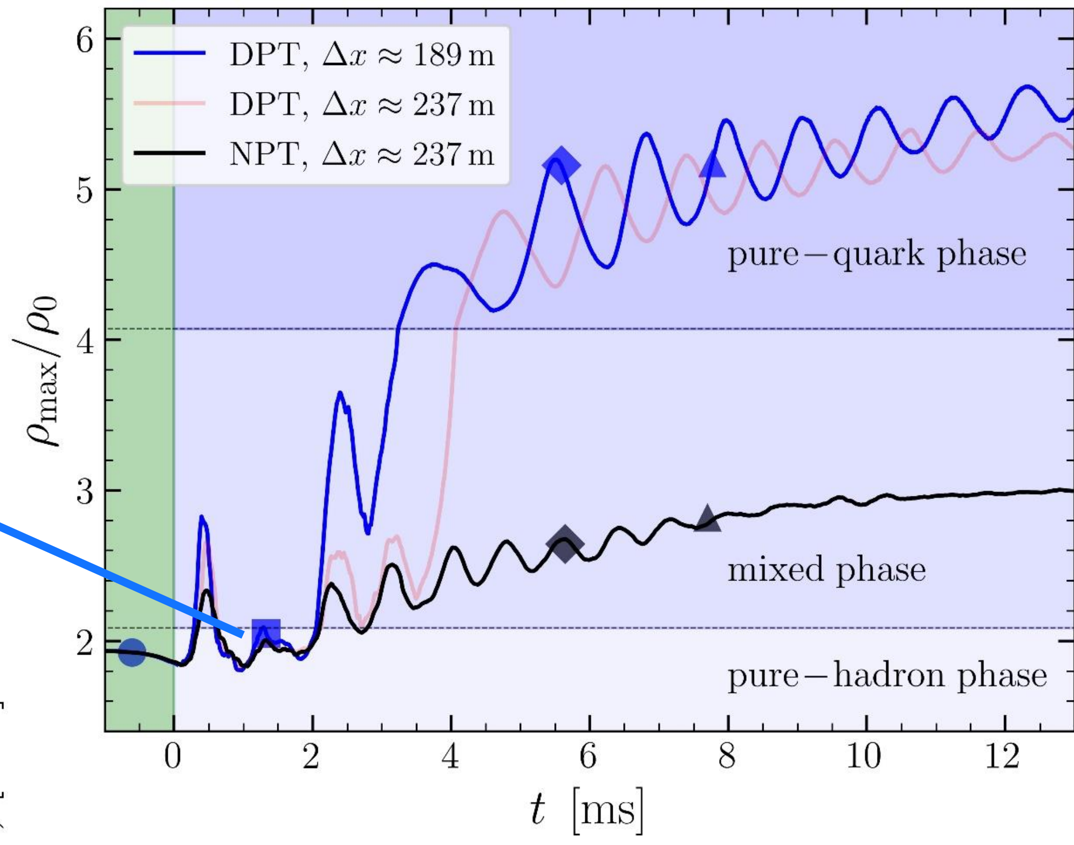

Additional article „ Neutron star collisions and gravitational waves" by M.Hanauske and L.Weih will appear soon in Astronomische Nachrichten (Astronomical Notes)

Without Phase Transition

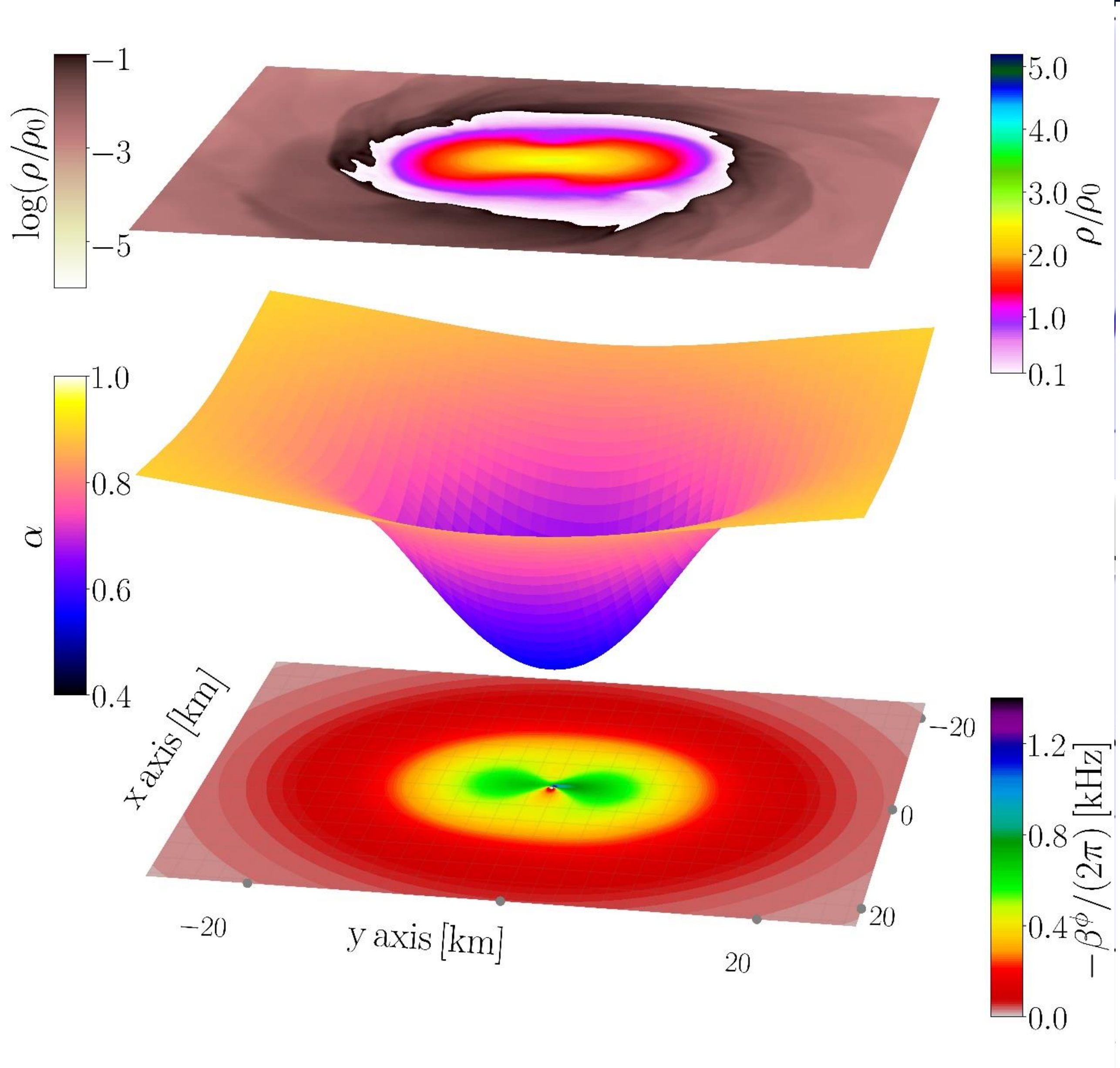

With Phase Transition

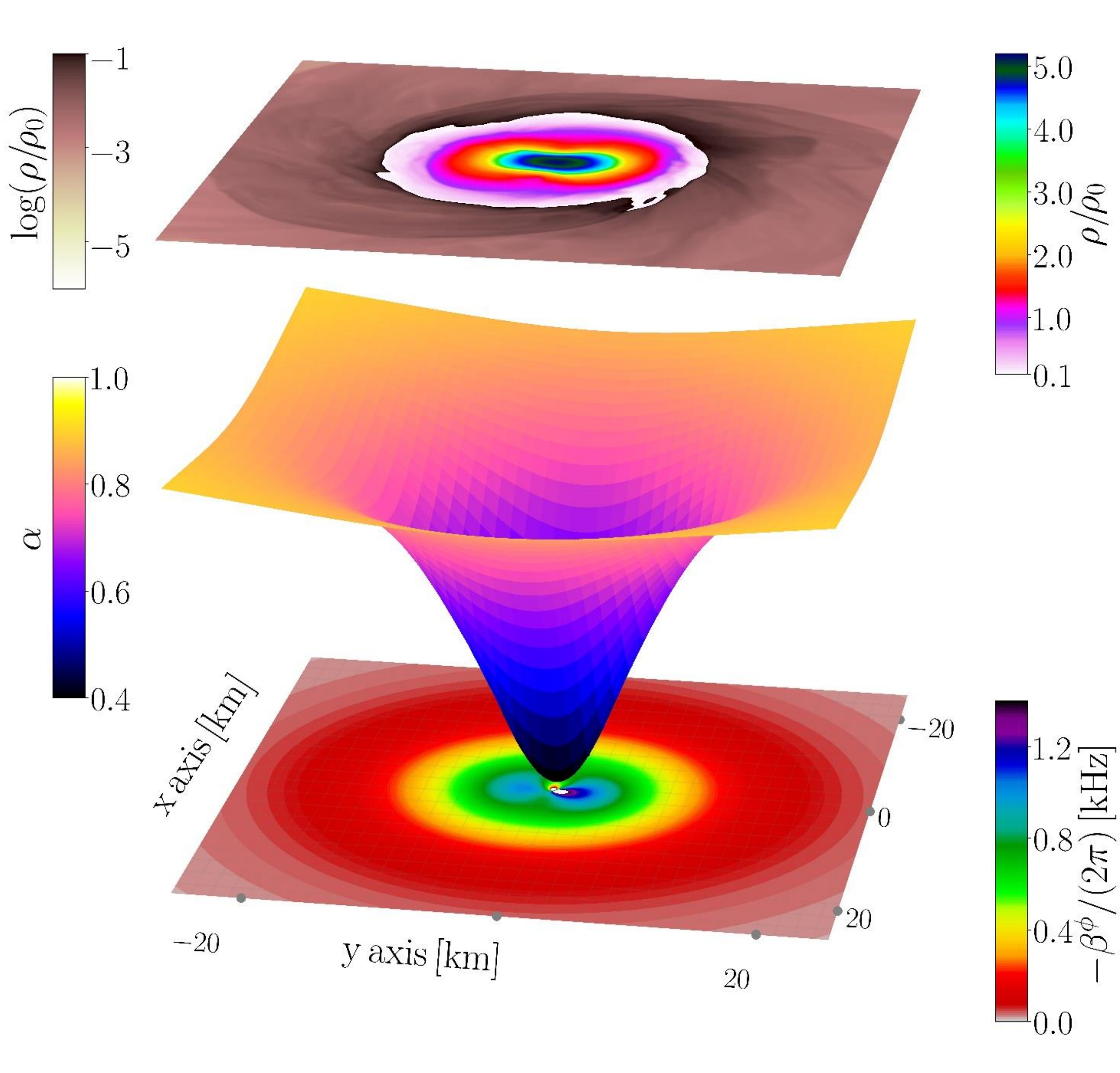

Without Phase Transition

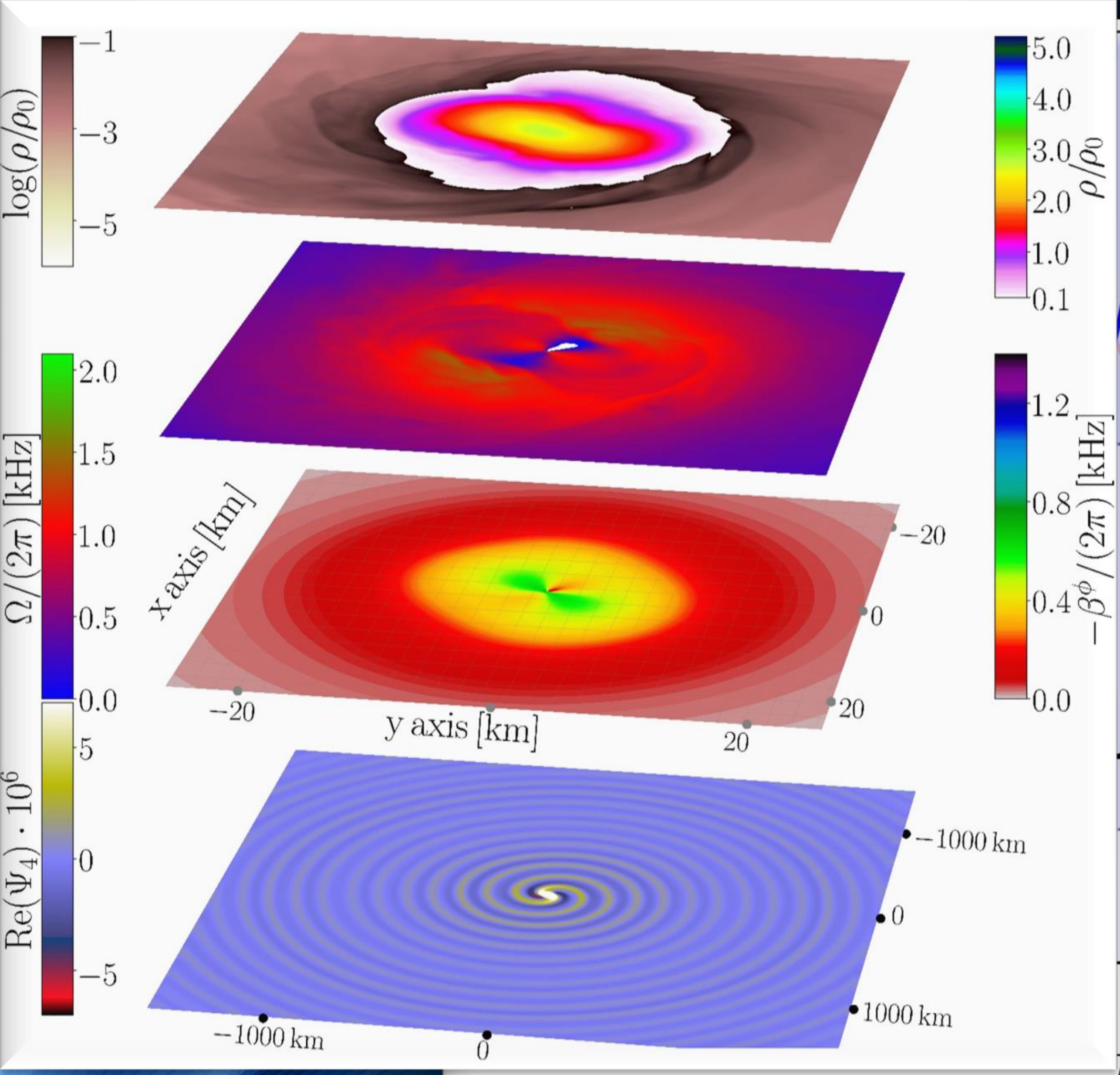

With Phase Transition

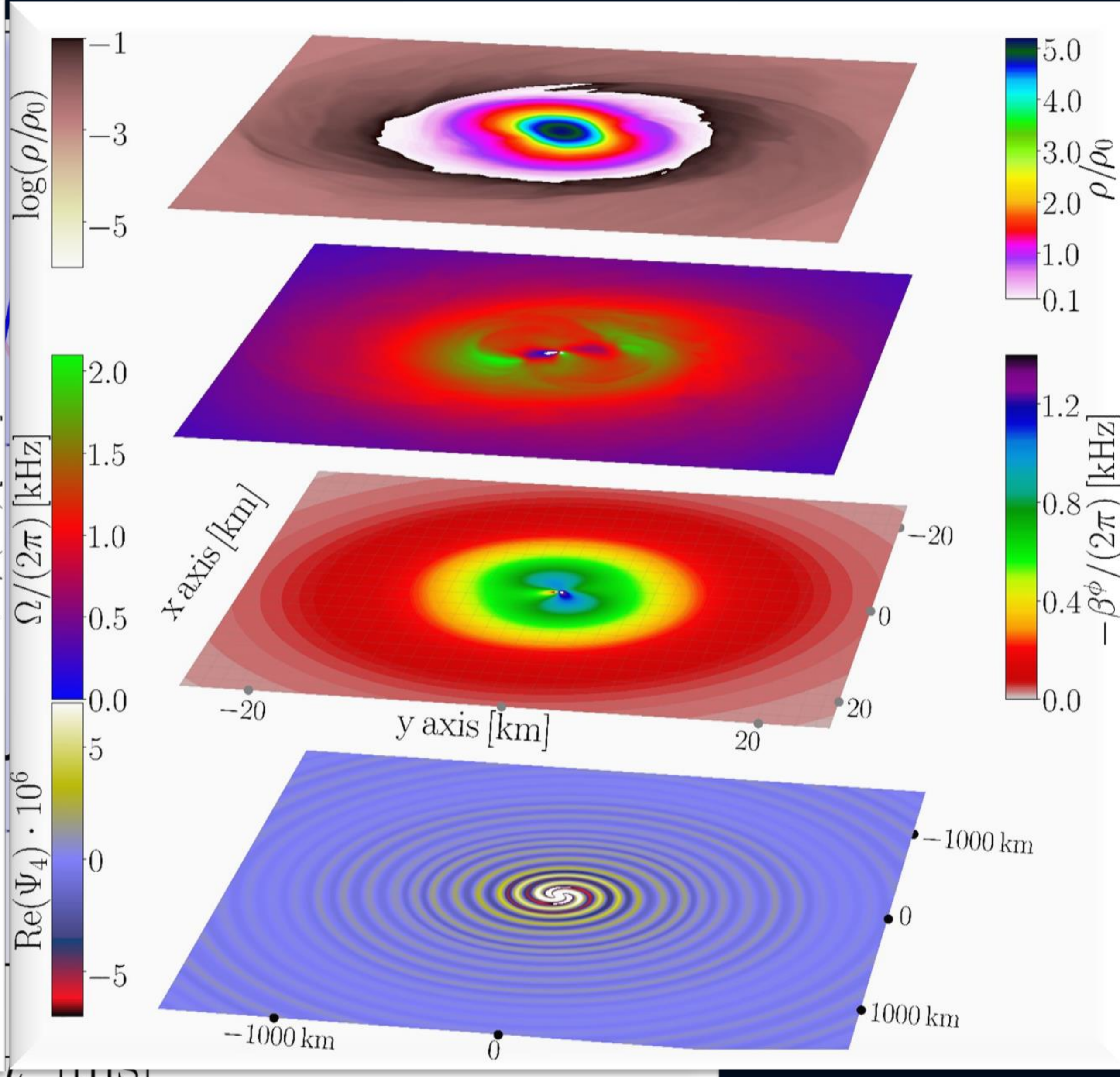

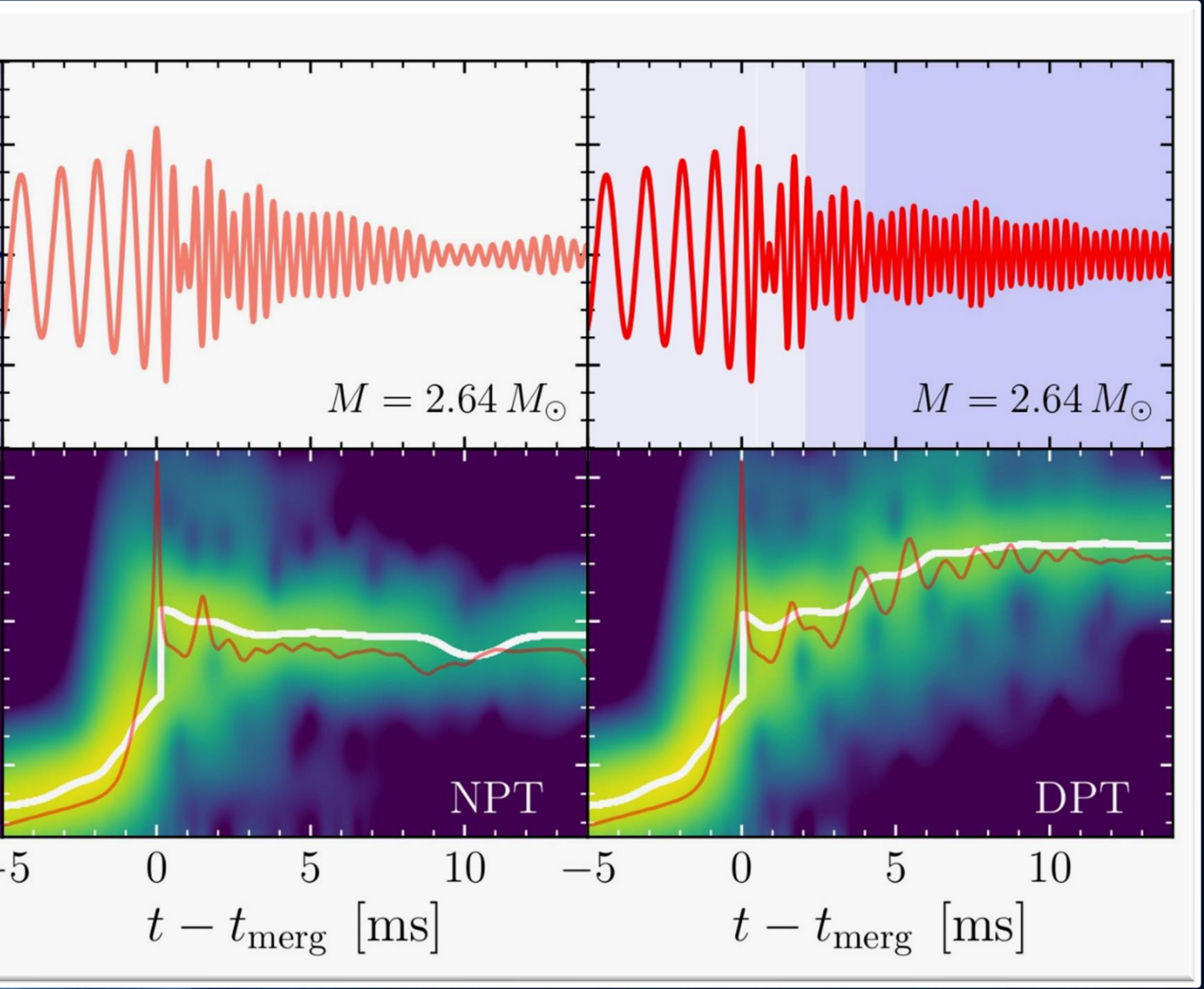

Strain h+ (top) and its spectrogram (bottom) for the binary neutron star simulation of the delayed phase transition scenario. In the top panel the different shadings mark the times when the HMNS core enters the mixed and pure quark phases.. In the bottom panels, the white lines trace the maximum of the spectrograms, while the red lines show the instantaneous gravitational-wave frequency.

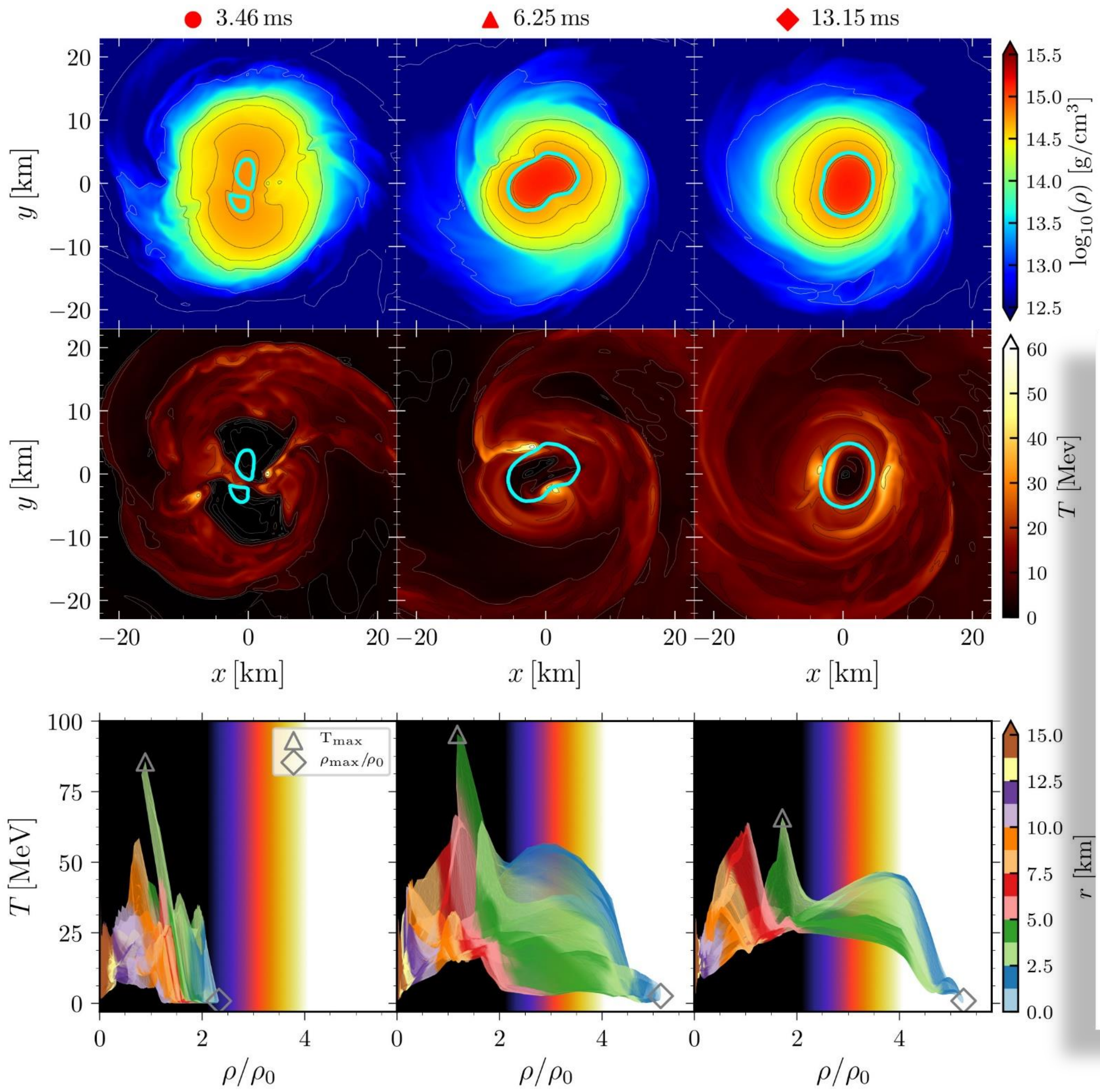

Article will appear in

EPJ Special Topics on
"Nuclear Astrophysics in Our
Time: Supernovae, Neutron Stars
and Binary Neutron Star Mergers"

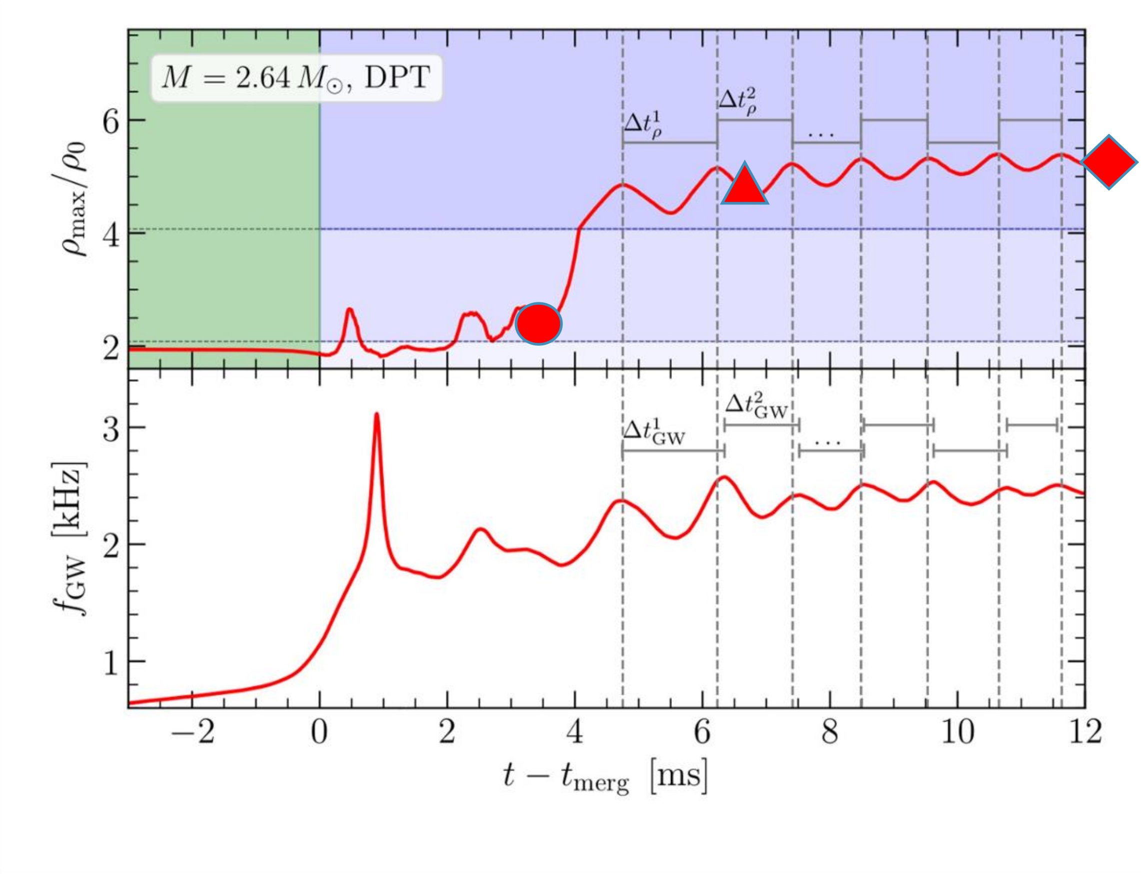

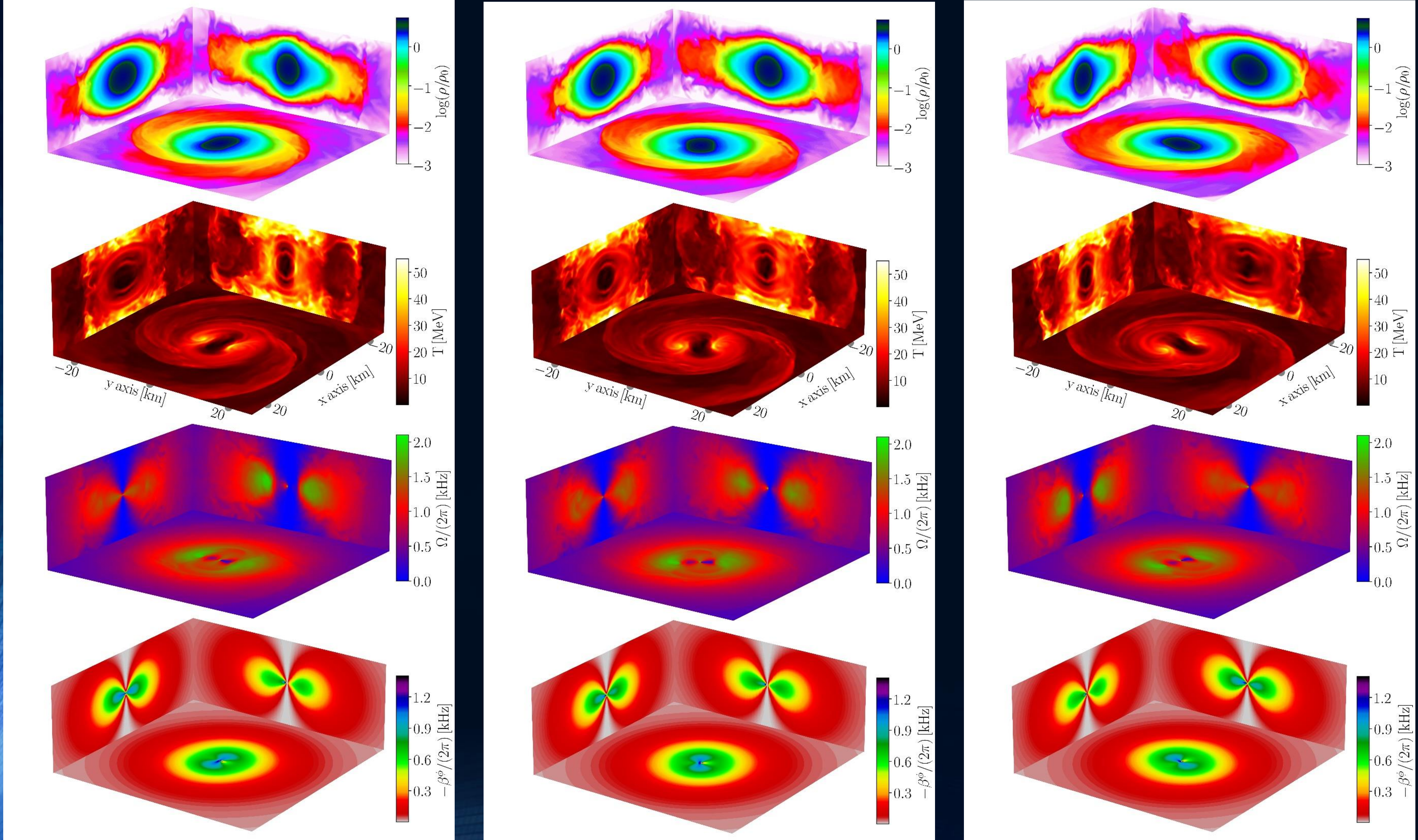

log(ρ/ρ0)
0
−1
−2
−3
T [MeV]
50
40
30
20
10
y axis [km]
x axis [km]
−20
0
20
Ω/(2π) [kHz]
2.0
1.5
1.0
0.5
0.0
−β^φ/(2π) [kHz]
1.2
0.9
0.6
0.3

Can we detect the quark-gluon plasma with gravitational waves?

- Gravitational-wave signatures of the hadron-quark phase transition in binary compact star mergers
  - *Signatures within the late inspiral phase (premerger signals)*
    - Constraining twin stars with GW170817; G Montana, L Tolós, M Hanauske, L Rezzolla; Physical Review D 99 (10), 103009 (2019)
  - *Signatures within the post-merger phase evolution*
    - **Phase-transition triggered collapse scenario**
      Signatures of quark-hadron phase transitions in general-relativistic neutron-star mergers; ER Most, LJ Papenfort, V Dexheimer, M Hanauske, S Schramm, H Stöcker, L. Rezzolla; Physical review letters 122 (6), 061101 (2019)
    - **Delayed phase transition scenario**
      Postmerger Gravitational-Wave Signatures of Phase Transitions in Binary Mergers; LR Weih, M Hanauske, L Rezzolla; Physical Review Letters 124 (17), 171103 (2020)
    - **Prompt phase transition scenario**
      Identifying a first-order phase transition in neutron-star mergers through gravitational waves; A Bauswein, NUF Bastian, DB Blaschke, K Chatziioannou, JA Clark, JA Clark, T Fischer, M Oertel; Physical review letters 122 (6), 061102 (2019)

Signatures within the post-merger phase evolution

Prompt phase transition scenario

Identifying a first-order phase transition in neutron-star mergers through gravitational waves; A Bauswein, NUF Bastian, DB Blaschke, K Chatziioannou, JA Clark, JA Clark, T Fischer, M Oertel; Physical review letters 122 (6), 061102 (2019)

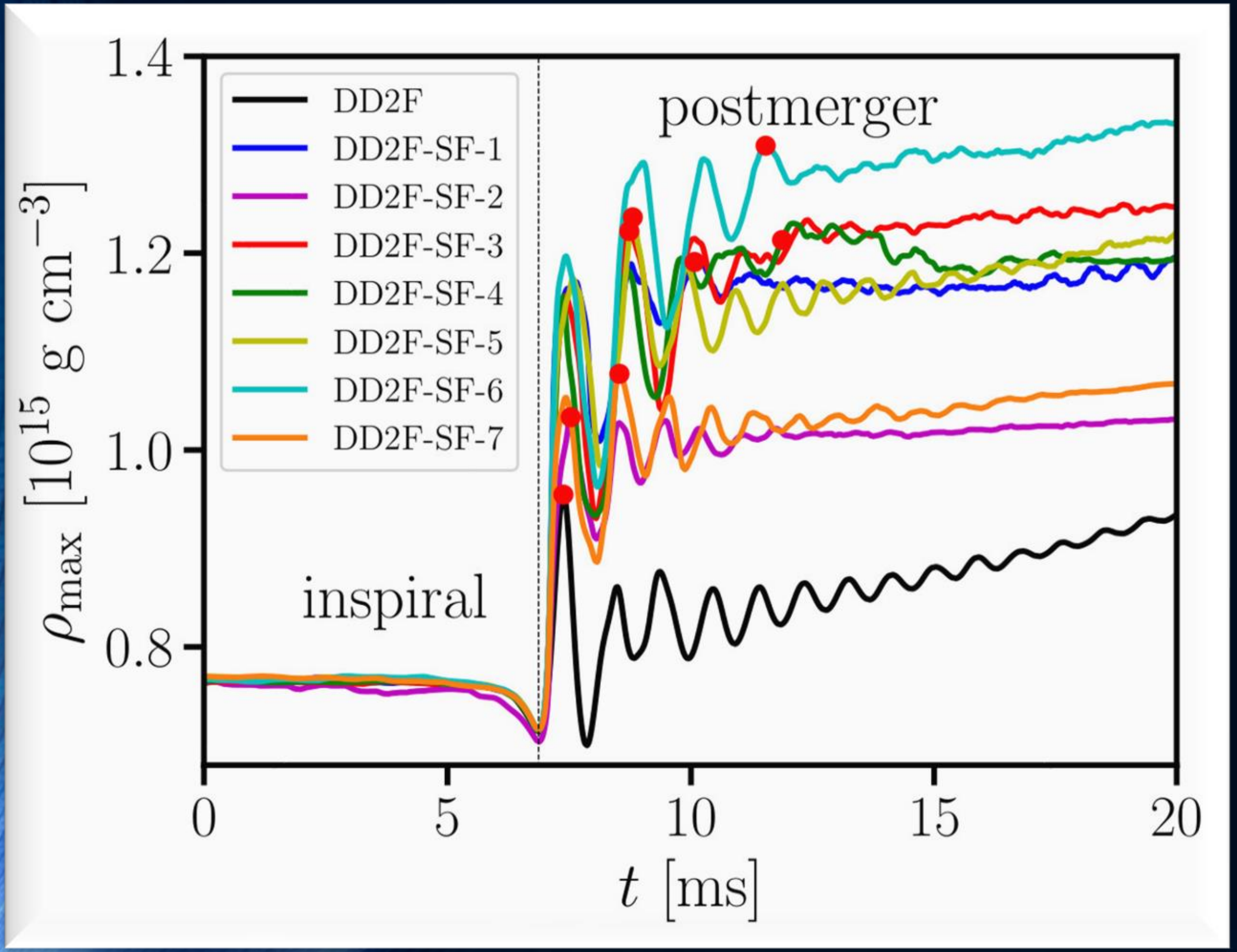

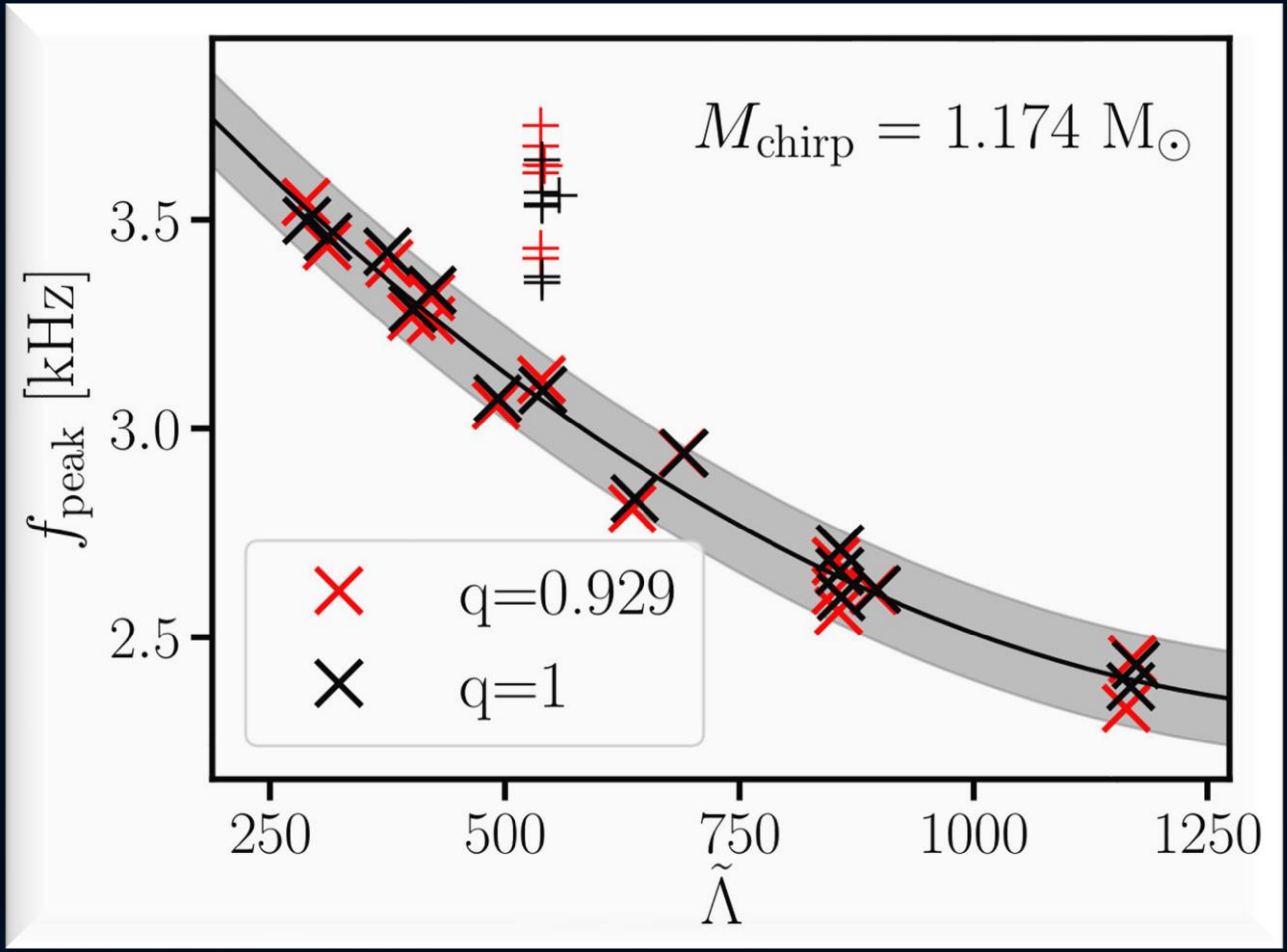

Can we detect the quark-gluon plasma with gravitational waves?

- Gravitational-wave signatures of the hadron-quark phase transition in binary compact star mergers
  - *Signatures within the late inspiral phase (premerger signals)*
    - Constraining twin stars with GW170817; G Montana, L Tolós, M Hanauske, L Rezzolla; Physical Review D 99 (10), 103009 (2019)
  - *Signatures within the post-merger phase evolution*
    - **Phase-transition triggered collapse scenario**
      Signatures of quark-hadron phase transitions in general-relativistic neutron-star mergers; ER Most, LJ Papenfort, V Dexheimer, M Hanauske, S Schramm, H Stöcker, L. Rezzolla; Physical review letters 122 (6), 061101 (2019)
    - **Delayed phase transition scenario**
      Postmerger Gravitational-Wave Signatures of Phase Transitions in Binary Mergers; LR Weih, M Hanauske, L Rezzolla; Physical Review Letters 124 (17), 171103 (2020)
    - **Prompt phase transition scenario**
      Identifying a first-order phase transition in neutron-star mergers through gravitational waves; A Bauswein, NUF Bastian, DB Blaschke, K Chatziioannou, JA Clark, JA Clark, T Fischer, M Oertel; Physical review letters 122 (6), 061102 (2019)

The Hadron-Quark Phase Transition and the Third Family of Compact Stars (Twin Stars)

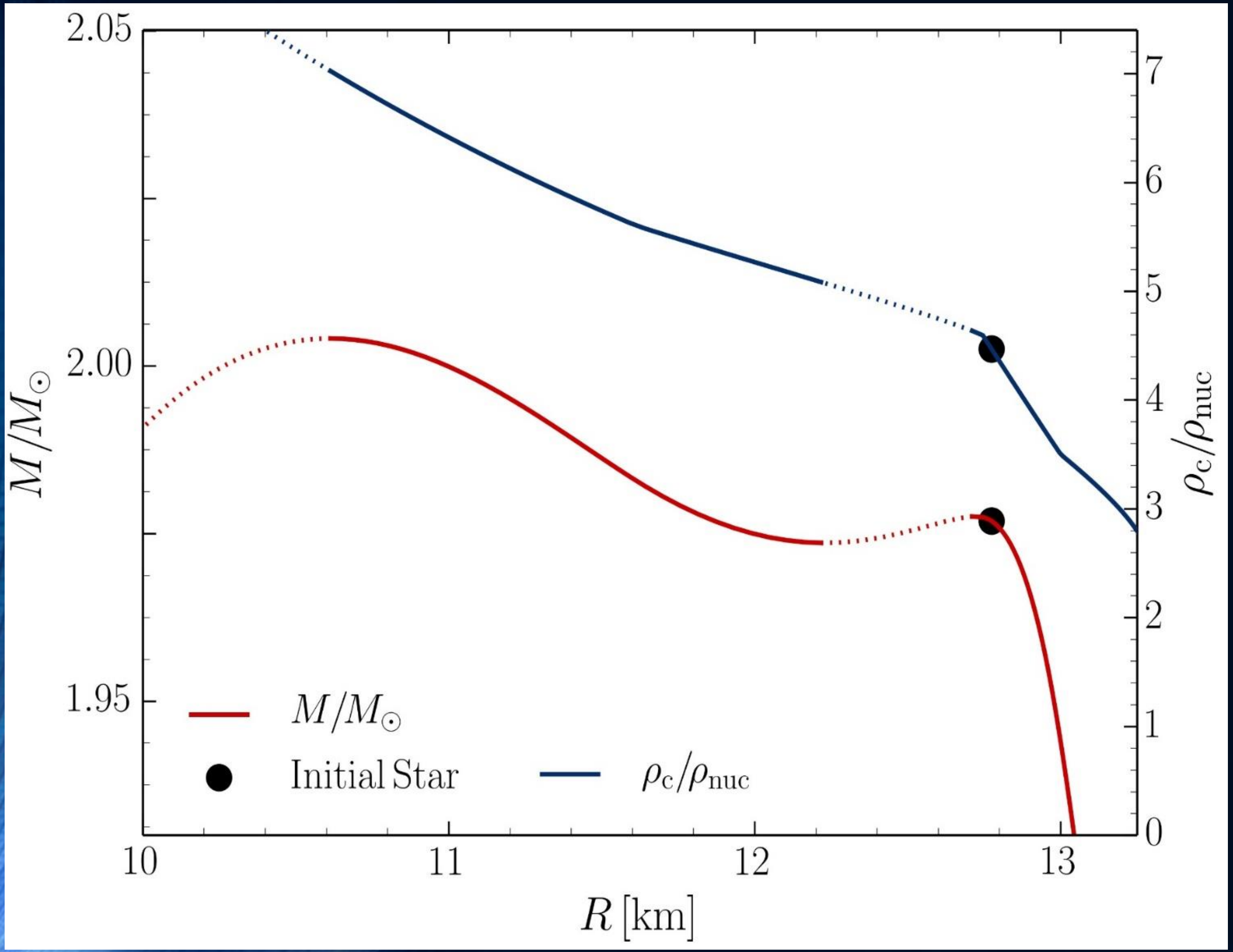

Glendenning, N. K., & Kettner, C. (1998). Nonidentical neutron star twins. Astron. Astrophys., 353(LBL-42080), L9.

Sarmistha Banik, Matthias Hanauske, Debades Bandyopadhyay and Walter Greiner, Rotating compact stars with exotic matter, Phys.Rev.D 70 (2004) p.12304

I.N. Mishustin, M. Hanauske, A. Bhattacharyya, L.M. Satarov, H. Stöcker, and W. Greiner, Catastrophic rearrangement of a compact star due to quark core formation, Physics Letters B 552 (2003) p.1-8

M.Alford and A. Sedrakian, Compact stars with sequential QCD phase transitions. Physical review letters, 119(16), 161104 (2017)..

D.Alvarez-Castillo and D.Blaschke, High-mass twin stars with a multipolytrope equation of state. Physical Review C, 96(4), 045809 (2017) .

A. Ayriyan, N.-U. Bastian, D. Blaschke, H. Grigorian, K. Maslov, D. N. Voskresensky, How robust is a third family of compact stars against pasta phase effects?, arXiv:1711.03926 [nucl-th]

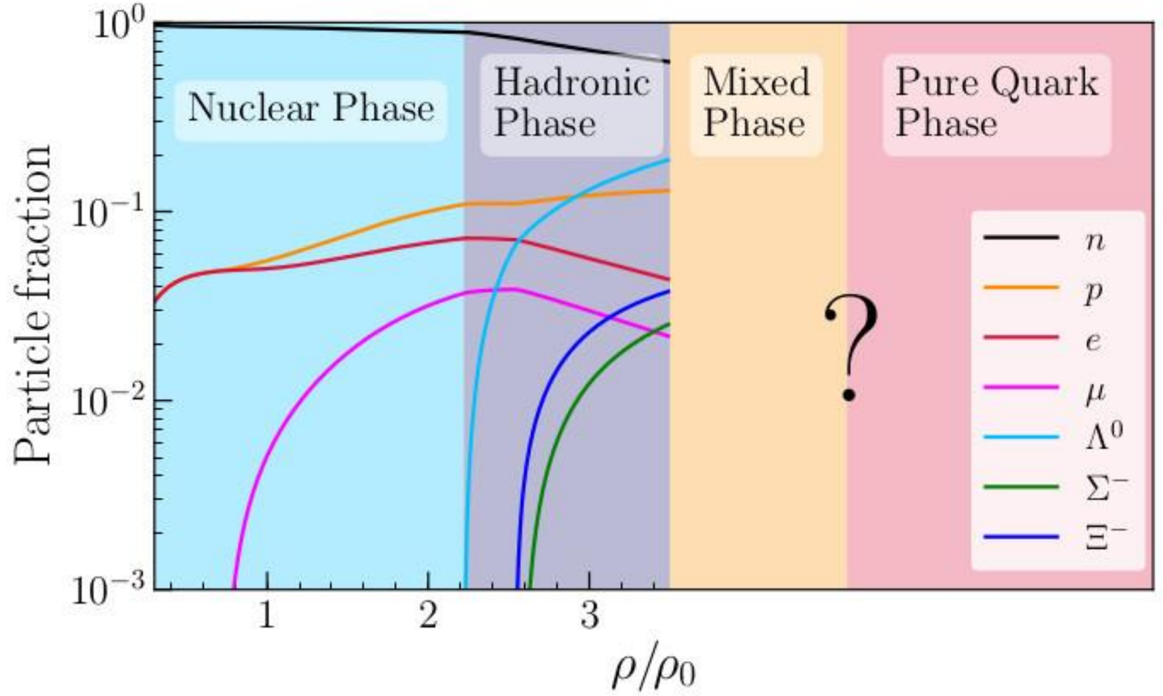

FIG. 1. Particle fractions as functions of the baryonic density for the FSU2H model [69, 70] up to the point where the HQPT is implemented, giving rise to a phase of deconfined quark matter which can be separated from the nuclear (or hadronic) phase by a mixed phase of hadrons and quarks. We note that the actual fractions of nucleons/hyperons and quarks u, d, s in the mixed and quark phases cannot be determined with the parametrizations used in this work.

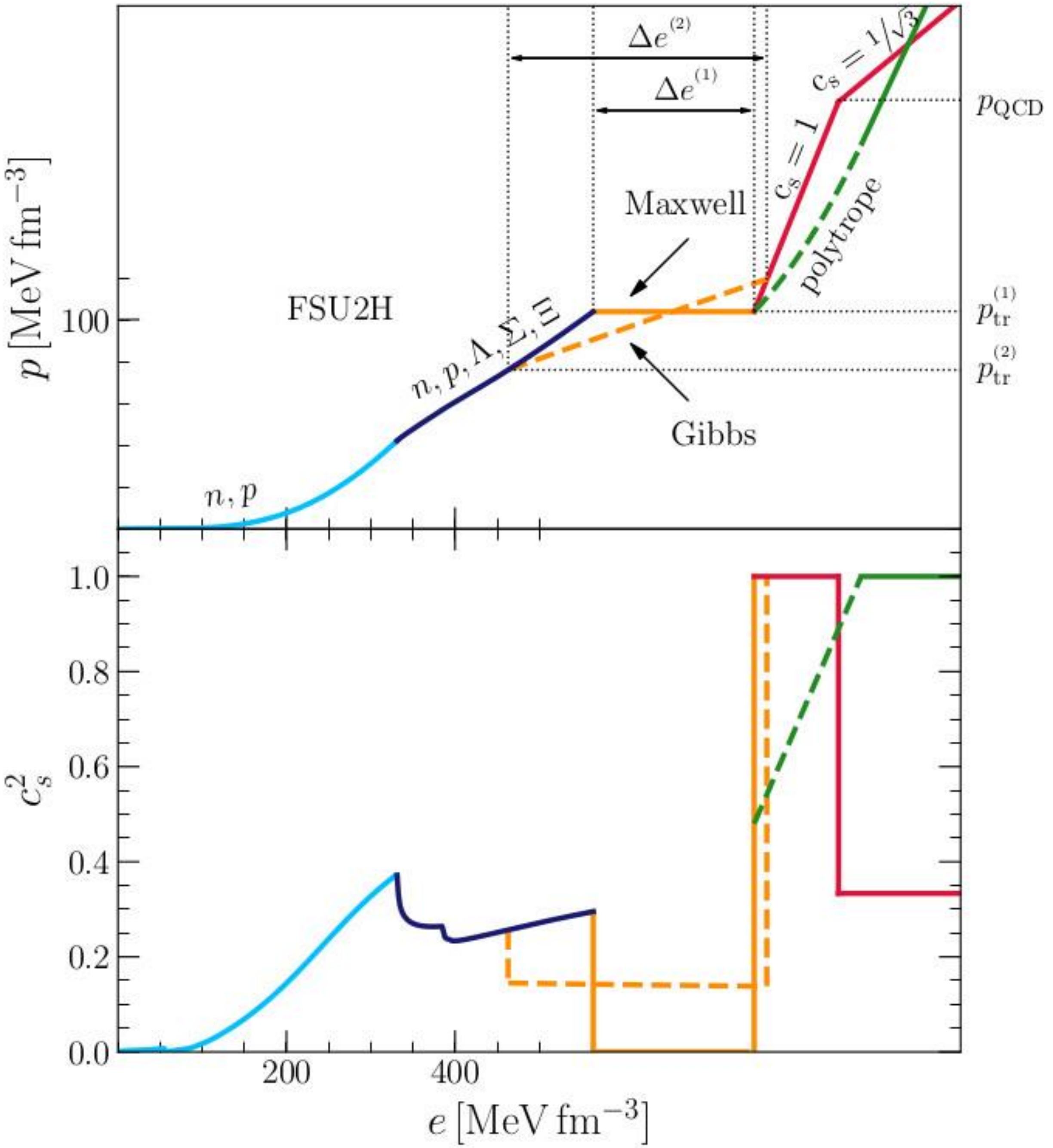

Mass-Radius Relations for Twin-Star EOSs

The mass and radius of a single, non-rotating and spherically symmetric neutron star can be easily calculated by solving the static TOV equation numerically for a given EOS.

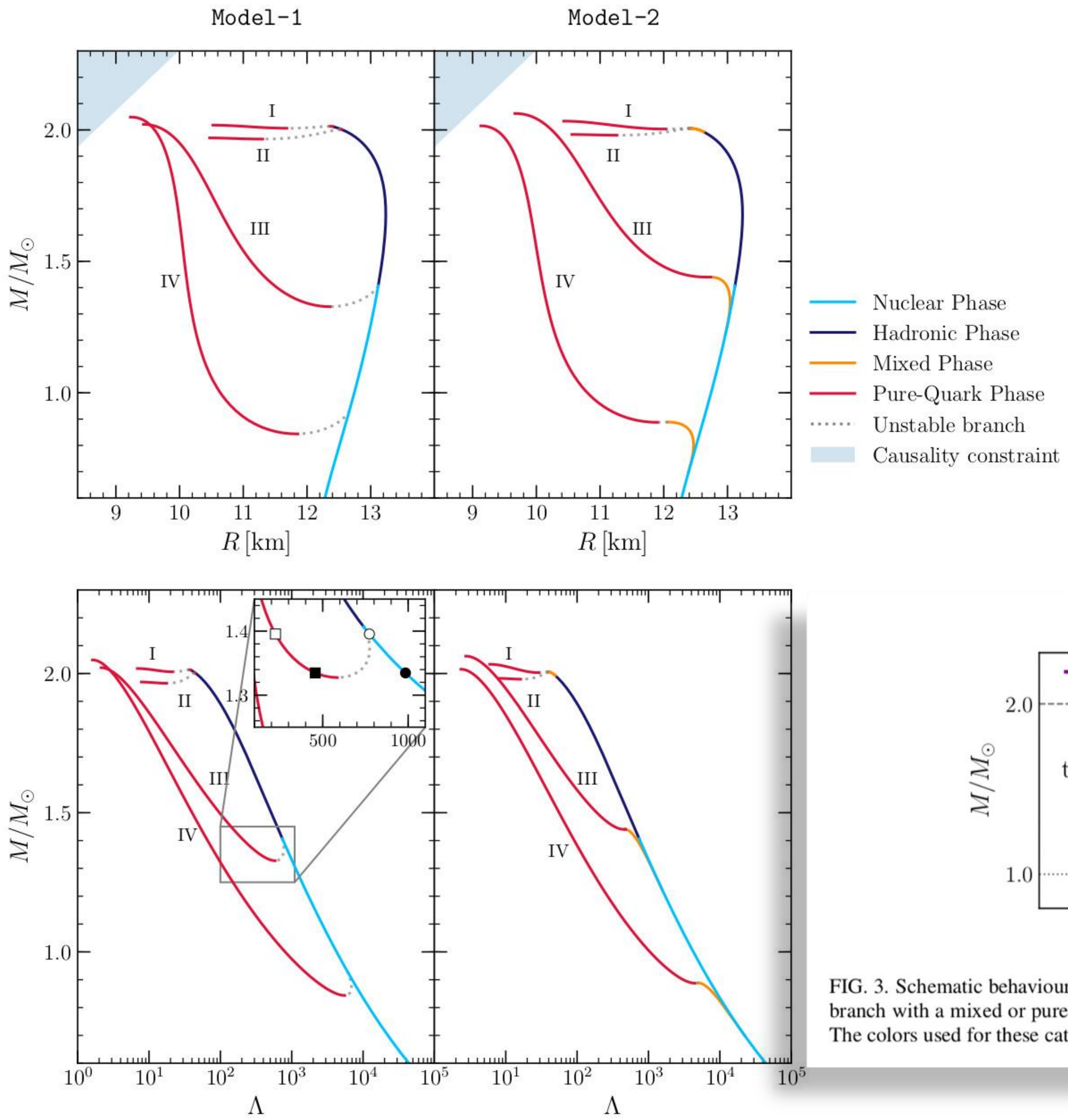

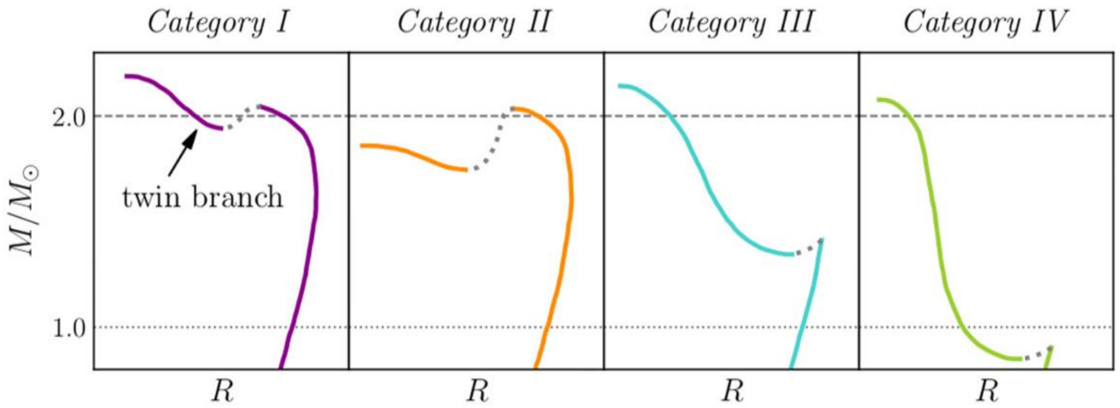

FIG. 3. Schematic behaviour of the mass–radius relation for the twin-star categories *I–IV* defined in the text. Note the appearance of a "twin" branch with a mixed or pure-quark phase; the twin branch has systematically smaller radii than the branch with a nuclear or hadronic phase. The colors used for these categories will be employed also in the subsequent figures.

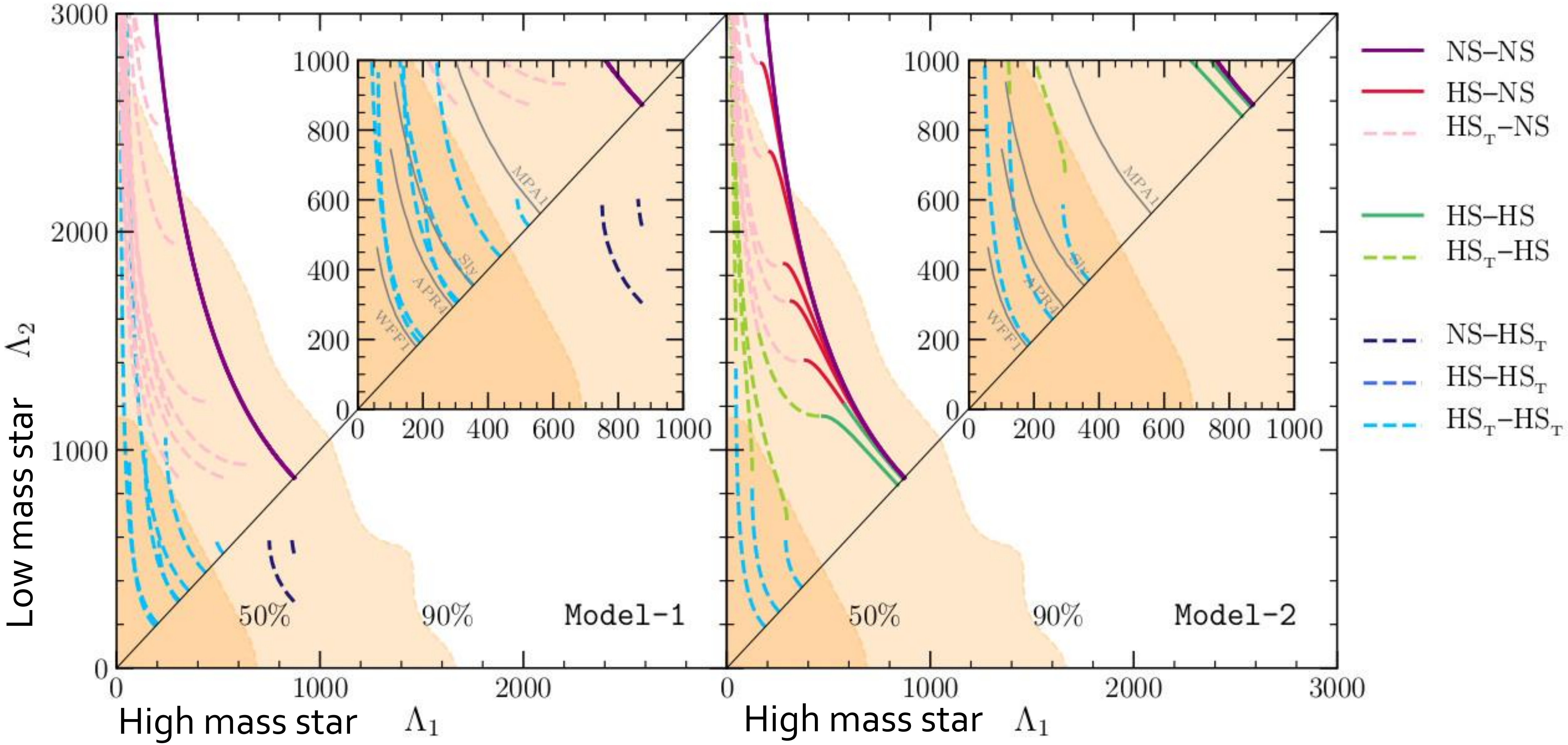

In a binary hybrid star merger the two masses of the individual stars can be different (q<1). As a result, the tidal deformability and the stars composition can be different. In this plot the total mass of the binary system has been fixed to the measured chirp mass of GW170817 (M=1.188 M_{solar}) and the different curve show results for EOSs of Category III.

Gravitational-wave signatures within the late inspiral phase

Construction of the EOS with a hadron-quark phase transition

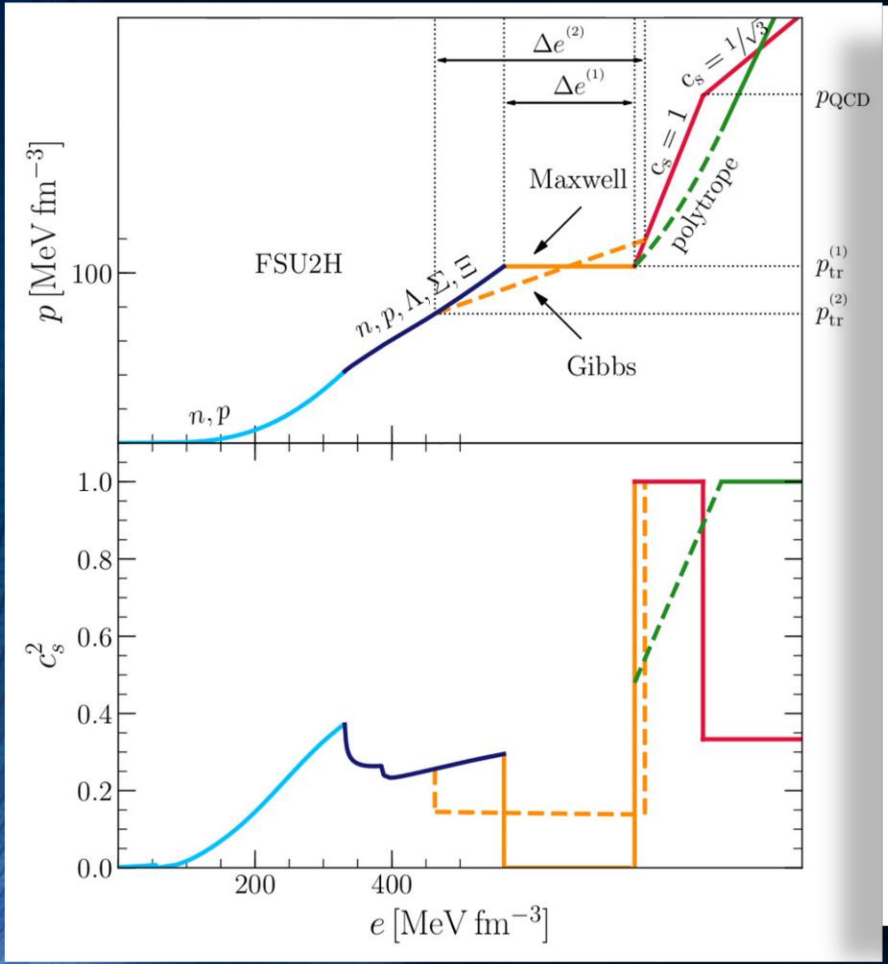

The Mass-Radius relation and the twin star property

Maxwell Construction Gibbs Construction

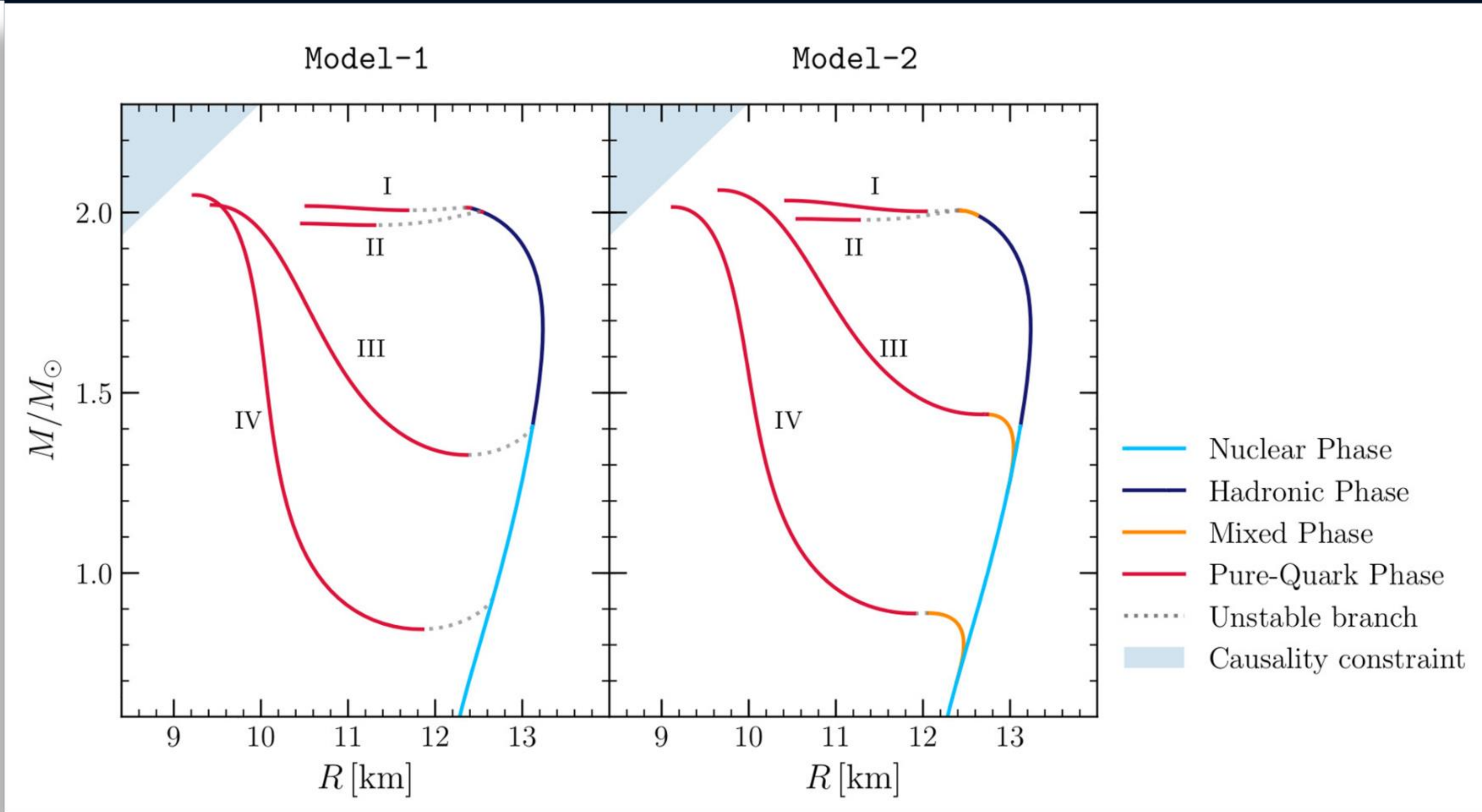

G. Montana, L.Tolos, M.Hanauske and L.Rezzolla
„Constraining twin stars with GW170817", PRD 99(10), 2019

Constraining the hadron-quark phase transition with GW170817

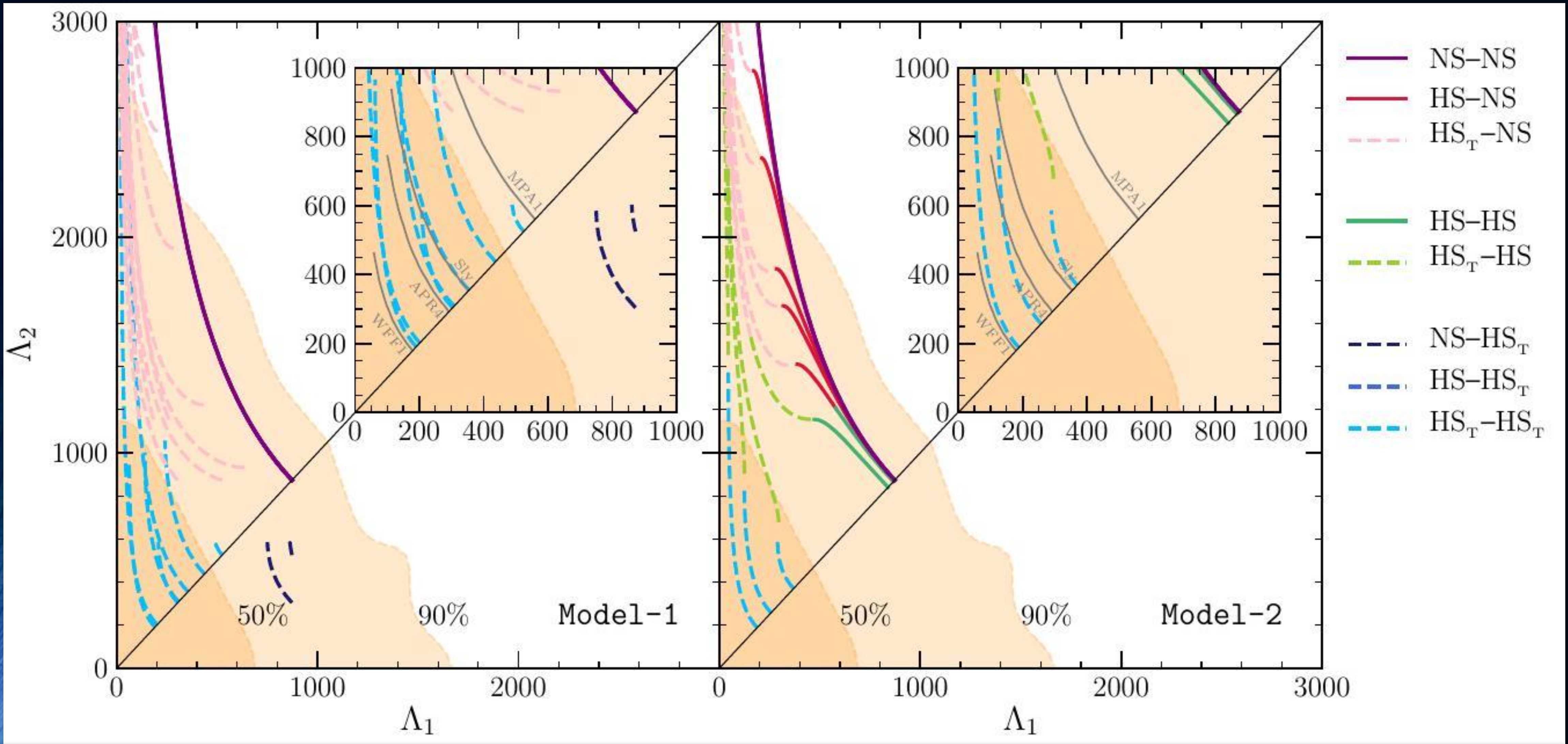

Assuming that the hadronic part of the EOS is given by the FSU2H model, the phase transition takes place already in the inspiral phase -> GW170817 was a hybrid star merger

Pre-merger signatures of the hadron-quark phase transition

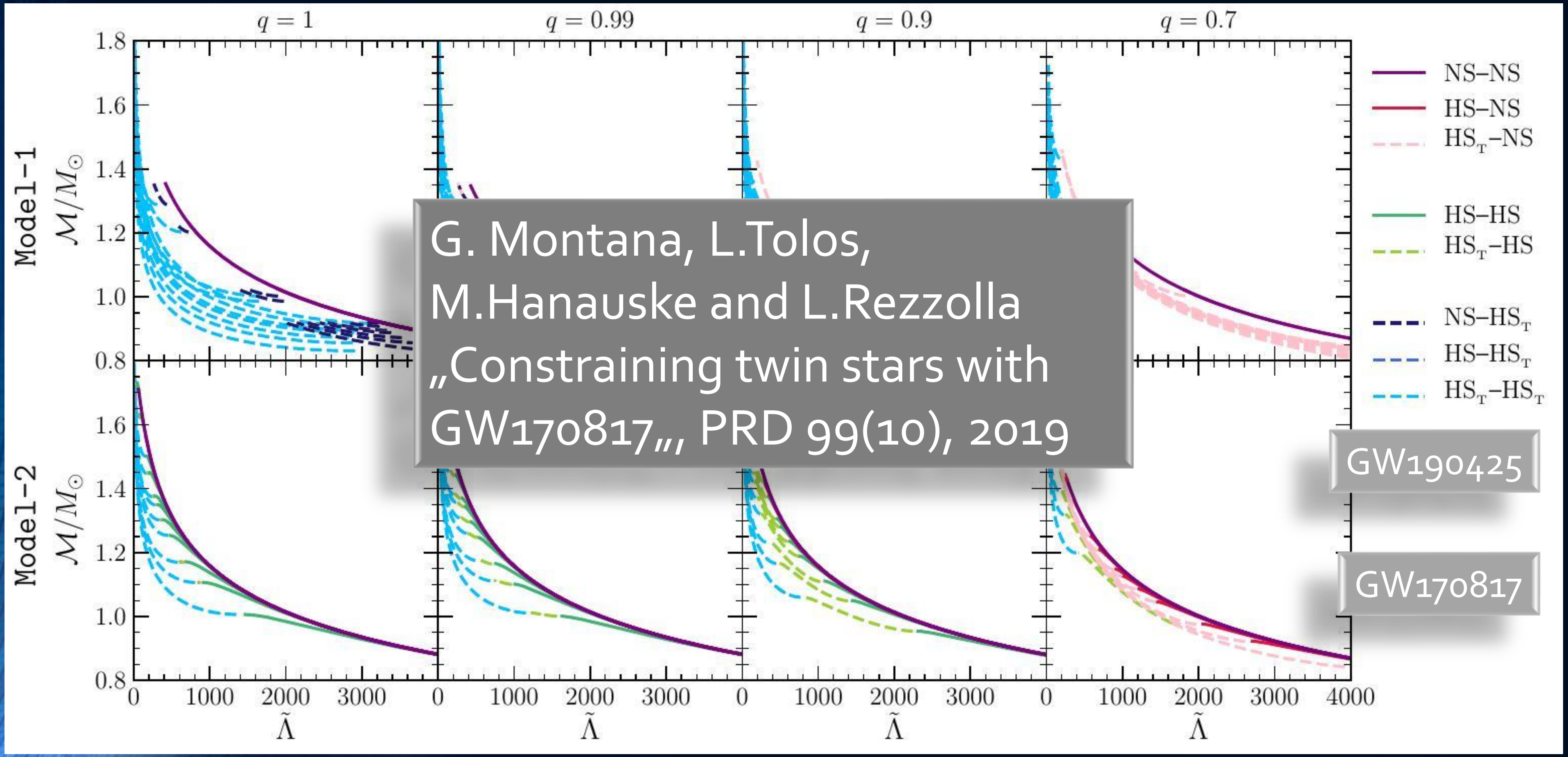

In the next few years, further gravitational waves from binary neutron star collisions with different chirp masses and mass ratios will be detected and thus the equation of state will be further restricted.

Chirp mass set to Mch as a function of the weighted dimensionless tidal deformability $\tilde{\Lambda} = \tilde{\Lambda}$ (M1,M2, Λ1, Λ2) for different mass ratios q

Die .par Datei des Einstein Toolkit

```
============
 Initial data
================================================================
============

ActiveThorns="LoreneID PizzaIDBase"

ADMBase::initial_data    = "LoreneBNS"
ADMBase::initial_lapse   = "LoreneBNS"
ADMBase::initial_shift   = "zero"
ADMBase::initial_dtlapse = "zero"
ADMBase::initial_dtshift = "zero"
HydroBase::initial_hydro = "LoreneBNS"
#HydroBase::initial_entropy  = "THCode"

LoreneID::lorene_bns_file =
"/dss/dsshome1/00/di36gaw4/ET/initial_data/FSU2H_PTv8_M135_
10000.d"
PizzaIDBase::eos_file    =
"/dss/dsshome1/00/di36gaw4/ET/EOSs/FSU2Hnew-v8.pizza"

# Geometric unit system for initial data, specified by length
unit.
# use CACTUS units
zaBase::length_unit           = 1476.7161818921163
================================
```

```
###################### SpaceTime
#######################
ActiveThorns = "ADMBase ADMCoupling ADMMacros CoordG
SpaceMask StaticConformal TmunuBase InitBase"
ActiveThorns = "GenericFD NewRad"

SpaceMask::use_mask = yes

ADMMacros::spatial_order = 4

ActiveThorns = "ML_CCZ4 ML_CCZ4_Helper ML_ADMConstraints
Dissipation"

ADMBase::evolution_method        = "ML_CCZ4"
ADMBase::lapse_evolution_method   = "ML_CCZ4"
ADMBase::shift_evolution_method   = "ML_CCZ4"
ADMBase::dtlapse_evolution_method  = "ML_CCZ4"
ADMBase::dtshift_evolution_method  = "ML_CCZ4"

ML_CCZ4::harmonicN       = 1.0    # 1+log
ML_CCZ4::harmonicF       = 2.0    # 1+log
ML_CCZ4::BetaDriver      = 0.5    # ~1/M (\eta)
ML_CCZ4::advectLapse        = 1
ML_CCZ4::advectShift        = 1
ML_CCZ4::shiftGammaCoeff             = 0.75
```

```
DF5::out2D_vars        = "
_ADMConstraints::ML_Ham
     ADMBase::lapse
     ADMBase::shift
     HydroBase::rho
     HydroBase::
```

Jupyter Notebook

Neutronenstern Kollisionen mit dem Einstein Toolkit

Allgemeine Relativitätstheorie m

General Theory of Relativity on t

Vorlesung gehalten an der J.W.Goethe- 2021)

von Dr.phil.nat. Dr.rer.pol. Matthias Hanauske

Frankfurt am Main 17.06.2021

Dritter Vorlesungsteil: Neutronenstern K

Einführung in den (3+1)-Split

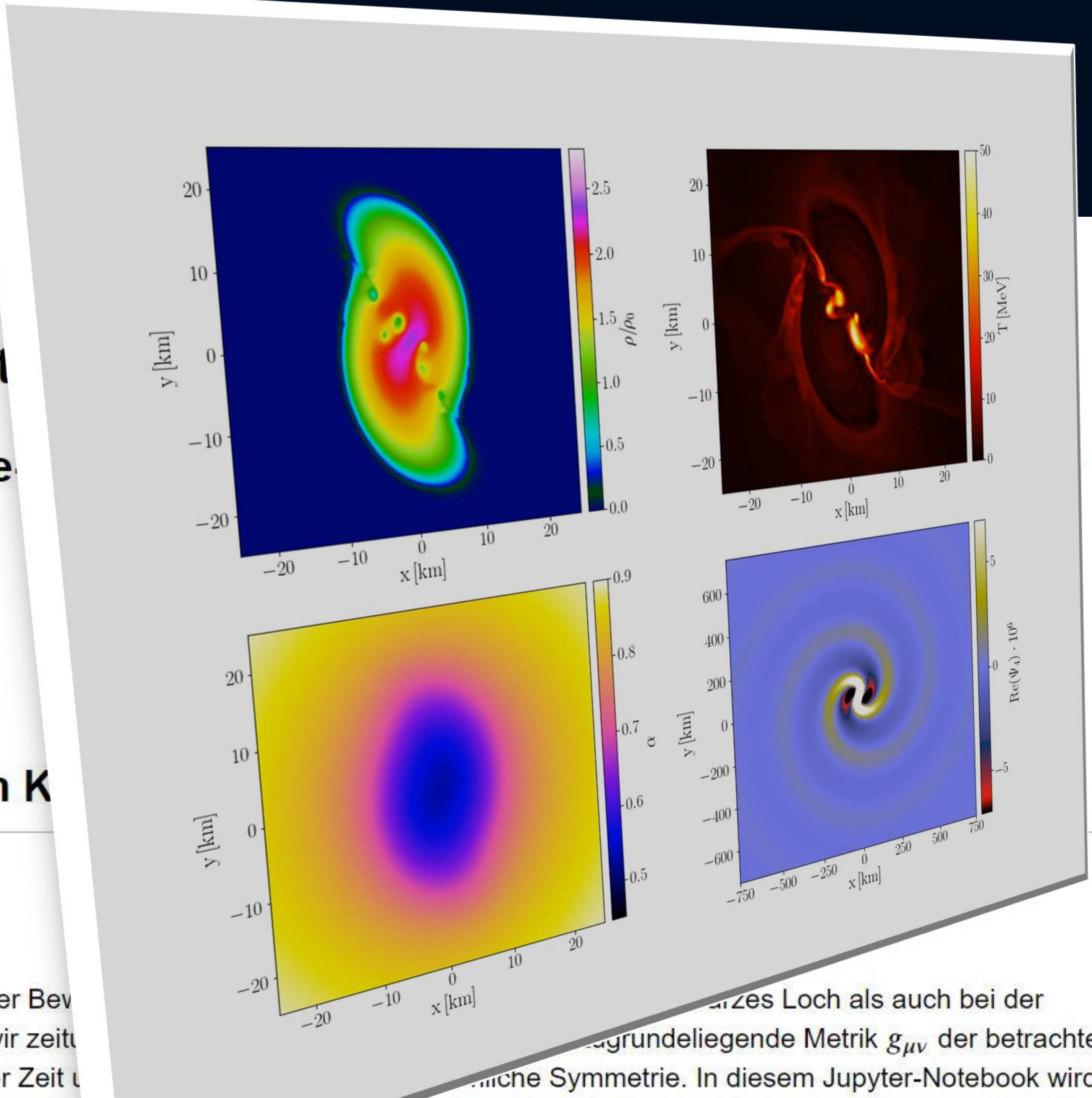

In den bisherigen Jupyter-Notebooks, sowohl bei der Analyse der Bew ...rzes Loch als auch bei der Berechnung der Eigenschaften von Neutronensternen, hatten wir zeitu ...ugrundeliegende Metrik $g_{\mu\nu}$ der betrachteten 4-dimensionale Mannigfaltigkeit $\mathcal{M}$ veränderte sich nicht mit der Zeit u ...liche Symmetrie. In diesem Jupyter-Notebook wird

Mögliche Vorlesungsprojekte

- Teil I: Simulationen und Berechnungen in Python
  - Weiterführende Themen der Kerr-Metrik
  - Kosmologie und die Robertson-Walker Metrik
- Teil II: C++ oder Python
  - Die Masse-Radius Beziehung von Zwillingssternen
  - Die Masse-Radius Beziehung von Compose Zustandsgleichungen
- Teil III: Simulationen mit dem Einstein Toolkit
  - Visualisierung der Neutronenstern Kollisionen von Herrn D. Goretzki